University of Southern Queensland

School of Engineering

Noncontact Distance and Vibration Measurement

A dissertation submitted by

Matthew Boden

in fulfilment of the requirements of

ENG4112 Research Project

towards the degree of

Bachelor of Electrical & Electronic Engineering

Submitted: October, 2023

Abstract

Vibration measurement is an important part of any machinery maintenance schedule, ensuring both correct operation and reliability. It can have devastating effects on rotating equipment and severly reduces the expected life span of said machinery. Being able to measure vibration remotely, without the need for physical contact with the device being assessed, allows for in-use servicing assessments which reduces down time of machinery and ensuring the health of the machine is being monitored.

To date, non-contact distance and vibration measurement has been extensively researched for use with medical patients, allowing for doctors to record accurate measurements of vital signs for heart and respitory rates of their patients. The research into the different algorithms used in this field predominately revolves around proving their ability to accurately capture the displacement under investigation. The gap in knowledge to close in order for this technology to have application in the industrial space is how this technology and algorithms are able to withstand the harsh environmental factors that are present in the areas these machinery operate.

It was found that the algorithms in question are able to operate in environments where noise and attenuation are abscent. It was discovered that the mathematical steps involved with some algorithms has made them less susceptible than others, making them the more robust choice for measurement in harsh environments when environmental noise has been introduced.

To complete the objectives of this project a literature review has been conducted which identified existing research around the operation of the algorithms. Determining how they operate so each could be replicated in simulation software. Literature review was also conducted around the environmental factors and the affect's they have on electromagentic waves to deterimine how noise imparted on the signals could be implemented in the

modelling software.

Each algorithm was then constructed and run through a series of tests concentrating on the error that is introduced by each attribute related to the electromagentic waves propogation through space. Data analysis was completed on the resulting datasets to highlight which factors affect the accuracy of each algorithm the most.

Once the behaviour of the algorithms had been confirmed theoretically, emperical testing was started to validate the results that were seen.

In summary each algorithm is affected by noise that impacts the amplitude of the recieved signal, each algorithm is accurate up to a point and the accuracy is heavily dependent on the carrier frequency chosen.

Two of the three algorithms were able to measure the vibration accurately in ideal conditions. Data anlysis proves that the attributes governing the recieved wave affect the error differently, with the amplitude attribute contributing more to the error than the phase attribute. All algorithms were suceptible to noise to the point where the accuracy is too far diminshed to be used in a practical sense and further pre-processing should be investigated.

University of Southern Queensland

Faculty of Health, Engineering & Sciences

ENG4111/2 *Research Project*

Limitations of Use

The Council of the University of Southern Queensland, its Faculty of Health, Engineering & Sciences, and the staff of the University of Southern Queensland, do not accept any responsibility for the truth, accuracy or completeness of material contained within or associated with this dissertation.

Persons using all or any part of this material do so at their own risk, and not at the risk of the Council of the University of Southern Queensland, its Faculty of Health, Engineering & Sciences or the staff of the University of Southern Queensland.

This dissertation reports an educational exercise and has no purpose or validity beyond this exercise. The sole purpose of the course pair entitled "Research Project" is to contribute to the overall education within the student's chosen degree program. This document, the associated hardware, software, drawings, and other material set out in the associated appendices should not be used for any other purpose: if they are so used, it is entirely at the risk of the user.

Dean

Faculty of Health, Engineering & Sciences

Certification of Dissertation

I certify that the ideas, designs and experimental work, results, analyses and conclusions set out in this dissertation are entirely my own effort, except where otherwise indicated and acknowledged.
I further certify that the work is original and has not been previously submitted for assessment in any other course or institution, except where specifically stated.

Matthew Boden

Acknowledgments

I would like to thank and recognise my family's support and commitment over the years. Particulalry my wife Louise for shouldering a large amount of the household and family duties, allowing me to focus on my study and complete this milestone.

I would also like to acknowledge Dr John Leis for his guidance and support throughout the completion of this research project.

Matthew Boden

Contents

List of Figures

List of Tables

Chapter 1

Introduction

1.1 Project Aim

The aim of this research project is to investigate the different algorithms related to the demodulation of phase encoded distance and vibration data and to then test the performance of the algorithms using both synthetic data generation and real world testing in adverse conditions. The adverse conditions in which these algorithms are believed to be subject to are atmospheres that are contaminated with dust/moisture particles. To accomplish this the project will have two main points of focus; the first being the implementation and testing of the algorithms using synthetic data and the second will be the use of the created and tested algorithms on real data.

1.2 Statement of objectives

To achieve the desired aim appointed for this project the following list of objectives has been created to plan and track the progress of this research project:

1. Conduct research on algorithms used in the continuous Doppler wave phase demodulation space.
2. Conduct investigation into adverse environmental impacts on radio/acoustic waves.
3. Investigate appropriate testing configurations and Doppler radio system designs.

4. Determine the properties that the algorithms are to be assessed on related to the accuracy of measurement and consistency of performance.
5. Conceptualize and design test arrangements for both synthetic and real data signals.
6. Select hardware and a suitable software development environment.
7. Develop the software algorithms and the synthetic data signals that are to be tested.
8. Test demodulation algorithms theoretically in the software environment with synthetic signals to prove understanding and operation of algorithms.

As time and resources permit:

1. Complete testing of algorithms using real world data in place of synthetic data.
2. Process and evaluate data from tests and recommend methods of improving algorithm performance.

1.3 Consequences and Ethics

In the completion of this research project the recording of data from the experiments will be conducted in an honest manner ensuring promotion of responsible research practices. No data will be doctored and all findings will be transparently communicated through the projects report.

1.3.1 Sustainability

Advances in the noncontact vibration measurement field will lead to improved condition monitoring of machinery which will allow for a longer life of parts and improved effectiveness in operation and manufacturing. This will reduce waste and the need to create new machinery. Improved monitoring of machinery expands company economic sustainability prospects by allowing for targeted maintenance routines to be put into affect reducing the down time of machinery due to critical failures. Improved economic outlook for companies directly affects the socioeconomic levels and economic prosperity via company expansion, research and development and job retention.

1.3.2 Safety

The outcome of this report will influence the devolpment of noncontact vibration sensors in the industrial space. This will lead to greater safety for personnel when monitoring equipment, specifically rotating machinery that would normally introduce risk to the person conducting the measurement. Through improved monitoring of equipment and machinery the user safety will be improved by determining the equipments service/repair requirements before a critical limit is reached. In completing this project there will be risks to safety present through the gathering of empirical evidence. These safety risks are assessed through the Univeersity of Southern Queensland's risk management plan and mitigation procedures have been put in place to reduce any risk associated with this project. The completed risk management plan can be found in Appendix B.

1.3.3 Ethics

When completing engineering works certain ethics are expected of the engineer undertaking the task. To ensure uniform performance and a base expectation of all engineers the Engineers Australia organization detailed a list of ethics that their cohort adhere to. Throughout this research project the following ethics will be followed and adhered to:

- Demonstrate integrity
  - Sound judgement is to be shown acting without bias when presented with decisions
  - Respecting deadlines and all contractual obligations associated with the project
  - Professional representation of the engineering profession showing honesty and trustworthiness
- Practise competently
  - Through the devlopment and management of knowledge and skills related to the completion of the project. Utilising peer review to confirm understanding and development of ideas related to the field
  - Act in a manner that ensures data is represented correctly without bias and within the appropirate competency
- Exercise leadership
  - Advocate for trustworthiness and responsible public debate regarding matters concerning the project
  - Support other professionals in the space through appropriate recognition of content
  - Engage in clear and timely communication regarding issues related to the project
- Promote sustainability
  - Promptly engage key stakeholders regarding concerns or consquences of completing the project
  - Actively balance the needs of the present with the needs of the future (Australia 2022)

Recording machine performance data creates a situation where a company's data can be recorded and analysed for nefarious means such as corporate espionage or intellectual property theft. To mitigate any occurance of this, the emperical testing being performed will perdominately be conducted on devices created to mimic the vibration profile that may be present on said machinery. If and where an opportunity is present to use actual machine data in the gathering of emperical evidence, such data will be stored in a manner to preserve any and all company IP and information regarding the machine's identity from which the data was collected.

The focus of this research project is around the use of the Doppler signal demodulation algorithms in the industrial sector. This technology has been and is currently in use in the medical field for the purpose of monitoring the vital signs of patients. It should be considered that advances in this technology could allow for the tracking and identification of personnel, leading to an invasion of privacy that could be used with malicious intent, possibly resulting in stolen identity, theft and extorsion. In mitigation towards this outcome and use of the technology, the focus of this project will be purely based on machinery and the application related to the industrial space.

A significant portion of the work being completed with this project is theoretical in nature. To ensure the engineering ethics depicted above are adhered to, all information utilised to support this project will be sourced from reliable and professional databases. All data collection and testing will be compeleted and communicated through the report without manipulation or doctorisation. This will allow for an unbiased conclusion to be drawn from the data.

Chapter 2

Background

Machinery and automation improvements have changed the way humanity manage the construction of new items and materials. As a result of the development of these mechanically driven machines, the need for maintenance has also arisen, along with the need to monitor a machine's operation and health. Recent research has shown that Doppler radar is effective for the detection of vibration through radio frequency signal reflection.

2.1 The Electromagnetic Wave

An electromagnetic wave differs from electrostatic and magnetostatic fields in that it is time varying. Time varying waves are typically the byproduct of accelerated charges or time-varying currents. Any pulsating current will produce a time varying electromagnetic wave (Sadiku 2018)

Henrich Hertz was the first to investigate the electromagentic wave and was able to prove their existence through maxwells equations and experimentation ultimately generating and detecting a radio wave. As a result electromagnetic waves are also known as Hertzian Waves. Traditionally, electromagentic waves are used to transport energy and information through some form of modulation (Sadiku 2018).

An electromagentic wave is a function of both time and space which can commonly be represented by the equation:

$$E = A\sin(\omega t - \beta z) \tag{2.1}$$

where:

A = Amplitude (Same unit as E)

t = time

z = space variable

ω = angular frequency (radians per second)

β = phase constant (radians per meter)

When electromagnetic waves are transmitted over distances they are modified by effects of the environment and structures in its path (Leis 2018). This modification is often referred to as modulation. Modulation refers to the change in parameters describing the electromagnetic wave.

A modulated electromagnetic wave can be broken down into two different equations with-the equations representing the modulated signal or the information being transmitted and the carrier signal, which the modulated signal is being superimposed onto.

Modulated signal as per (Leis 2018):

$$m(t) = A_m\sin(\omega_m t + \psi_m) \tag{2.2}$$

Carrier Signal as per (Leis 2018):

$$x_c(t) = A_c\sin(\omega_c t + \psi_c) \tag{2.3}$$

where:

$m(t)$ is the modulated signal

x_c is the carrier wave

A is the Amplitude

t is the time sequence

ω is the angular frequency

ψ is the phase constant

An electromagnetic wave can be modulated in different ways. The most common forms of modulation are amplitude, frequency and phase modulation (Leis 2018). For the purposes of this report the phase modulation is of particular interest as this is the affect imparted on the waveform when the signal reflects off a vibrating body.

The electromagnetic wave with time varying phase shift as per (Leis 2018) is represented by:

$$x_r(t) = A_c \sin(\omega_c t + k_p m(t)) \tag{2.4}$$

where:

x_r is the reflected waveform containing the phase modulation

A is the Amplitude

t is the time sequence

ω is the angular frequency

k_p is the constant phase multiplier

$m(t)$ is the modulation waveform

2.2 Doppler Vibration Detection Principle

Doppler radar vibration detection works on the principle of simple harmonic motion that modifies the transmitted carrier signal by imparting a phase shift on the reflected signal. The reflected signal's phase shift can be broken into three components; one being a component that represents the distance the object is located from the receiver another component being the vibration modulation and the last component being the residual phase noise applied to the signal (Rakshit, Roy & Chakravarty 2018), as can be seen below:

$$x_r(t) = \cos(\theta_0 + \frac{4\pi x(t)}{\lambda} + \Delta\theta(t)) \tag{2.5}$$

Where:

t is the time sequence

θ_0 is the phase shift present due to the distance between transmitter and reciever

$\frac{4\pi x(t)}{\lambda}$ is the phase shift due to the object

$\Delta\theta(t)$ is the residual noise/external noise

The total phase displacement can be represented by the frequencies present in the signal. The lowest frequency in the signal represents the vibration component embedded in the signal. (Rakshit et al. 2018)

2.3 Quadrature Demodulation

Interpretation and demodulation of modulated signals is commonly achieved through quadrature demodulation and is the employed approach of the algorithms being investigated. This method employs two orthoganal signals generated at the same frequency as the carrier frequency that are then combined with the reflected signal. The resultant signals are termed the I and Q signals, which are to be used in conjunction with the algorithms to determine the phase shift present in the reflected signal with reference to the transmitted carrier signal. (Leis 2018)

The following block diagram from (Leis 2018) shows the operations involved with generation of the I and Q orthogonal signals.

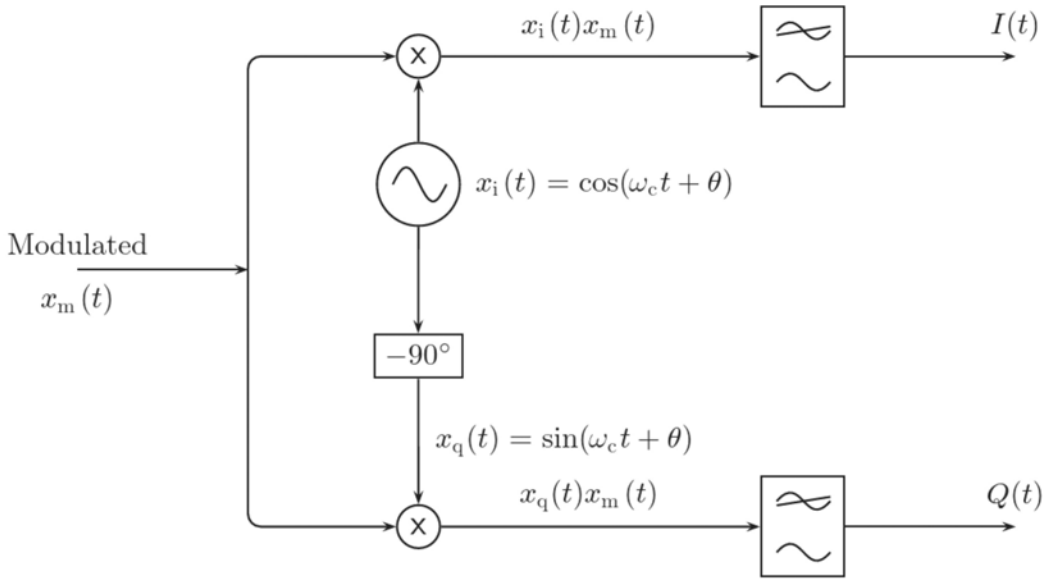

Figure 2.1: Quadrature demodulation block diagram (Leis 2018)

Traditionally the I and Q signals can be considered as an in phase signal and an out of phase signal. With reference to the transmitted carrier signal the I and Q signal are represented by the following equations as shown in figure above:

$$x_i(t) = \cos(w_c t + \theta) \tag{2.6}$$

$$x_q(t) = \sin(w_c t + \theta) \tag{2.7}$$

Where:

x_i is the I quadrature signal

x_q is the Q quadrature signal

w_c is the carrier wavaes angular frequency

t is the time sequence

θ is the phase constant

2.4 Industry Background

Typically, vibration measurement is used to measure and determine the health of machinery. The amount of vibration in a piece of rotating machinery can often be directly related back to the health of the following components:

- Shafts
- Bearings
- Gearboxes
- Engines
- Fans
- Blowers

It is common practice for a technician familiar with a machine to observe the equipment and determine which component requires the vibration study conducted (CAS & DataLoggers 2016).

Vibration in the above components can be caused by several issues, the following list is a collection of the main contributors to machine vibration:

Imbalance This situation occurs when a heavy spot has developed in a rotating component of the machine. The vibration in this instance is developed by the centrifugal force of the "heavy spot".

Misalignment This situation can arise when components of the machine are not correctly in alignment. There are two categories of misalignment assigned to this issue; angular misalignment and parallel misalignment. The first indicates that two shafts of a machine are not parallel and the later indicated that two shafts of a machine are parallel but are not in alignment.

Wear This situation is created through use of the machine and should ideally be combated with regular monitoring and maintenance as required. The main cause of vibration from wear is when a roller or ball becomes pitted after extensive use, and when in use, cause a vibration whenever the damaged area is travelled over.

Looseness In this instance, vibration that is not addressed can often lead to disastrous consequences as the vibration will often exacerbate the situation. The initial condition that can cause this situation does not need to be vibration existing in the machine, this can be caused by the likes of a loose fastener or mounts. (Wright 2010)

The applications of noncontact distance and vibration measurement are not limited to the industrial space with many applications being identified within the medical field. The applications of note are predominately focused around the monitoring of life signs such as the respiration and heart beat of a patient.

2.5 Idea Development

The idea for this project originated from the identified need for a method to remotely measure accurately the vibration present in machinery. This led to further investigation around the methods of vibration measurement of mechanical items, with the most appropriate solution being that of a non-contact form versus the traditional sensor mounted approach.

This method is better suited to mechanical applications, as quite often the mass of a sensor would influence the vibrating structure and subsequently the result being measured. In addition to this, rotating equipment is extremely difficult to wire sensors too. (Hanly 2021)

In addition to the industrial aspects the ability to measure a patients lifesigns remotely and without the need for obstructive wires or sticky pads, improves the patients comfortability as well as increasing the accessbility of the attending physician to the patient.

Non-contact vibration measurement can be facilitated through several different methods, these methods predominately revolve around the use of microphone or acoustic sensors, laser displacement sensors or eddy current and capacitive displacement sensors(Hanly 2021) The aim of this research project is to investigate another method of noncontact vibration measurement using radio frequencies and the factors affecting the measurement accuracy.

Chapter 3

Literature Review

3.1 Chapter Overview

The Literature review completed in this report will explore in detail the available published literature on the different types of phase demodulation algorithms that are used with continuous wave Doppler systems. The review will be broken up into the following different sections:

- Demodulation Algorithms
  - Arc Tangent Demodulation
  - Extended Differentiate and cross multiply (EDACM)
  - Modified Differentiate and cross multiply (MDACM)
- Application of Vibration Technology
- Knowledge Gap identification
- Adverse environmental factors on electromagnetic/acoustic waves
- Calculating vibration displacement from angular phase shift

3.2 Demodulation Algorithms

3.2.1 Arctangent Demodulation

The traditional method of determining phase modulation of a received signal is the arc tangent method. The arctangent algorithm is used in many applications and to date, existing literature focuses around the use of this method to aid in the detection of heart beats and respiratory rates. The Arctangent demodulation method uses a traditional Doppler radar setup to transmit and receive a signal to determine the phase modulation imparted on a reflected signal by a vibrating source, the image below displays this(Wang et al. 2014).

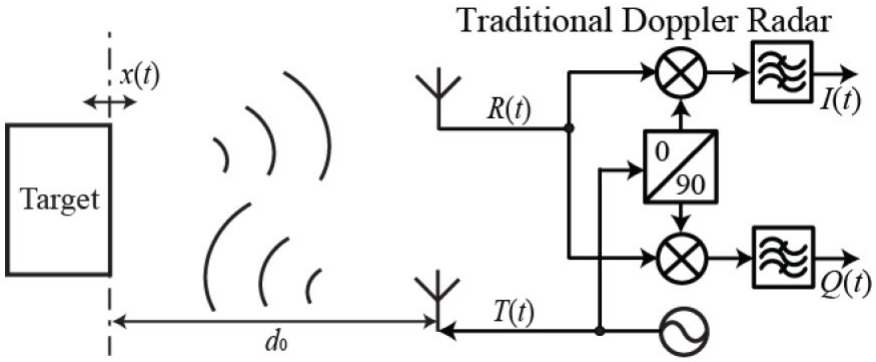

Figure 3.1: Common configuration of a traditional Doppler radio used in signal modulation detection (Wang et al. 2014)

The carrier signal being transmitted by the Doppler radar can be represented by the following equation:

$$x_c(t) = A_c \cos(w_c t + \Psi(t)) \tag{3.1}$$

The received signal is passed through a quadrature de-modulater where the two I and Q signals are created:

$$I(t) = A_I \cos[\Phi(t)] \tag{3.2}$$

$$Q(t) = A_Q \sin[\Phi(t)] \tag{3.3}$$

Where

$$\Phi(t) = \theta + \frac{4\pi x(t)}{\lambda} + \Delta\theta(t) \tag{3.4}$$

Where:

t is the time sequence

θ_0 is the phase shift present due to the distance between transmitter and reciever

$\frac{4\pi x(t)}{\lambda}$ is the phase shift due to range of object

$\Delta\theta(t)$ is the residual noise/external noise

Taking the arctangent of the two quadrature outputs results in the phase difference between the transmitted signal and the reflected signal. The arctangent operates within the range -$\pi/2$,$\pi/2$ because of this when the output exceeds this range the demodulated output creates discontinuities in the resultant waveform. (Wang et al. 2014) Such waveform irregularities can be witnessed in the testing completed by (Wang et al. 2014) in the below graph.

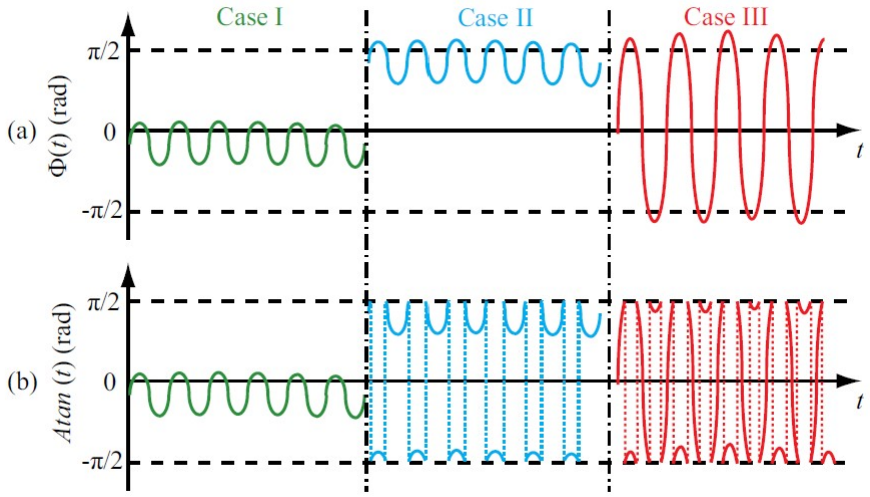

Figure 3.2: (a) This shows the desired phase demodulation output (b) This shows arctangent demodulated output image sourced (Wang et al. 2014)

In the above graph three cases are presented that show the behaviour of the arctangent's

demodulated output:

Case I The phase modulation is within the confines of the domain (Wang et al. 2014)

Case II Where the phase modulation is offset and oscillation is located at the limits of the domain (Wang et al. 2014)

Case III Where the modulation amplitude is larger than an eigth of the wavelength (Wang et al. 2014)

3.2.2 Extended Differentiate and Cross Multiply - EDACM

The extended differentiate and cross multiply algorithm is similar to the arctangent algorithm. The EDACM algorithm applies differentiation to the arctangent operator resulting in the equation below. This differentiation operation calculates the amount of angular acceleration change in the received signal. By differentiating the quadrature outputs the domain limit issue that is experienced with the arctangent algorithm when used directly on the quadrature signals is removed because the differentiation operator yields the angular frequency acceleration rather than the phase value (Wang et al. 2014).

$$\omega(t) = \frac{d}{dt}[\arctan\frac{Q(t)}{I(t)}] = \frac{I(t)\dot{Q}(t) - \dot{I}(t)Q(t)}{I(t)^2 + Q(t)^2} \tag{3.5}$$

Due to the added mathematical operations in this algorithm, the EDACM algorithm is inherently highly susceptible to noise, specifically high frequency noise. In addition to the noise, the added operations in this algorithm also make it highly dependant on the calibration of the I/Q quadrature signals.(Xu, Gu & Mao 2020) To reduce the noise added by the differentiating portion of the algorithm an integration procedure can be added to the algorithm which will allow all noise with a mean of zero to be suppressed. (Wang et al. 2014) The following block diagram shows the method of application for the DACM algorithm.

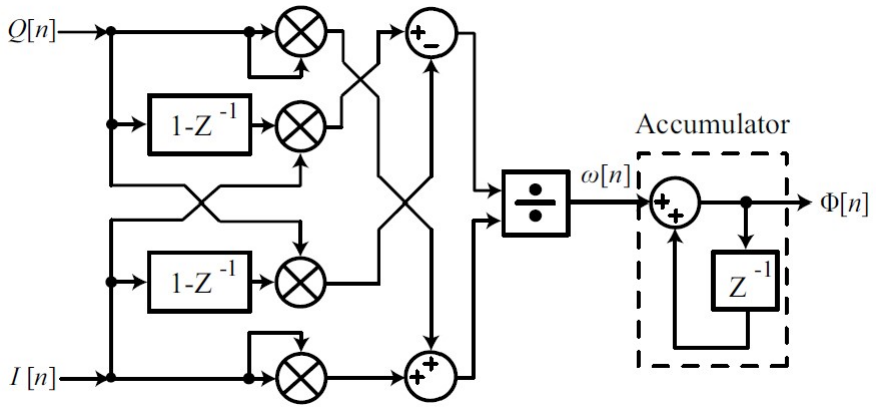

Figure 3.3: The above block diagram represents the operations of the EDACM algorithm, including the accumulation operation (Wang et al. 2014).

With the added accumulation process the EDACM algorithm can be represented mathematically by:

$$x(t) = \frac{\lambda}{4\pi} \sum_{k=2}^{t} \frac{I(k)\dot{Q}(k) - \dot{I}(k)Q(k)}{I(k)^2 + Q(k)^2} \tag{3.6}$$

3.2.3 Modified Differentiate and Cross Multiple - MDACM

A variation of the EDACM algorithm is the modified differentiate and cross multiply algorithm which differentiates the quadrature I and Q signals before processing, this method works by removing the arc tangent operator all together and replacing it using trigonometric relationships. This procedure allows for the removal of the additive noise by the additional nested operations present in the EDACM algorithm and suppresses approximation errors. (Xu et al. 2020)

$$\omega(t) = \frac{\lambda}{4\pi}[I(t)\dot{Q}(t) - \dot{I}(t)Q(t)] \tag{3.7}$$

The following block diagrams show the procedured of application of the MDACM algorithm.

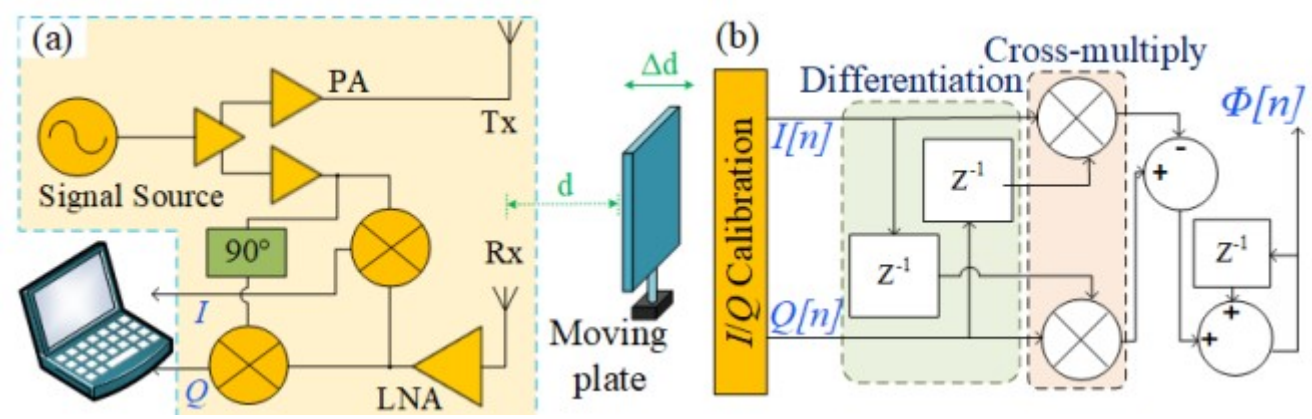

Figure 3.4: Block diagram of the MDACM without using the arctangent operator(Wang et al. 2014).

Like the EDACM algorithm the MDACM algorithm also incorporates an accumulation procedure to convert the calculated angular frequency acceleration into the phase being measured. This is represented mathmatically below:

$$x(t) = \frac{\lambda}{4\pi} \sum_{k=2}^{t} [I(k)\dot{Q}(k) - \dot{I}(k)Q(k)] \tag{3.8}$$

3.3 Application of Vibration Technology

From the literature review it has been observed that different algorithms are inherently being used for different functions. These range from vibration detection in machinery to heart beat and respiration monitoring of a patient. It is the purpose of this report to conduct research into each algorithm's performance when exposed to environments that would affect the accuracy of the measurement.

3.4 Knowledge Gap Identification

In the reviewed literature some limited comparisons have been made between the different algorithms available, predominately the arc tangent and extended differentiate and cross multiply algorithms. These are compared with very little mention of the modified differentiate and cross multiply algorithm. In these comparisons, the existing literature is

focused on theoretical shortcomings and confirming operation of these algorithms through simulation. It is for this reason that these comparisons must be confirmed through trials. In completing trials of all algorithms in different scenarios the benefits of each algorithm will clearly be observed and the advantages and diadvantages of each will be identified. This study will provide industry with a guide to the selection of phase demodulation algorithms so they can better measure the vibration in their specific scenario.

3.5 Environmental factors

Electromagnetic waves travelling through space and time are affected by the structures and environments in its path (Leis 2018). It is therefore reasonable to assume that random environmental events such as rain and dust storms and sources of electromagentic noise will have an effect on the performance of the algorithms. Mathematically the impact of external noise is represented by $\Delta\theta$ in the wave equation representing the modulated wave:

$$x_r(t) = \cos(\theta + \frac{4\pi x(t)}{\lambda} + \Delta\theta(t)) \tag{3.9}$$

Where:

$x_r(t)$ is the reflected wave

t = time

θ_0 is the phase shift present due to the distance between transmitter and reciever

$\frac{4\pi x(t)}{\lambda}$ = the phase shift due to modulation from the vibrating displacement $x(t)$

$\Delta\theta(t)$ = residual noise/external noise

The ITU-R P.618-10 details the propogation losses present in an earth to space transmission path as being:

- Attenuation by atmospheric gases
- Attenuation by rain, other precipitation and clouds

- Focusing and Defocusing
- Decrease in antenna gain due to wave-front incoherence
- Scintillation and multipath effects
- Attentuation by sand and dust storms (Union n.d.)

Of the above list, the events that are believed to be of particular impact to the measurement of vibration through non contact methods is the following environmental events:

- Rainfall
- Dust storms

The effects of rain particles in the path of an electromagnetic wave is something that is commonly experienced and is typically experienced when attempting satellite communication or communications over a large distance (Singh, Bonev, Petkov & Kumar 2018). Propogation affects caused by moisture in the atmosphere are often attributed to the absoprtion and scattering of the wave as it travels through the element (Abuhdima & Saleh 2010).

A common model often employed for the estimation of the effects of rainfall on electromagentic waves is the ITU-R P.618-10 Model (Singh et al. 2018). Section 2.2 of the guide lists methods and suggestions for estimating the attenuation caused by rainfall and clouds highlighting that moisture in the atmosphere leads to attenuation of radio waves.

In addition to attenuation, moisture also adds a phase shift to the signal as was shown by (Fares, Fares & Ventrice 1997) in the analysis of signal attenuation and phase shift when affected by moist snow.

The effects caused by moisture in the atmosphere have been proven to be severly detremental to signals operating at frequencies above 10Ghz (Singh et al. 2018, Fares et al. 1997). Although it is possible for vibrations to be measured at a frequency this high, the computational requirements make it unsuitable with the techonology at present. The proven affects of moisture in the atmosphere can be summised to attenuation of the signal and added phase noise, both of which are believed to impact the accuracy of measurement.

The affects of dust and sand in the atmosphere are similar to that of the moisture, in that attenuation and phase shift are imparted on the signal. This is because the attenuation and phase affect are a function of the moisture content in the sand/dust particles (Abuhdima & Saleh 2010).

3.6 Calculating vibration displacement from angular phase shift

Each algorithm outputs the phase difference in radians from the quadrature signals I and Q. The breakdown of the phase shift present in the output can be expressed as follows:

$$\Phi = \theta + \frac{4\pi}{\lambda}x(t) + \Delta\theta(t) \tag{3.10}$$

Where:

Φ represents the phase shift in radians

θ represents the phase shift due to distance between transmitter and device being measured

λ represents the wavelength of the carrier frequency

$x(t)$ represents the physical displacement caused by the vibration

$\Delta\theta$ represents residual phase noise (Often neglected) (Wang et al. 2014)

The vibration displacement is focused around the second element of the above equation rearranging and neglecting the two other elements we can determine the displacement $x(t)$ with the following:

$$x(t) = \frac{\Phi\lambda}{4\pi} \tag{3.11}$$

Chapter 4

Methodology

4.1 Scientific Method

This research project follows the scientific method. The scientific method details a process in which investigation into scarcely understood or under investigated topics is to be conducted. This method is preferred among the scientific community as it aknowledges that certainty of knowledge concerning our understanding of the world and the rules governing it is unattainable. The preferred method being to instead recognise that science is fallible but still rationally justifiable (Hepburn & Andersen 2021).

4.2 Overview

To understand the performance of each algorithm and the factors that affect the error present within the demodulation, the theoretical testing will be concentrated on the attributes that characterise the reflected waveform. This testing will predominately conclude with a sound understanding of how each attribute interacts with the algorithm and an understanding of the values that allow for optimum performance of each algorithm.

On succesful completion of the theoretical testing of the algorithms, time permitting, it is the aim of this project that a test rig be developed to conduct real world experiments on each algorithm in the adverse environments. The vibration source will be a traditional plate and speaker setup mimicking that of a chladni plate with the speaker generating

vibration on a metallic plate. This vibration source will allow for a highly configurable frequency of vibration that can be replicated numerous times to complete the data collection and verify the simulated results.

4.3 Parameters to be Measured

In the field of noncontact vibration measurement the most obvious parameters to be measured are those that correlate with the overall desired output from use of the algorithm. On this basis the theoretical analysis will measure the error present between the demodulated output and the known signal. Furthermore the emperical testing will focus on the accuracy of the algorithms which relates to the repeatability of the measurements being taken and the precision of each algorithm. This relates to the error between the known value and the calculated value.

Assessing these parameters over multiple tests will provide a clear picture as to which algorithm can better handle the environments expected in the industrial/manufacturing space. In the process of evaluating and testing these parameters values such as carrier frequency, vibration frequency and the reflected waves amplitude will also be measured and assessed to determine their affect on the results.

4.4 Theoretical Testing

For completion of the theoretical testing each algorithm was created as a function. A script was written that would pass each algorithm the test parameters and the error was returned this allowed for efficient and consistent testing to be run. The theoretical testing has been broken up into four different sections, with each section containing sub tests as can be seen below.

Table 4.1: A table depicting the theoretical test being conducted to determine the affects of attribute variation.

Theoretical Tests		
Parameter	Test Number	Description
Amplitude	1	Measures the error present when the peak amplitude of the reflected wave is a static value that is varied in relation to other parameters
	2	Measures the error present when the peak amplitude of the reflected wave is a time varying value in relation to other parameters
	3	Measures the error present when the peak amplitude is a time varying value that cycles at varying frequencies
Carrier Frequency	1	Measures the error present when the carrier frequency is varied against a unit vibration frequency
	2	Measures the error when a fixed carrier wave measures varying vibration displacements
	3	Measures the error present when a fixed carrier frequency is measuring a time varying vibration frequency
Phase Noise	1	This test imparts a phase offset onto the reflected signal and measures the resultant error.
Wavefrom Samples	1	Measures the error introduced by the number of points used to create the carrier wave

4.4.1 Amplitude Testing

The first attribute being analysed is the amplitude of the reflected wave. This parameter representing the power of the signal being recieved is often the first to suffer the affects from external sources, measuring its affect on the error is critical to understanding the behaviour of the algorithms. A break down of each test detailing the aim of each is below:

$$x_r = A\cos(w_c t + (\alpha x_m)); \tag{4.1}$$

where:

A is the amplitude peak

w_c is the angular velocity of the carrier wave.

t is the time sequence.

α is the phase displacement caused by the vibration.

x_m is the vibration frequency.

- Test 1 - This test varies the peak amplitude of the reflected waveform. Represented by equation 4.1 the element under investigation can be seen as A where the amplitude peak value is being varied from $0.1....10^6$ to allow for behaviour analysis.
- Test 2 - This test varies the peak amplitude of the reflected wave form, introducing a time varying peak amplitude with regard to the reflected wave. Where A is the amplitude peak value calculated by $A = A_t\cos(w_c t)$ with A_t being varied from $0.1....10^6$.
- Test 3 - This test measures the error when the amplitude of the reflected wave is a time varying value from which the peak value is static and the frequency of the amplitudes variation is being varied. Where A is the amplitude peak value calculated by $A = A_t\cos(w_t t)$ with A_t being a static value and w_t representing the different frequencies varying from $0.1...10^6$.

4.4.2 Carrier Frequency Testing

The carrier wave frequency directly relates to the precision of the algorithms. It determines how many times the vibration displacement is sampled and the phase shift imparted onto a cycle of the carriers wave. If the carrier frequency is set too low in comparison to the vibration frequency there is the possibility that the algorithms will measure no phase displacement due to a correlation between the zero crossings of both the carrier and vibration waves.

- Test 1 - This test captures the relationship between vibration frequency and carrier frequency highlighting the values where the accuracy is at it's best and conversly at it's worst. This test is conducted on a unit vibration frequency to show the ratio relationship between the two values. Mathematically the testing being conducted is represented by the w_c attribute in the carrier wave equation being varied between $0.1...10^6$.

- Test 2 - This test identifies the relationship between the carrier frequencies wavelength and the physical displacement of the vibration being measured. The carrier frequency will be a fixed value with the displacement being a fraction of the carriers wavelength represented by $\frac{\lambda}{k}$ where k varies between $0.1...10^6$. Completing this test will identify each algorithms sensitivity to phase shift which relates to the displacement being measured.

- Test 3 - This test identifies the relationship between the carrier frequency and a time varying vibration frequency. This test aims to replicate the effects of potential noise or time varying vibrations as is the case found with most machinery. The carrier frequency will be varied between $0.1...10^6$ hertz to showcase the relationship adequately and the vibration frequency being a time varying signal.

4.4.3 Phase Noise

The phase noise added as part of the environmental affects will be tested by the addition of a static phase offset ranging from 0 to 2π. This will show each algorithms response to a static phase shift applied to the reflected signal. In doing this will highlight each algorithms perfromance to variations in phase.

4.4.4 Waveform samples

This test will analyse the affects of sampling on the error. This has been completed to understand how the error correlates with the number of samples being used to generate the waveforms. This can be related directly with the sampling of a waveform by a microprocessor. To control the manner in which the testing is completed the waveforms have been generated on a number of samples per cycle scheme. This allows for easy modification to the number of samples being used to generate the waveform allowing for assessment of the effects. The samples will be varied between $10^0...10^6$ for a fixed carrier and fixed vibration signal with the error being recorded for analysis.

4.5 Empirical Testing

A test rig assembled for the puposes of recording a reflected waveform will facilitate the empirical testing data collection so that the algorithms can be assessed against real world data. The enclosure will be purpose built to allow for exposure of the wave length to the different environments under test. In order to comply with the scientific method, data will be collected of the generated waveform and the reflected waveform for each variation of test required and each algorithm will use this same data to demodulate allowing for accurate assessment of each algorithms performance. This arrangement will allow for validation of theoretical testing and analysis completed on the behaviour of how the algorithms are affected by interferance to the waveforms.

4.5.1 Experiment Construction Details

Each experiment to be conducted as a part of this research project will target the environmental effects identified by the literature review. These environments are as follows:

- Atmospheric moisture (Rain) - To control the amount of water entering the enclosure a valve will be used to control the water entering the rain attachement of the enclosure. To ensure repeatability through testing the valve will be fed by a head of water situated above the enclosure and filled with enough water to maintain the pressure induced by the head of water.

- Varying Atmospheric pollutents from sand or dust - Atmospheric pollutents will be introduced into the test rig via a hopper filled with sand being fed into a compressed air line blowing into the path of the electromagentic wave.

4.6 Data Analysis Methodology

To focus the testing in a method that will yield a definitive result regarding the impact the variations in environmental conditions and wave parameters have on the results measured; the "analysis of variance" (ANOVA) methodology has been followed. This statistical analysis methodology was chosen above others as it allows for the testing and comparison of multiple variables and results in a variance result indictating the effect each parameter has on the output and can be easily implemented through readily accessible data processing applications such as Excel. (Chandrakantha 2014).

The ANOVA method is a parametric test in the parametric branch of statistical anaylysis known as general linear modelling (GLM) techniques (Sauro 2015). Parametric statistics assumes that sample data comes from a population that can be adequately modelled by a probability distribution that has a fixed set of parameters. To complete the ANOVA analysis parameters affecting the outcome need to be sorted into independent and dependent variables. The below table indicates the breakdown of the variables being tested(Chandrakantha 2014):

Table 4.2: ANOVA Testing breakdown highlighting the dependant variable being investigated with each test.

ANOVA Variable breakdown		
Attribute	Independant Variable	Dependant Variable
Amplitude	Test 1	error
	Test 2	error
	Test 3	error
Carrier Frequnecy	Test 1	error
	Test 2	error
	Test 3	error
Phase Testing	Test 1	error
Sampling	Test 1	error

Comparison of different variables is completed quantitatively by what is know as the F-test. This equation results in a value that represents the relationship between mean values calculated from the samples of the population where the variables were differed allowing the effects of each variable to be determined.

$$F = \frac{VariationbetweenSampleMeans}{Variationwithinthesamples} \tag{4.2}$$

The ANOVA methodology confirms that a parameter is contributing more to the dependant variables result by disproving the "null hypothesis". The null hypothesis dictates that each attributes contribution to the error is equal through calculation of the F value. To disprove this if the F value calculated is larger than the F critical value that represents the value for equal contribution then the hypothesis is proved invalid.

4.7 Resources Required

This project has been broken up into two different testing arrangements in order to have the resources that are required. In order to conduct the computer simulated tests the following has been identified as being needed:

- PC capable of running MATLAB
- Matlab Licence

Similiarily, in order to conduct the physical tests the following items have been identified:

- PC capable of running MATLAB
- Matlab Licence
- Signal generator
- Antenna for transmission of signal
- Antenna for receiving of reflected signal
- AC Motor

- Speaker
- Metallic plate - preferably copper
- Raspberry Pi or similar device for experiments
- Power supply
- Accelerometer for vibration measurement so results can be confirmed
- Construction equipment for building of the enclosure to control environmental parameters
  - Wood for framing
  - Perspex
  - silicon
  - poly pipe
- Various electronic items

4.8 Timeline

In order to ensure completion of this project a timeline has been outlined and the tasks associated have been defined and assigned a certain number of hours believed to be sufficient to allow for completion. The project has been broken up into three main sections and are as follows:

- Research Proposal/Research - relates to the finalisation of the research proposal and the background research into the literature to sufficiently ensure the completion of this research project.
- Experiment and data recording - relates to the experimentation and recording of data as well as the theoretical confirmation of the algorithms that confirms their performance for the experiments. This portion of the project represents the main body of work associated with the project.
- Analysis and Conclusions - The results from the experiments will be analysed and drafted into the report ready for finalisation before submission. This will conclude the project and will signify the completion of the research.

The project has been further broken down into sub tasks and milestones to ensure completion of each portion of the project in a controlled manner.

- Research Proposal/Research
  - Literature Review - This portion of the project relates to the review of existing literature
  - Project Goals - This portion is allocated to the confirmation and determination of project goals.
  - Experiment Design - On completion of this portion of the project the experiments will be finalised and ready for construction.
  - Resource Identification - This portion of the project is reserved for the identification and acquiring of resources.
- Experiment and Data Recording

  - Development of Algorithms - This phase of the project relates to the development of the algorithms that are being tested.
  - Confirmation of Algorithms Performance - This phase of the project is related to the testing of the developed algorithms to ensure their functionality.
  - Building of Test Rigs - This part of the project is reserved for the construction of the test rigs.
  - Experiments - This portion of the project is reserved for carrying out the tests and recording of data.
  - Completion of Experiments with data recorded - This is a milestone that signifies the completion of stage two of the project.

- Analysis and Conclusions
  - Review of data and conduct analysis - The portion of the project is reserved for the review and analysis of the collected data.
  - Develop Conclusion based on data - In this part of the project the conclusions will be developed based on the results from the data.
  - Finalise report and provide recommendations - This part of the report will serve to finalise the report and develop the recommendations based on the data collected.
  - Submission of Research Project - This is a Project Milestone that signifies the completion of the Research Project.

See the ghant chart in appendix C for a graphical break down of the project, The project began on February the 20th and is set to be completed on the 16th of October, these are subject to change once confirmed.

4.9 Timeline Limitations

Because this research project is a final year graduate project associated with a bachelor degree, it is required to be completed over eight months, approximately two standard schooling semesters. This time constraint creates strain on the scope that can be covered by this research project. Because of this, this research will only focus on the algorithms discussed previously and the key performance factors of each of those algorithms, other

aspects that may affect the performance of the algorithms, whilst they may be mentioned, will not be explored in detail.

Chapter 5

Test Data Creation

This project involves the testing of each algorithm against a generated data set. The testing and creation of the algorithms for this portion of the project is to be completed in MATLAB. MATLAB was chosen as the development environment because of its ability to handle complex operations and its signal processing strengths. In addition MATLAB is also accompanied by a detailed support manual to allow for understanding in its use and tools. Creation of the waveforms has been acomplished in the manner prescribed in (Leis 2018) which details a sample program for the creation of a phase modulated wavelength.

For each algorithm being tested the generation of the carrier wave, reflected wave and quadrature signals does not differ and are covered below ahead of the sections detailing the algorithms operations.

5.1 Creation of Carrier Wave

The waveform simulating the carrier wave is created through the standard circular wave function of:

$$x_c = A_c \cos(2\pi f_c t) \tag{5.1}$$

Where:

x_c is the carrier wave

A_c is the Amplitude of carrier wave

f_c is the frequency of oscillation of the carrier signal

t is the time sequence

For the simulation the amplitude of the waveform has been set to a magnitude of one to aid in interpretation of results and the time has been set from zero to twenty seconds. In creation of the digital signal in MATLAB the signal is generated through calculation of its points at alloted sample intervals. To ensure enough accuracy in the waveform creation is present, the number of samples per cycle needs to be set so that the wave is modelled correctly and the phase shift detected efficiently. To determine the appropriate number of points per cycle testing will be completed to review the impact to error that is present and a value chosen that minimises the effect.

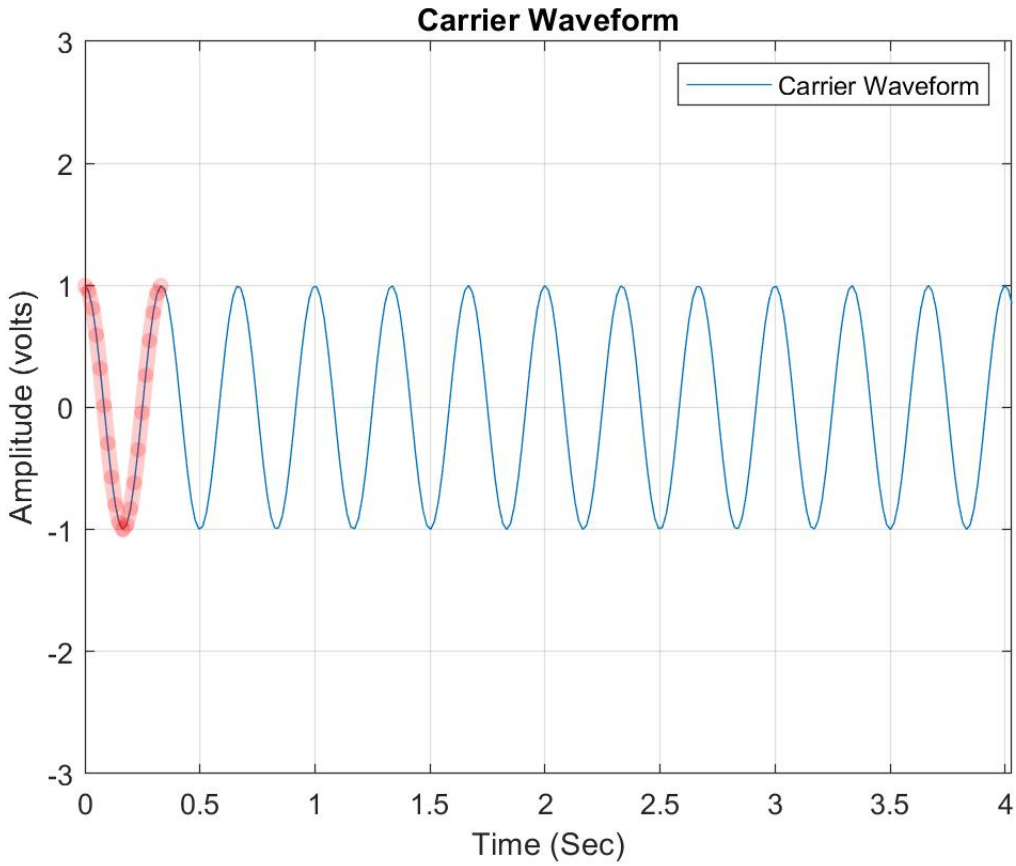

Figure 5.1: Carrier wave with sampling points highighted showing construction of sinusoidal wave

To faciliate the theoretical testing in the MATLAB environment a frequency of twenty

hertz was chosen for the carrier wave as this allowed for clear visibility of the waveform features in plots and should not affect the theorised outputs of the tests. The figure below demonstrates twenty hertz over three seconds.

For the theoretical testing the values chosen for the creation of the carrier wave are summarised below:

Table 5.1: Parameters used in construction of Carrier wave

Variable	Value
A_c	1
f_c	20
t	0...3

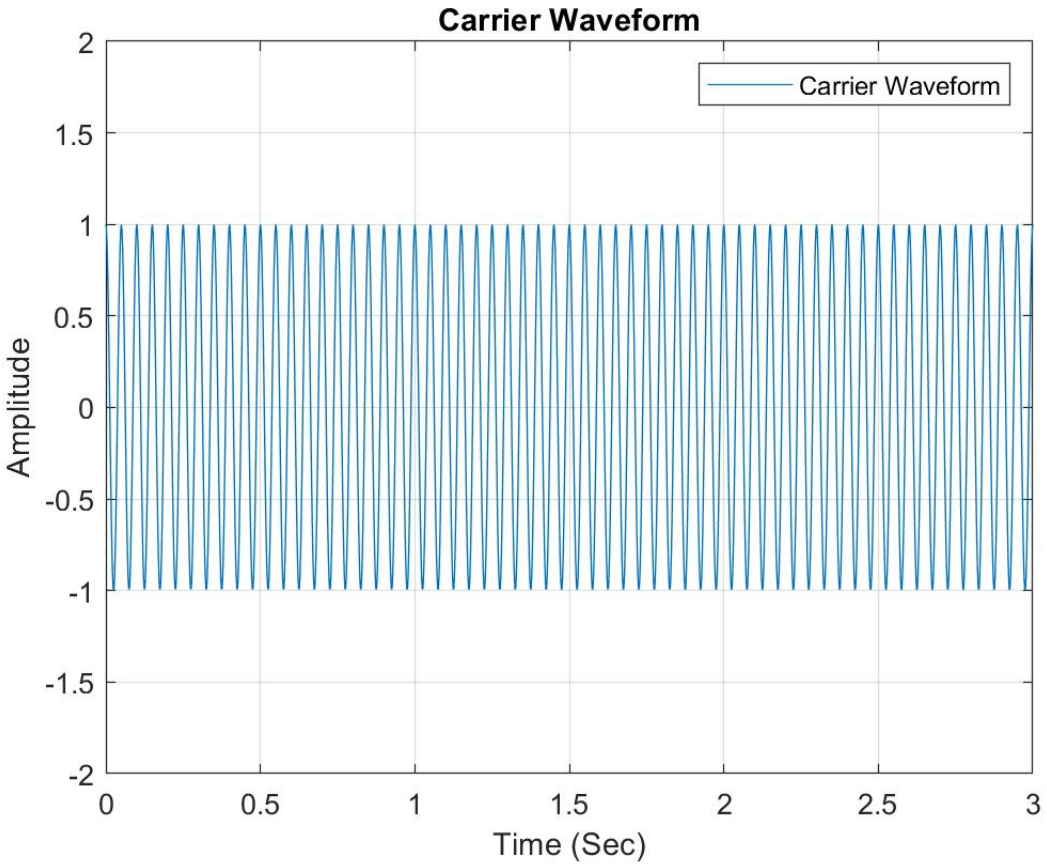

Figure 5.2: Carrier waveform used in theroretical tests shown across full time scale

5.2 Creation of Reflected Wave

Creation of the phase shifted reflected wave in MATLAB has been generated using the additive noise model (Leis 2011).

$$x_r(t) = x_c(t) + \alpha x_m(t) \tag{5.2}$$

Where:

$x_r(t)$ is the observed phase shifted signal

$x_c(t)$ is the underlying periodic signal (Carrier wave)

α is the amount of additive noise (i.e the maximum phase shift)

$x_m(t)$ is the time varying noise signal

Use of the above model allows for a time differing phase shift to be applied to the carrier for the algorithms to extract. The time varying signal $x_m(t)$ can be seen implemented in the figure below. The mathematical function used for its generation is:

$$x_m(t) = A_m \sin(w_m t) \tag{5.3}$$

Where:

A_m is the amplitude of the vibration

w_m is the frequency of the vibration

t is the time sequence

For the theoretical testing the values chosen for the creation of the vibration wave are summarised below:

Table 5.2: Parameters used in construction of the vibration profile wave

Vibration Wave variables	
Variable	Value
A_m	1
w_m	1
t	0...20

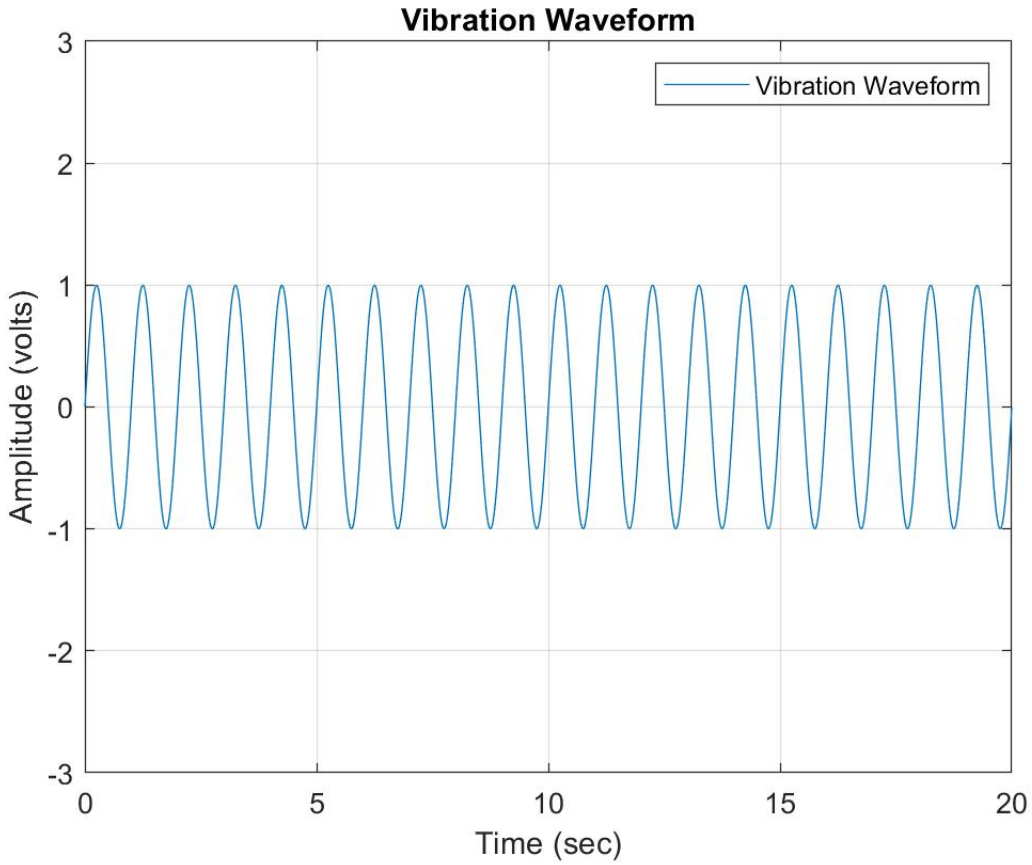

Figure 5.3: Time varying vibration wave

Using the additive noise equation 5.2 the reflected wave has been generated and the resultant waveform can be seen in the figture below.

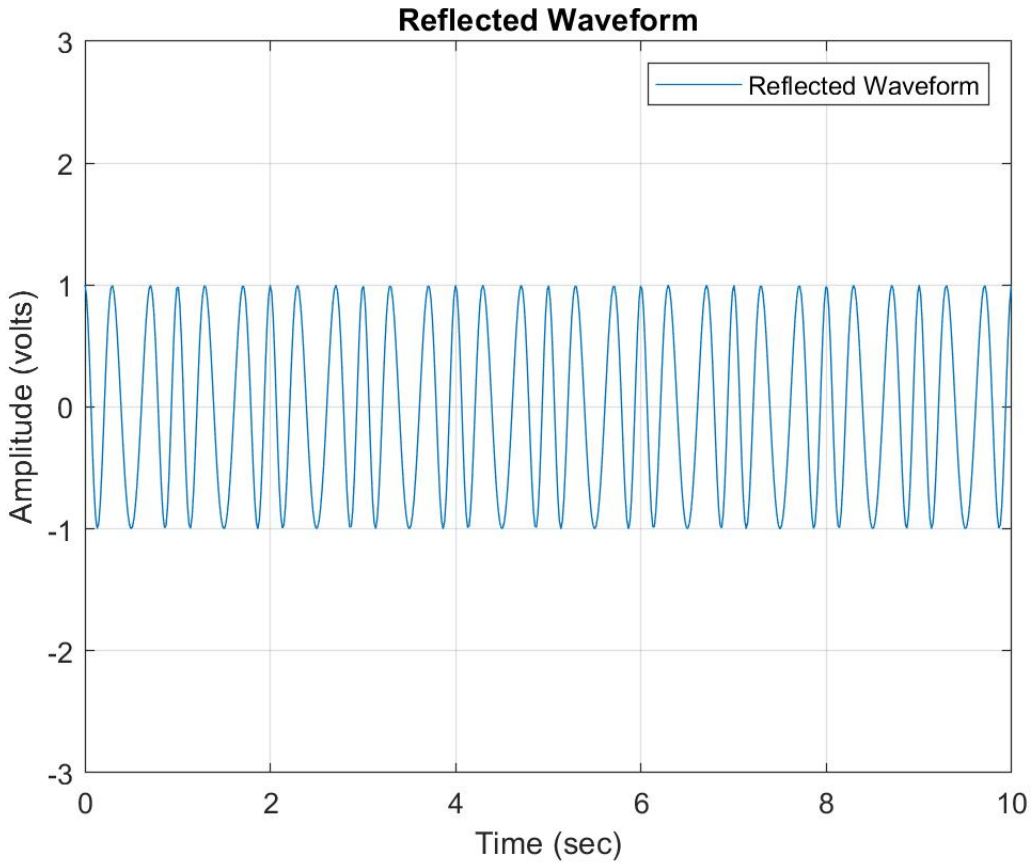

Figure 5.4: Reflected waveform modulated with vibration

5.3 Quadrature Signal I and Q generation

Creation of the quadrature signals in MATLAB has been facilitated by the multiplication of the reflected wave with both the in phase and the phase shifted carrier signal (Leis 2018).

$$I(t) = \cos(w_c t) x_r(t) \tag{5.4}$$

$$Q(t) = \sin(w_c t) x_r(t) \tag{5.5}$$

Where:

$I(t)$ is the in phase quadrature signal

$Q(t)$ is the out of phase quadrature signal

w_c is the carrier wave frequency

$x_r(t)$ is the reflected waveform

t is the time sequence

The result of equations 5.4 and 5.5 the creation of the quadrature waveform can be seen in the figure below:

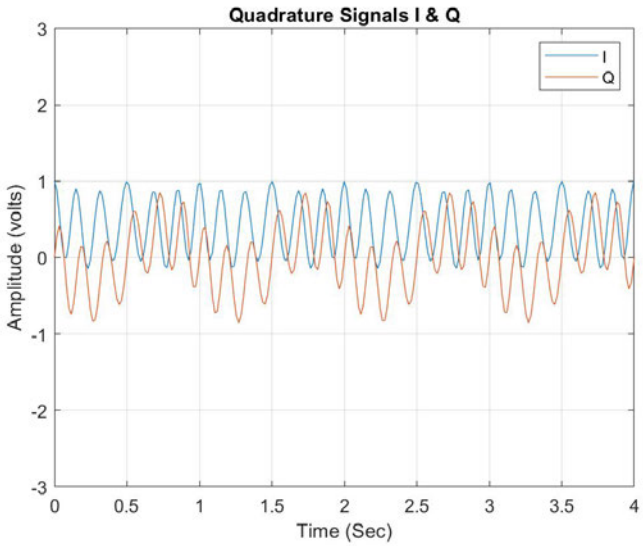

Figure 5.5: Quadrature I and Q signals plotted on single graph

5.3.1 Filtering applied

The successful operation of the algorithms is dependant on the clarity of the generated I and Q signals. The creation process for these two signals creates high frequency noise on the resultant wave. This noise was proven to impact the accuracy of the algorithms demodulated output, to combat the high frequency noise a low pass filtering operation was introduced to the algorithms that averaged out the values over the period of one cycle of the carrier wave.

5.4 Creation of Algorithms

5.4.1 Arctangent Phase Demodulation

The implementation of the arctangent demodulation algorithm was achieved through the use of the built in MATLAB function "atan". This function was used instead of the "atan2" MATLAB function as the "atan2" built in function operates in all four quadrants of the unit circle domain as opposed to the standard arctan which is constrained by the codomain restriction(Leis 2018).

The arctangent calculation has also been multiplied by -1 to introduce a $180°$ phase shift to the resultant waveform. This negates the phase shift applied to the calculated result by the algorithms processing.

The displacement measured and calculated is extracted from the waveform and compared to the known displacment and the error is presented. See the below figure for the results of the arctangent algorithm with a displacement of $\lambda/4$ which translates to a phase shift of $\frac{4\pi\frac{\lambda}{4}}{\lambda} = 1.57rad$ applied.

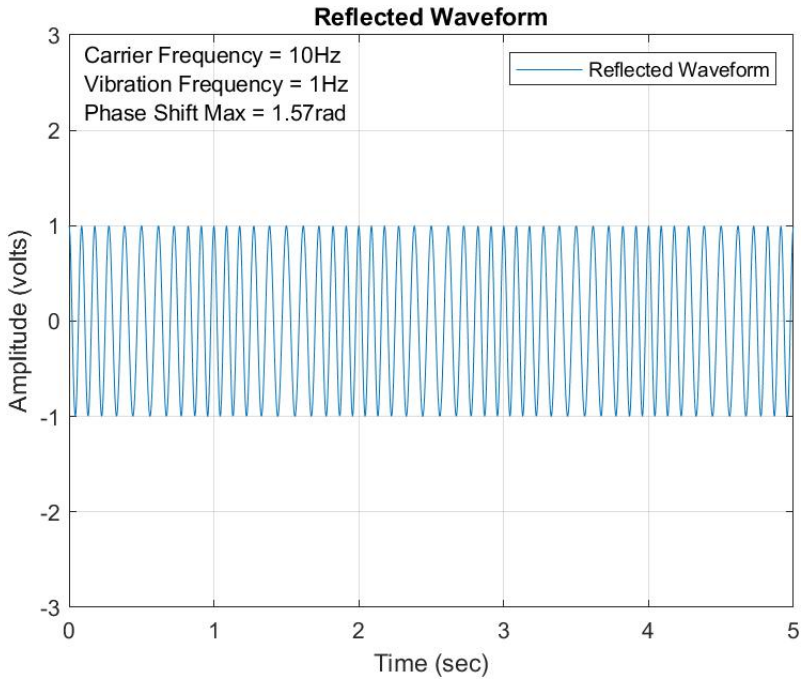

Figure 5.6: The above figure depicts the recieved waveform reflected off of the vibrating object

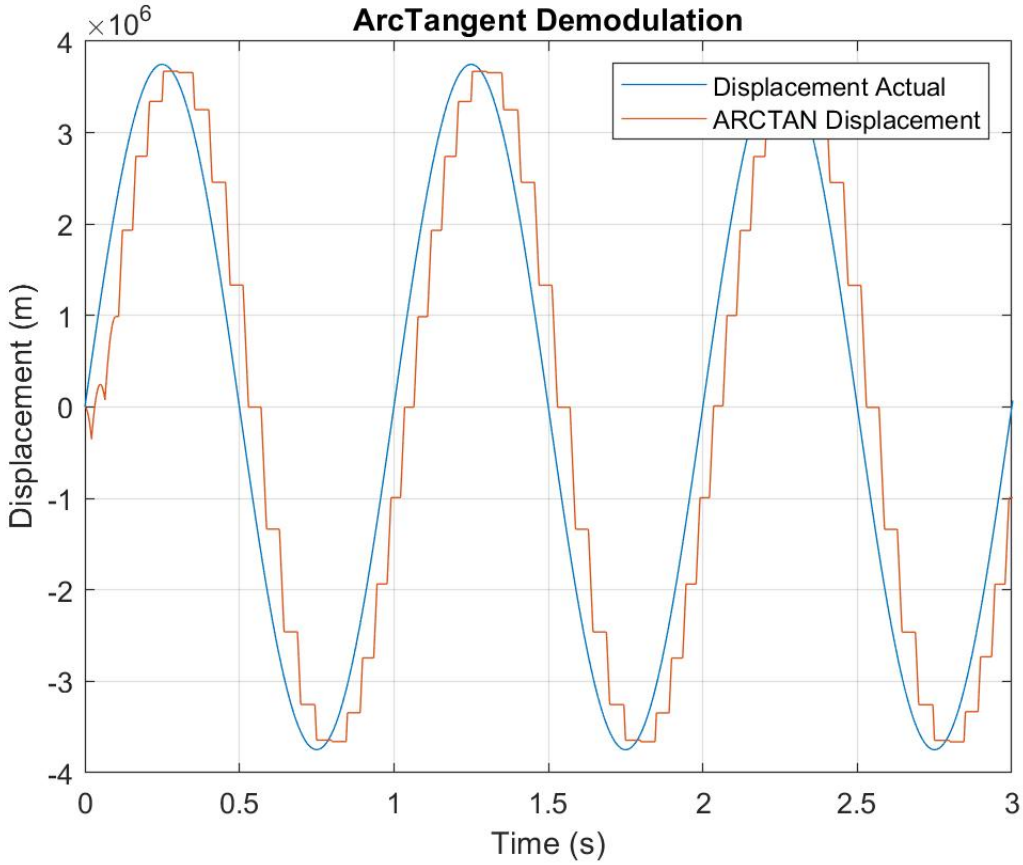

Figure 5.7: Resultant displacement calculated by Arctangent algorithm

The quantized appearance of the waveform is directly related to the filter applied and the carrier frequency being used. The carrier frequency will be varied to reduce any quantisation error introduced. The MATLAB code created for the arctangent algorithm can be located in appendix.

5.4.2 Extended Differentiate and Cross Multiply - EDACM

The implementation of the EDACM algorithm has been achieved through vectorised computations allowing for improved efficiency in the processing of the EDACM algorithm. This algorithm is considered computationally straining and this approach mitigates the perfromance impact.

After the I and Q signals have passed through the filtering stage the differentiation and cross multiply portion of the algorithm is implemented which creates the angular velocity signal w, accumulation of this signal is carried out to determine Φ the phase shift present

in the reflected signal, the mathematical functions and figures shown below represents these operations.

$$\omega(k) = \frac{I(t)(Q(t) - Q(t-1)) - Q(t)(I(t) - I(t-1))}{I(t)^2 + Q(t)^2} \tag{5.6}$$

$$\Phi(n) = \sum_{k=2}^{n} \omega(k) \tag{5.7}$$

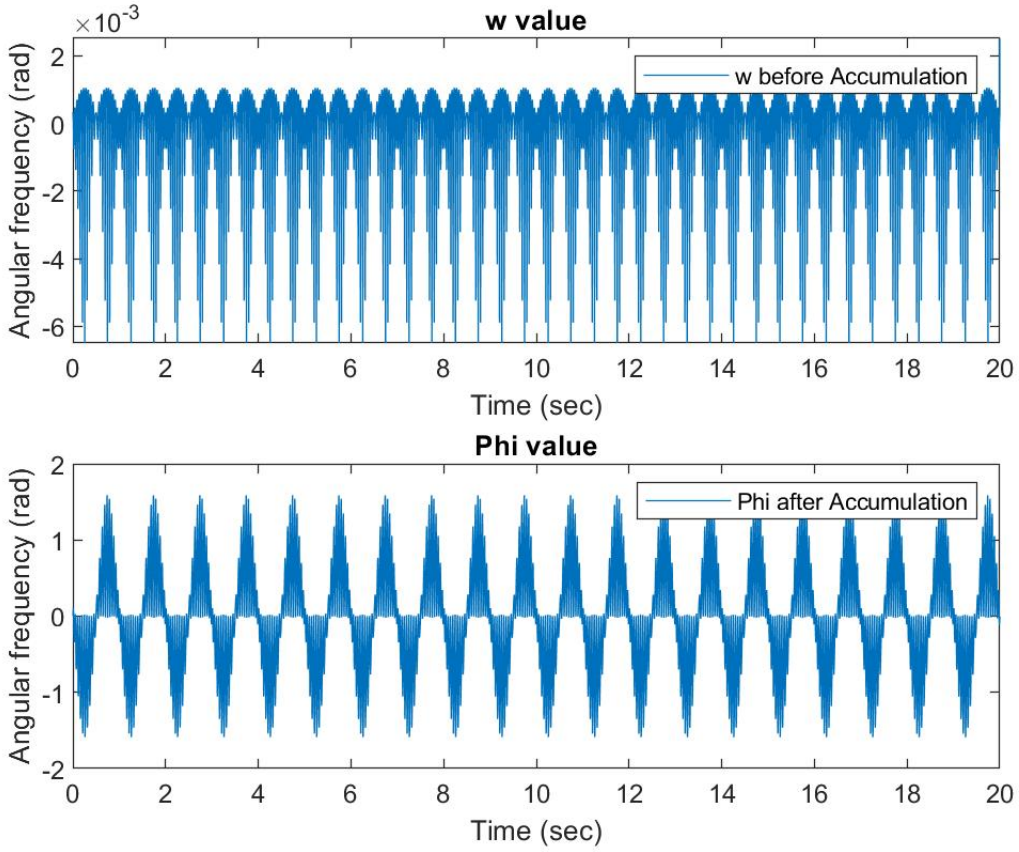

Figure 5.8: Waveforms showing raw output of the angular velocity signal w and the subsequent accumulated output Φ.

From the accumulated value Φ the displacement can then be calculated. The output of the algorithm plotted against the original vibration can be seen below.

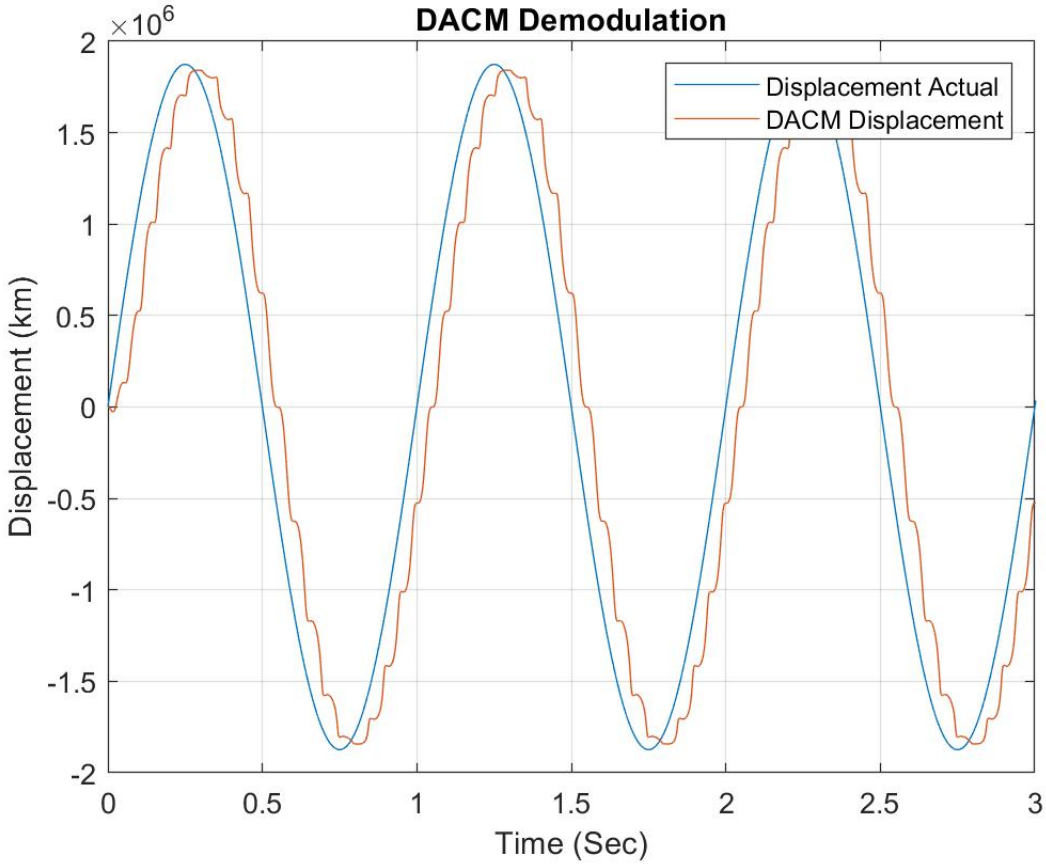

Figure 5.9: Waveforms EDACM algorithm output plotted against the known vibration waveform.

5.4.3 Modified Differentiate and Cross Multiply - MDACM

The MDACM algorithm operates in a similar manner to the EDACM algorithm in that the algorithm takes the derivative of the I and Q signals to extract the phase shift imparted from the vibrating body. Unlike the EDACM algorithm the MDACM algorithm applies the differentiation directly to the quadrature signals I and Q rather than the arctan operator (Zhang, Fu, Zhuang, Yang, Ding, Hong & Zhu 2022). This results in the following equation representing the angular phase shift:

$$\Phi(t) = (I(t)Q'(t)) - (Q(t) - I'(t)) \tag{5.8}$$

With the physical displacement being calculated by (Zhang et al. 2022):

$$x(t) = \frac{\lambda}{4\pi} \int [I(t)Q'(t) - Q(t)I'(t)] \tag{5.9}$$

The literature covering this algorithm indicates that similar performance to the EDACM algorithm can be achieved. When implementing the algorithm as depicted the results detailed in the literature were not able to be recreated, as can be seen below with the demodulated output matching the vibration source in frequency but not amplitude, with the resultant displacement being heavily attenuated.

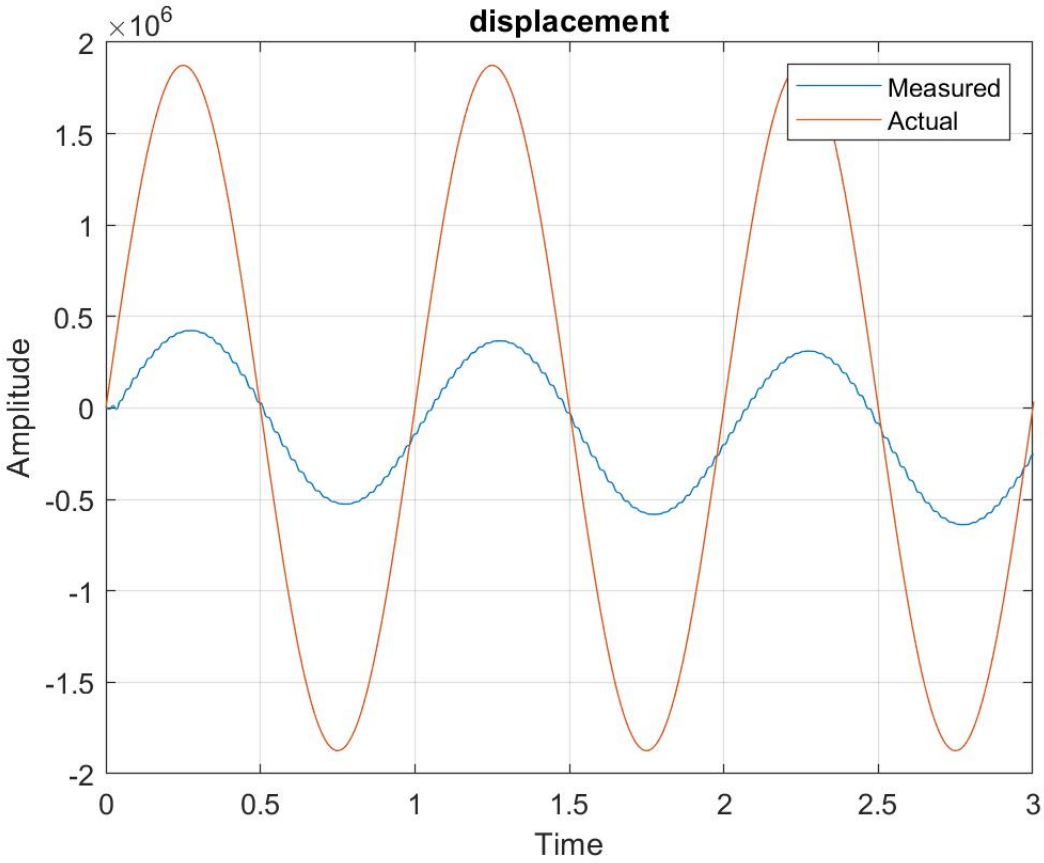

Figure 5.10: MDACM algorithm's output plotted against the known vibration waveform.

Through testing it was found that adjusting the extraction factor of $\Phi\frac{\lambda}{4\pi}$ to $\Phi\frac{\lambda}{\pi}$ resulted in a less attenuated signal being extracted.

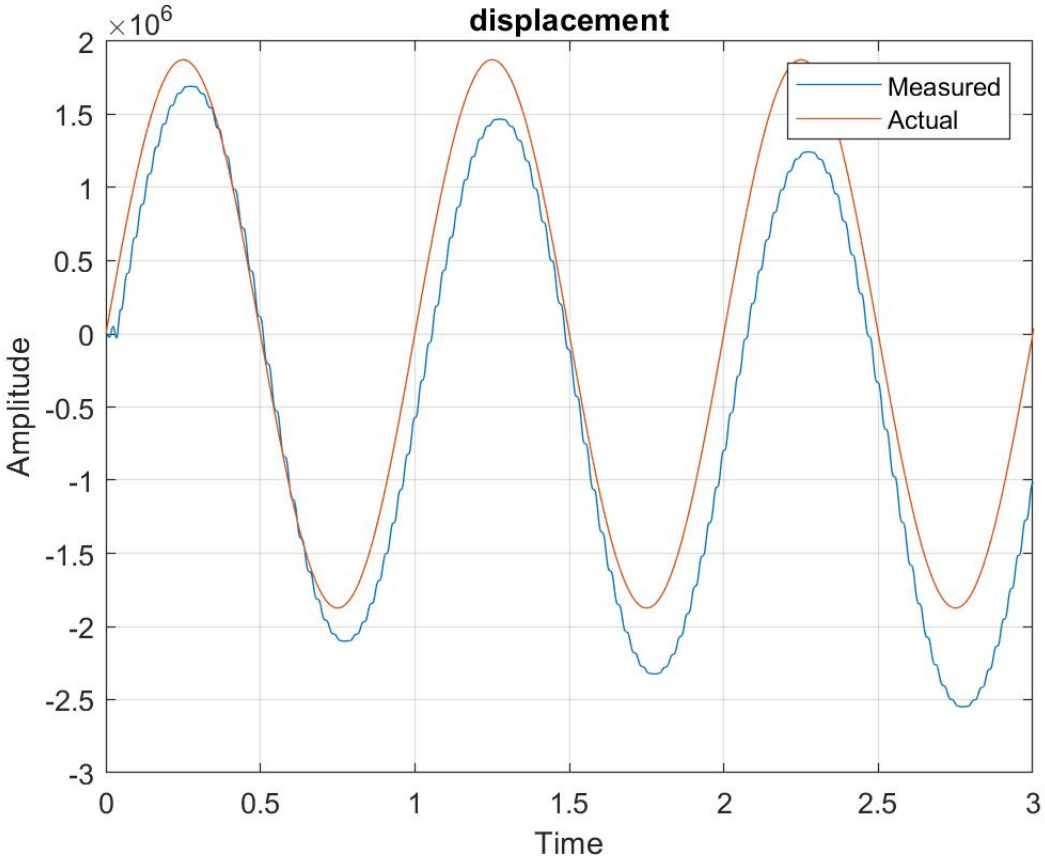

Figure 5.11: MDACM demodulation using $\Phi\frac{\lambda}{\pi}$

This signal now created shown above contained a decaying DC shift. This was mitigated by calculating the mean value for the waveform and subtracting it from the waveform to produce the resultant wave below.

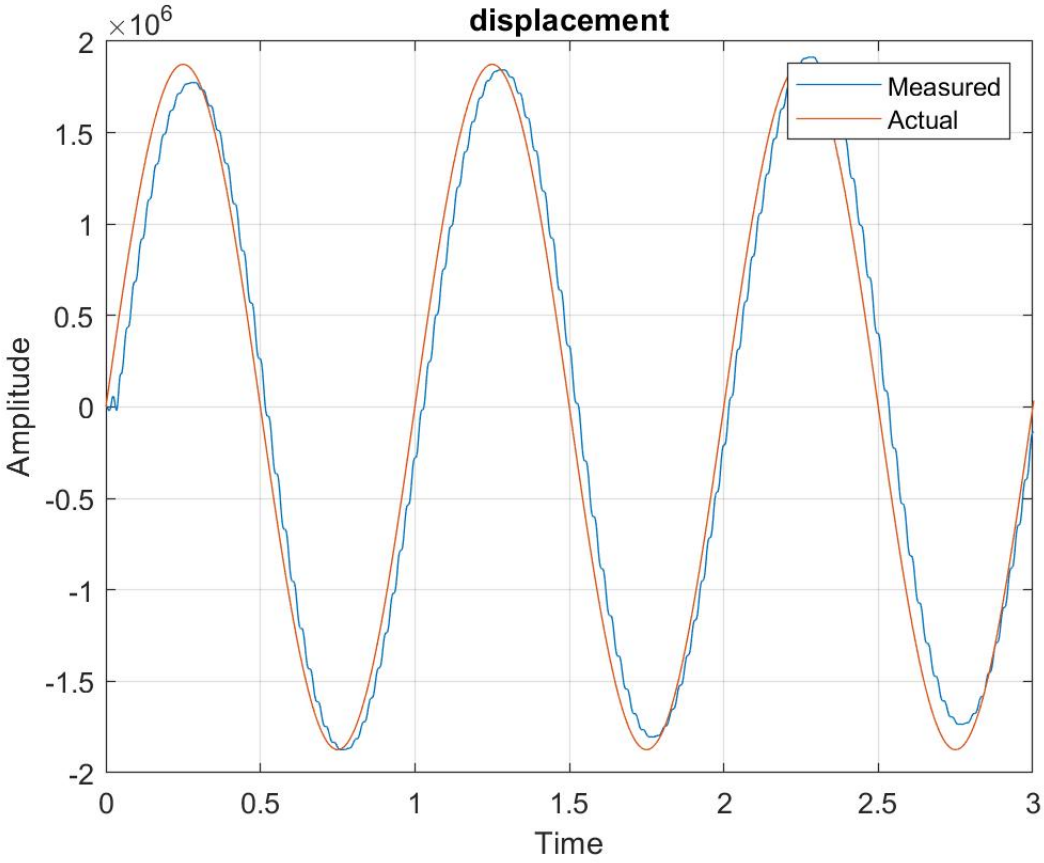

Figure 5.12: MDACM demodulation using $\Phi\frac{\lambda}{\pi}$

The testing carried out on the MDACM algorithm will be carried out on the algorithm as dipicted in the literature available. The exploration completed above was carried out in an attempt to achieve the results detailed in the literature.

The resultant mathematical representation for the MDACM algorithm for this paper is as follows:

$$x(t) = \frac{\lambda}{4\pi} \int [I(t)Q'(t) - Q(t)I'(t)] \tag{5.10}$$

Chapter 6

Theoretical Testing Results

This section details the results obtained from the tests outlined in the methodology. The section has been presented so that each algorithms performance in a particular test has been reviewed before the next test is presented.

6.1 Amplitude Testing

The amplitude testing of each algorithm will involve the variation of the amplitude attribute whilst the other attributes are fixed this allows for the analyses of the amplitudes affect on the resultant demodulated output.

6.1.1 Test 1 - Static Peaks of different Amplitudes

This test varies the peak amplitude of the reflected waveform. Represented by the following equation, the element under investigation can be seen where:

$$x_r = A\cos(w_c t + (\alpha x_m)) \tag{6.1}$$

where:

x_r is the reflected waveform

A is the amplitude peak varied from 0.1....10^6

w_c is the angular velocity of the carrier wave.

t is the time sequence.

α is the phase displacement caused by the vibration.

x_m is the vibration frequency.

ARCTAN Results

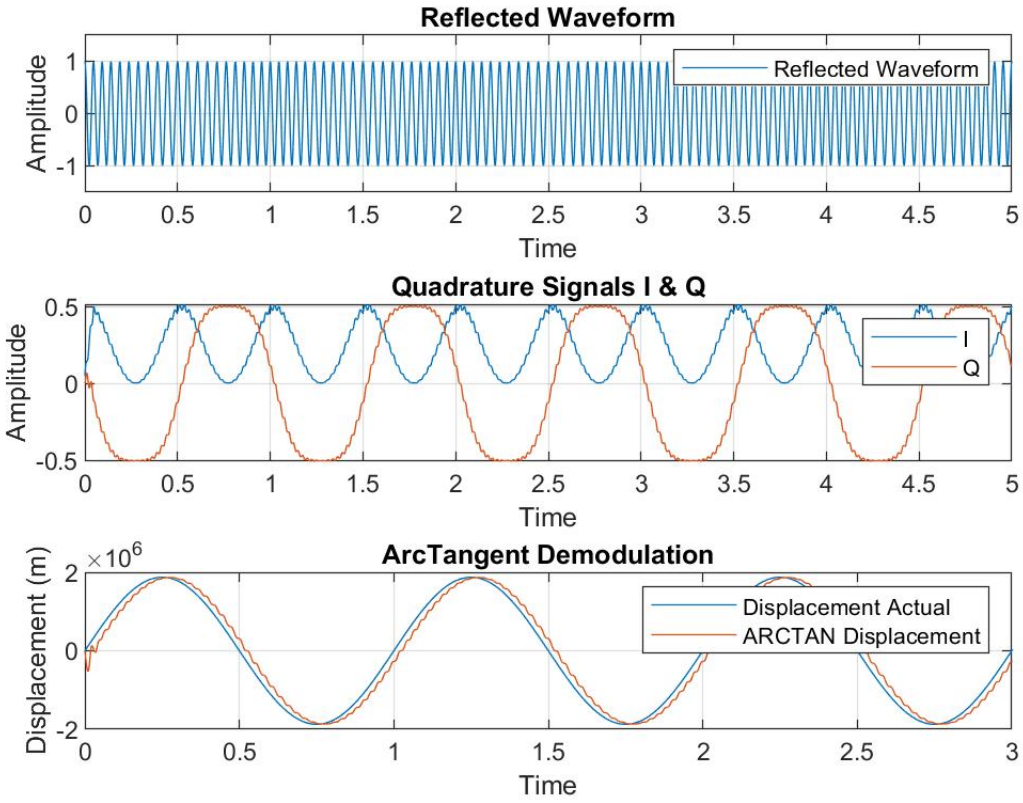

Figure 6.1: The results of the arctangent algorithm with Test 1

The resultant waveforms from the test can be seen above, with the results across the range of testing seen in the figure below. When the amplitude of the reflected wave is differed, either caused by attenuation of amplification, there is no additional effect on the accuracy of the algorithms demodulation. With the error remaining constant at 10.694%

indicating an accuracy of 89.306%. This would imply that the algorithm is capable of handling standard attenuation of the signal stemming from environmental conditions. It can be further summarised that the error that is present is the result of a combination of the remaining attributes to be tested.

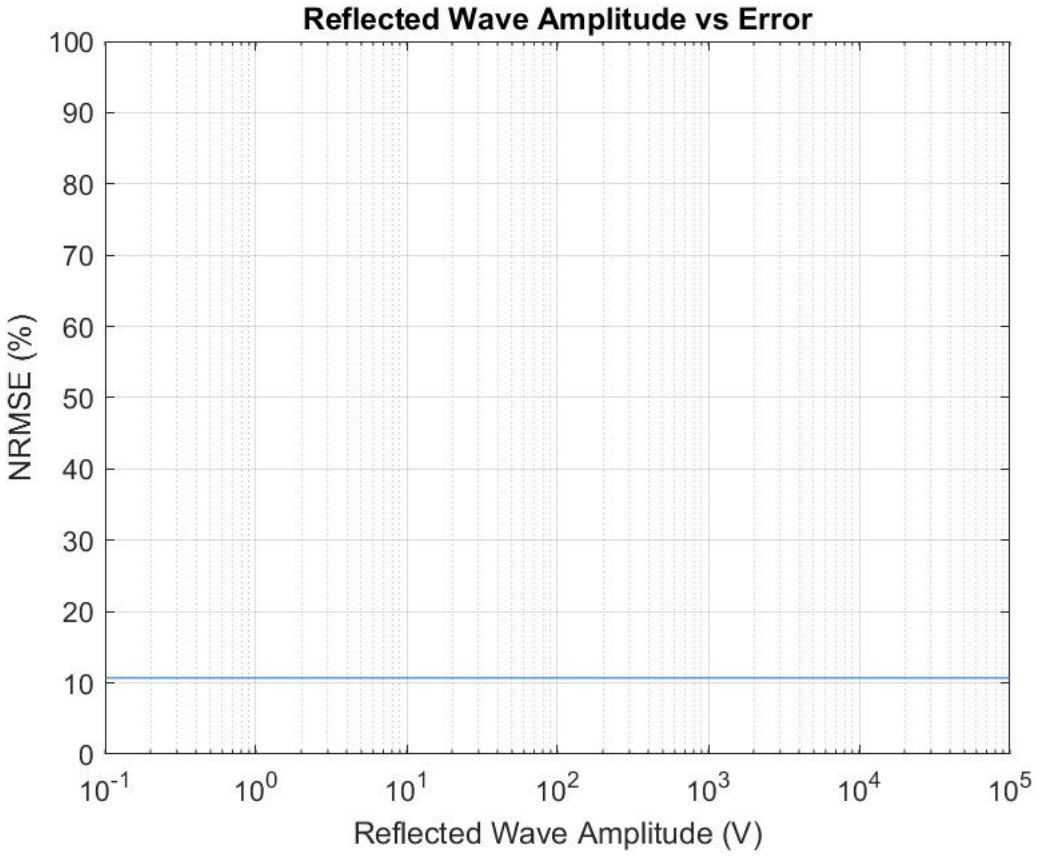

Figure 6.2: Arctangent results showing error when the static peak amplitude of reflected wave is modified

EDACM Results

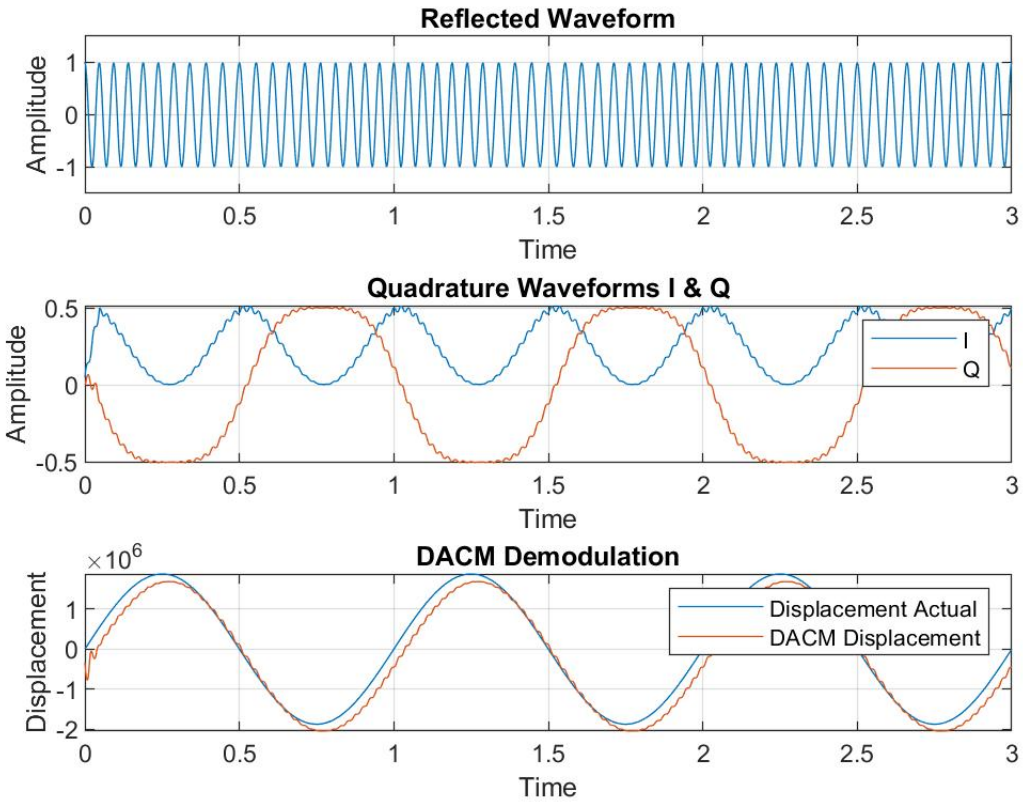

Figure 6.3: EDACM waveforms generated from Test 1

Similar to the arctangent results the EDACM algorithm is resilient to variations in the peak amplitude derived from attenuation or amplification from external environmental conditions acting on the waveform. The EDACM experienced an error of 13.7009%. An error of 13.7009% correlates to an accuracy of 86.2991%.

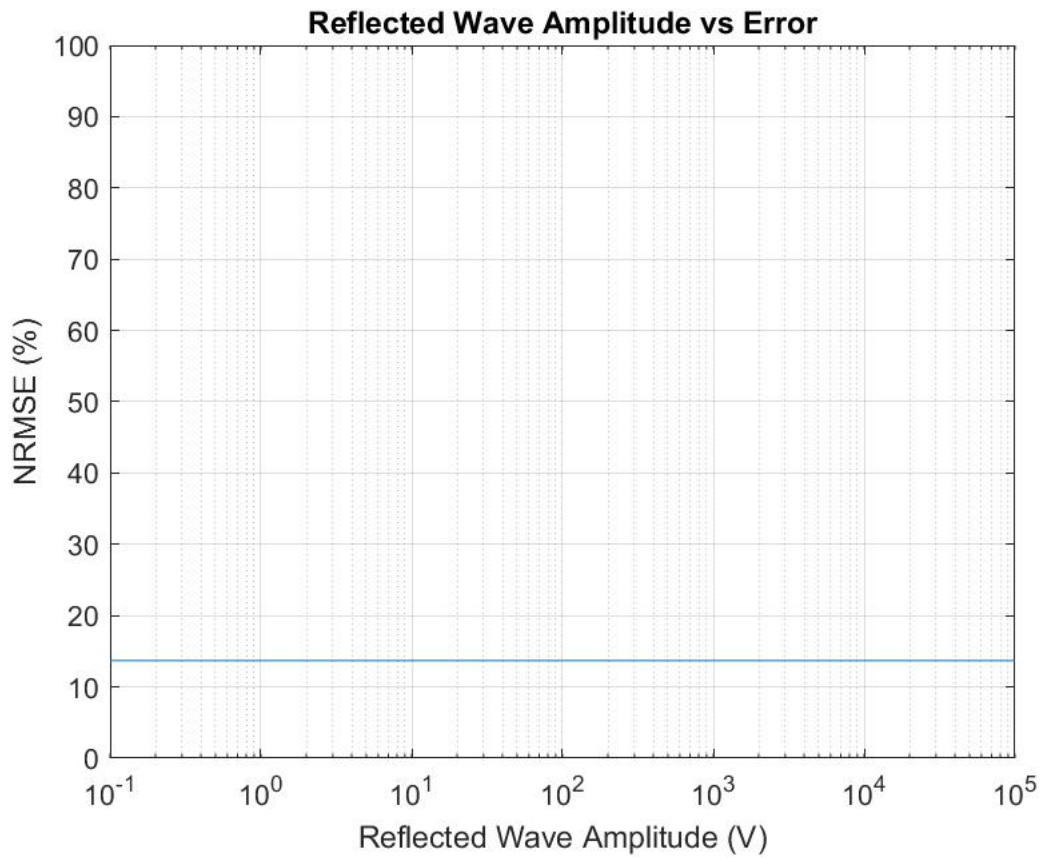

Figure 6.4: Differentiate and cross multiply results showing error when the static peak amplitude of reflected wave is modified

MDACM Results

The results recorded for the MDACM algorithm indicate that it is particularly suceptible to attenuation/amplification of the reflected signal when compared to the carrier signal.

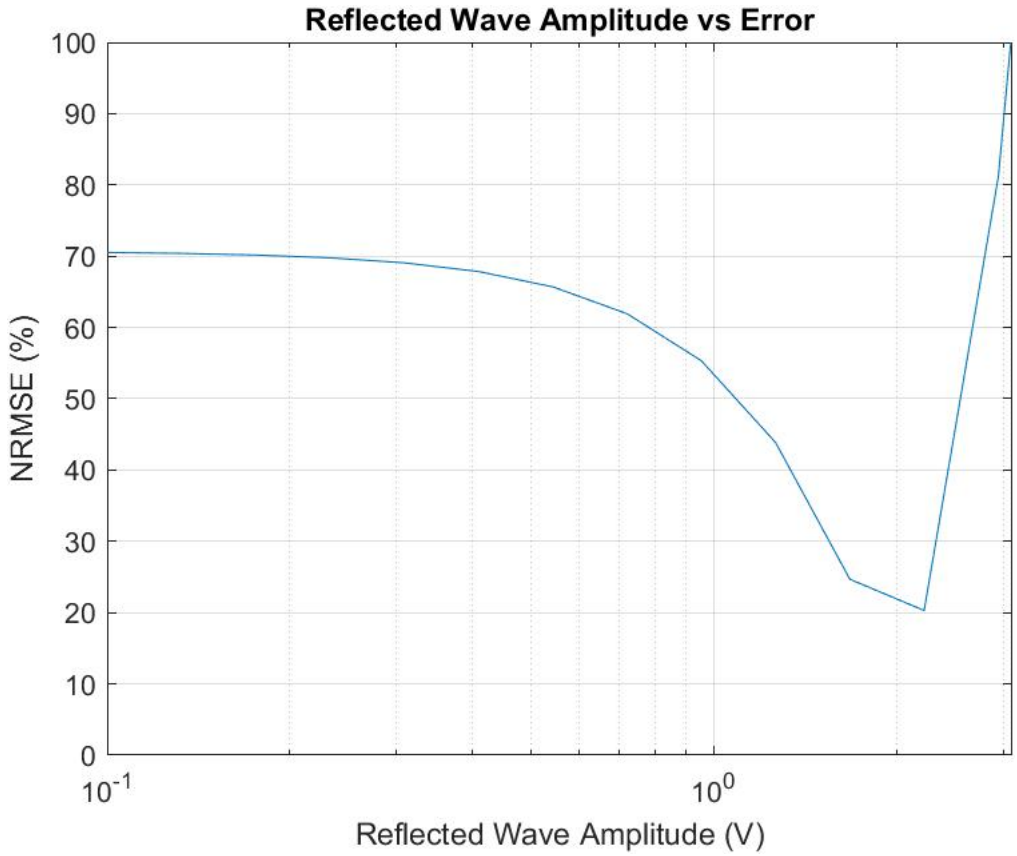

Figure 6.5: MDACM results showing error when the static peak amplitude of reflected wave is modified

The results show that the error is at its lowest when the amplitude of the reflected wave is roughly double that of the carrier frequency. The signals of the MDACM algorithm can seen below when the reflected signals amplitude is double that of the carriers amplitude.

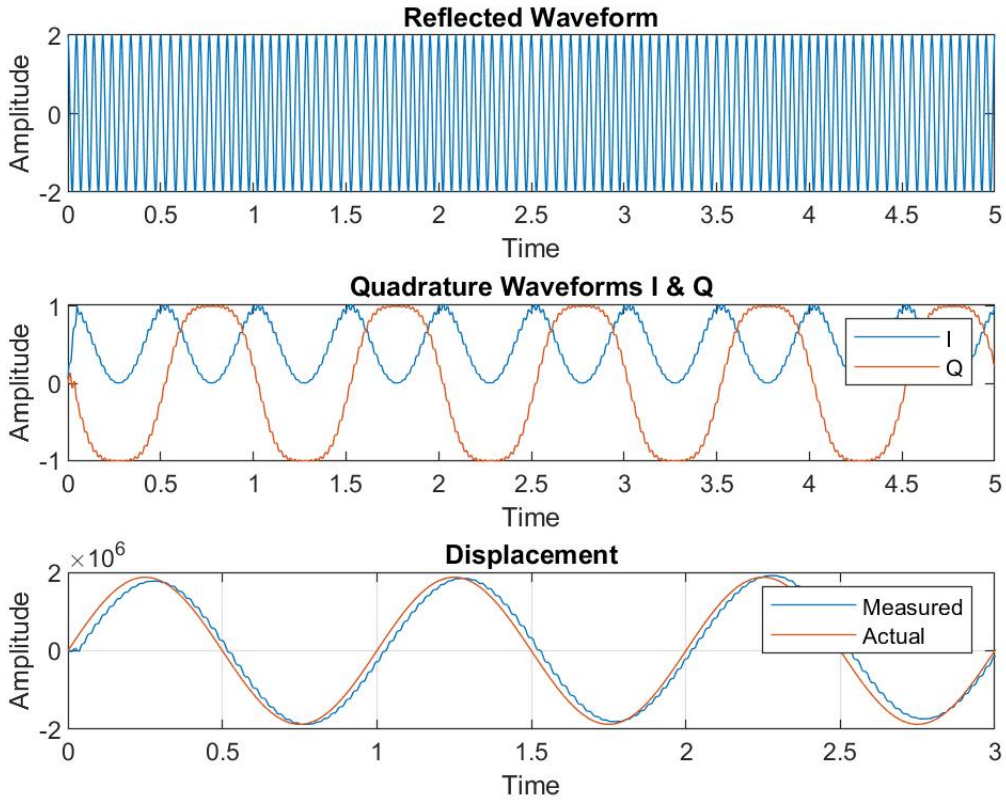

Figure 6.6: MDACM waveforms when reflected signal's amplitude is double that of the carriers.

6.1.2 Test 2 - Static Peaks of different Amplitudes varying with time

This test varies the peak amplitude of the reflected wave form, introducing the affects of a time varying peak amplitude with regard to the reflected wave. Where A is the amplitude peak value calculated by $A = A_t \cos(w_c t)$ with A_t being varied from $0.1....10^6$.

ARCTAN Results

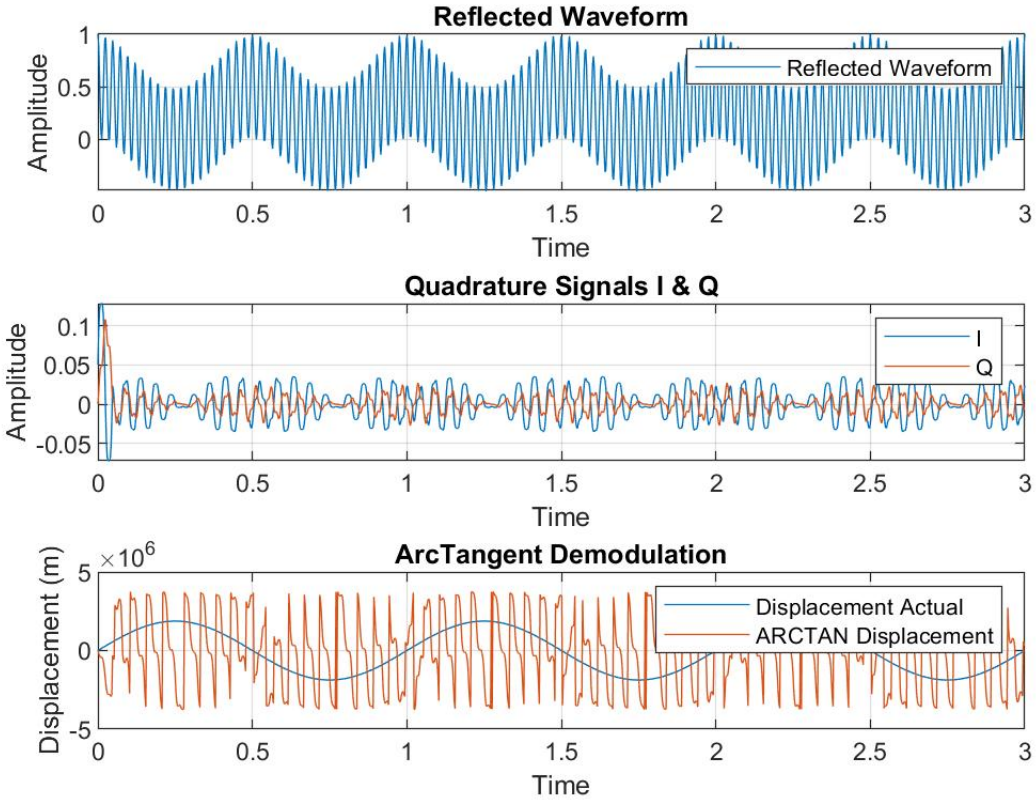

Figure 6.7: Arctan waveforms of Test 2

When the peak amplitude of the reflected wave is being varied with relation to time, i.e changing the value of the peak amplitude of the reflected waveform. The error introduced into the resultant demodulated output is significantly larger, but remains constant at different levels of attenuation or amplification as seen in the figure below. This indicates that the accuracy of the arctangent algorithm is suceptible to frequency shifts of the time varying amplitude peaks but not changes to the actual peak amplitude.

The demodulated output of the algorithm is being driven outside of the codomain range of arctan as is visible above indicating that any cyclic oscillation of the amplitudes peak value translates to added phase shift through the algorithm.

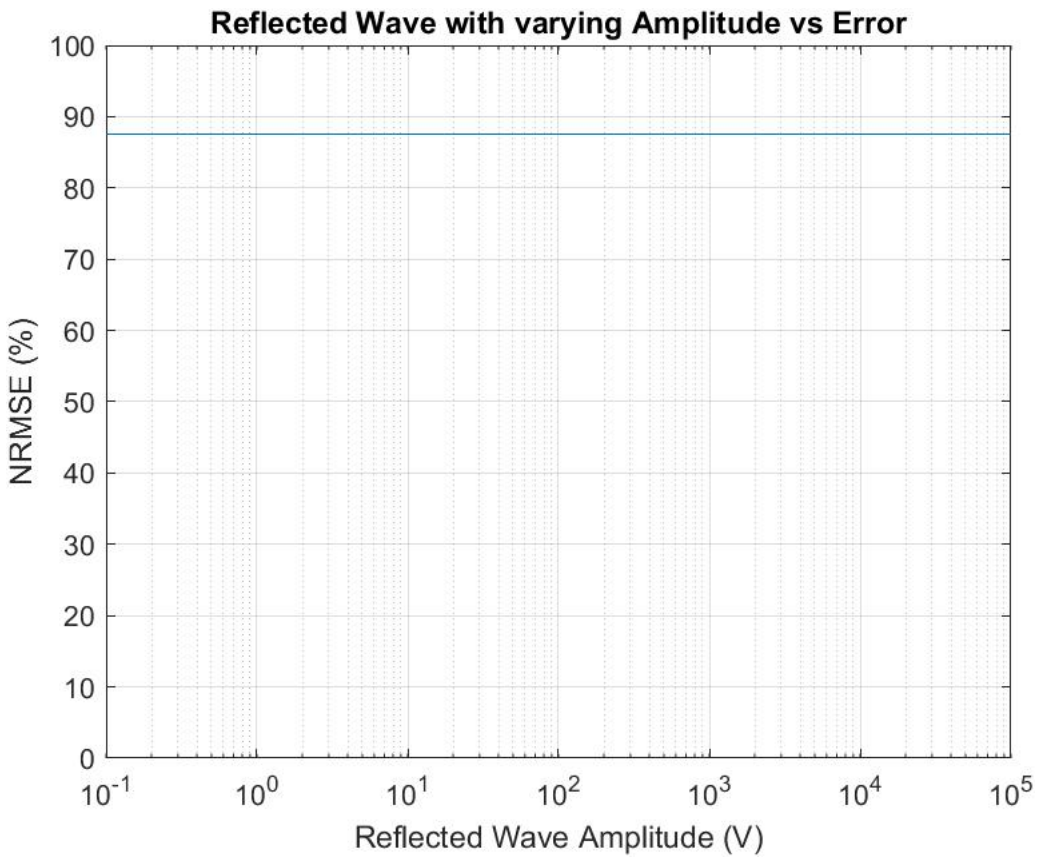

Figure 6.8: Arctangent results showing error when the peak amplitude of reflected wave is Time Varying

EDACM Results

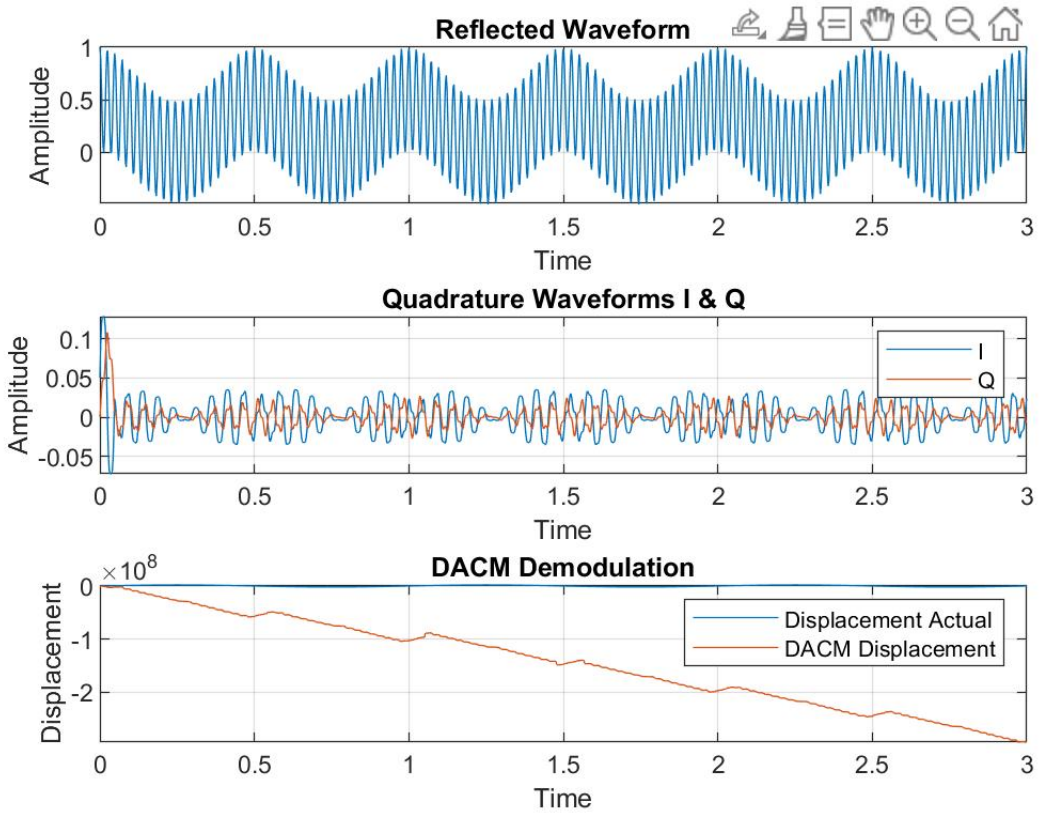

Figure 6.9: DACM waveforms generated by the completion of Test 2

The EDACM algorithm shows similar results to the arctangent algorithm when the amplitude is time varying. As can be seen in the figure below the error has increased significantly with the expected error averaging around 12861% indicating that the EDACM algorithm is highly suceptible to cyclic oscillation of the amplitudes peak value.

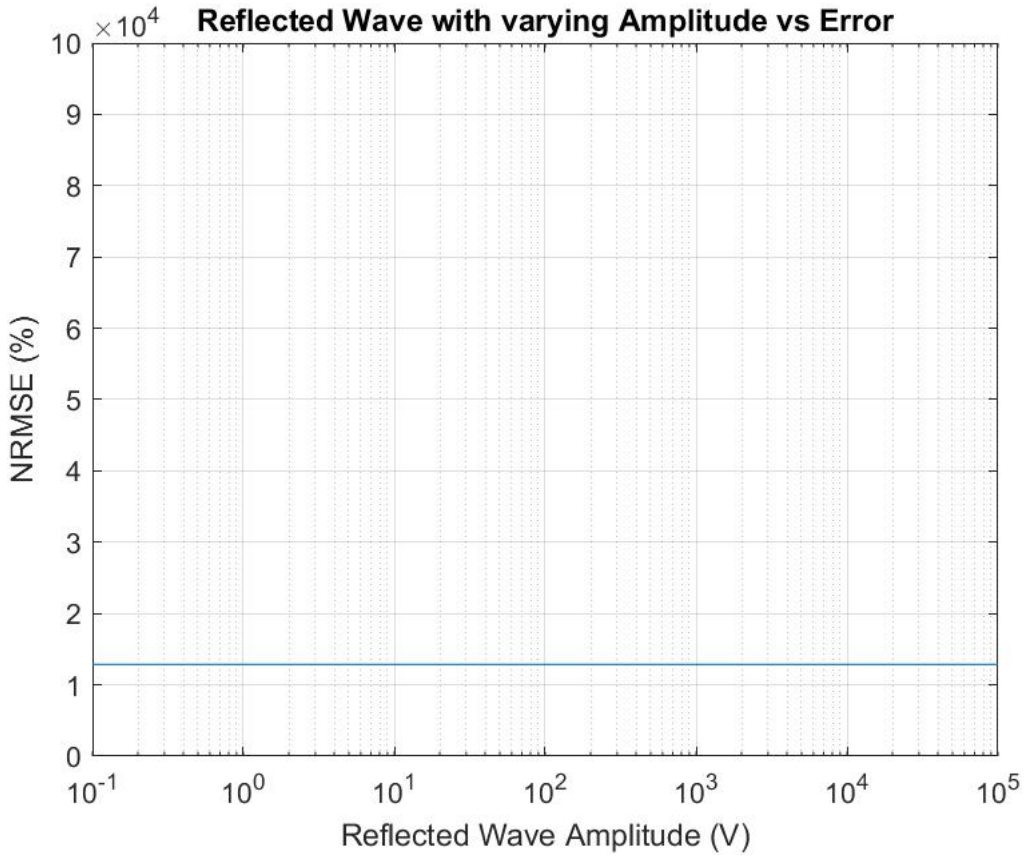

Figure 6.10: EDACM results showing error when the peak amplitude of reflected wave is Time Varying

MDACM Results

The results obtained from the MDACM's performance with a time varying amplitude on the reflected signal resemble that of the results obtained in the first test in that it is highly suseptible to noise affecting the amplitude of the reflected signal.

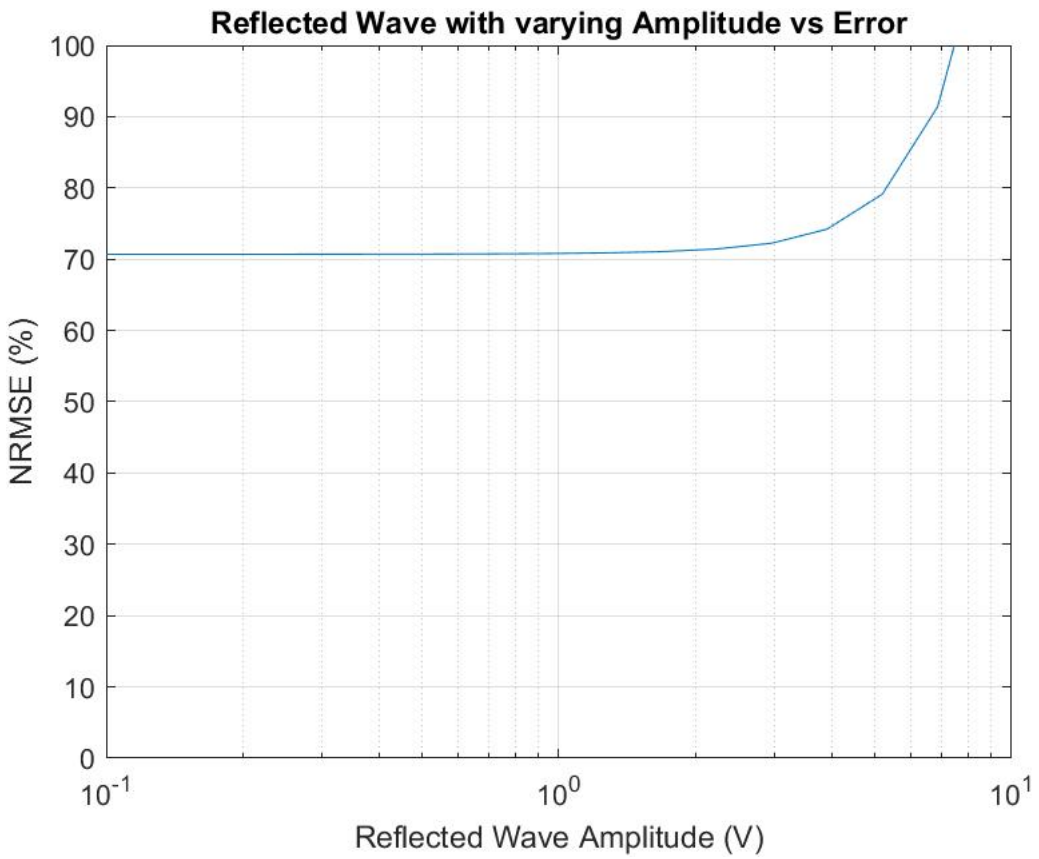

Figure 6.11: MDACM results showing error when the peak amplitude of reflected wave is Time Varying

As with the test of varying static amplitudes the results obtained indicate an increasing error with increasing variation between the carrier's amplitude and the recieved signals amplitude.

6.1.3 Test 3 - Static Peaks of Amplitude varying with time at differing frequencies

This test measures the error when the amplitude of the reflected wave is a time varying value from which the peak value is static and the frequency of which the amplitude cycles is being tested where A is the amplitude peak value calculated by $A = A_t \cos(w_t t)$ with A_t being a static value and w_t representing the different frequencies varying from $0.1...10^6$.

Arctan Results

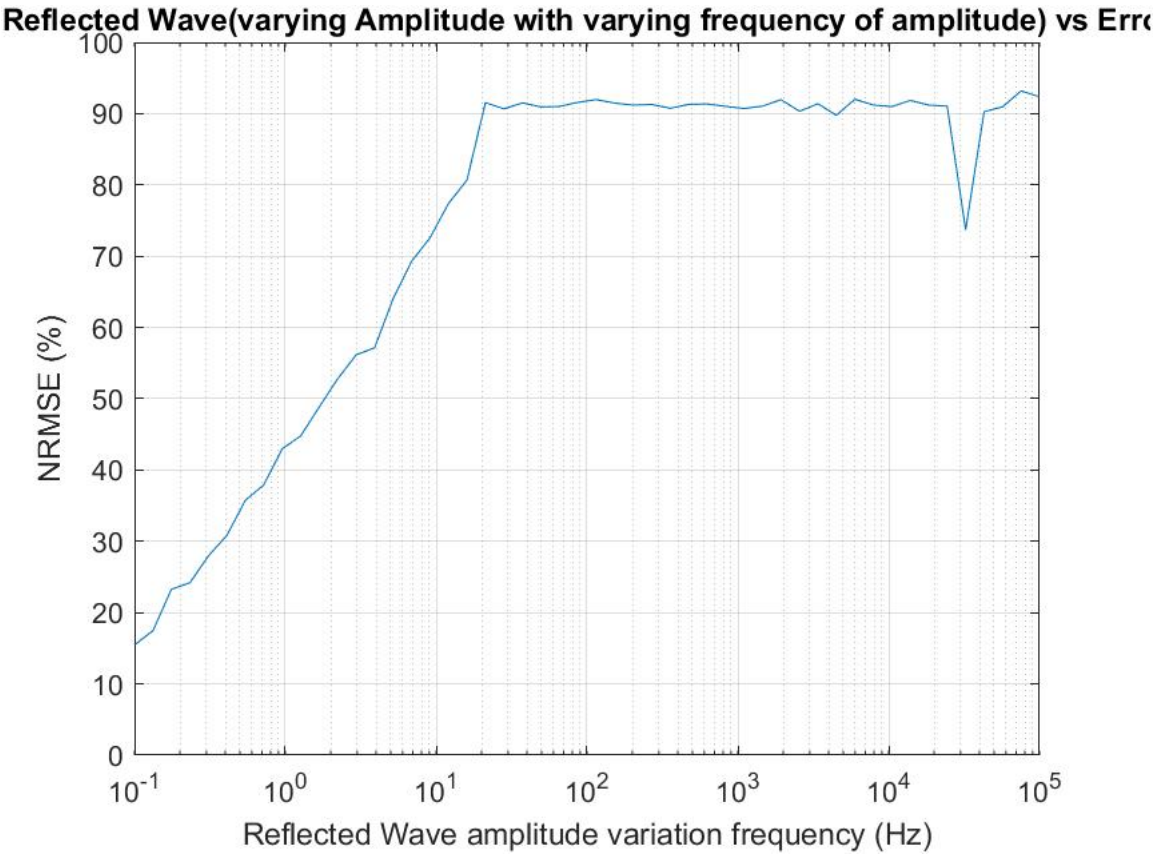

Figure 6.12: Arctan results showing error when the peak amplitude of reflected wave is Time Varying with differing frequencies

This test confirms the effects of varying frequencies of amplitude oscillation. As can be seen from the above the arctangent algorithm is susceptible to cyclic ocsillation of the amplitudes peak value steadily rising until the error starts to faltten out as the arctangent result is being driven to the limits of the codomain range.

EDACM Results

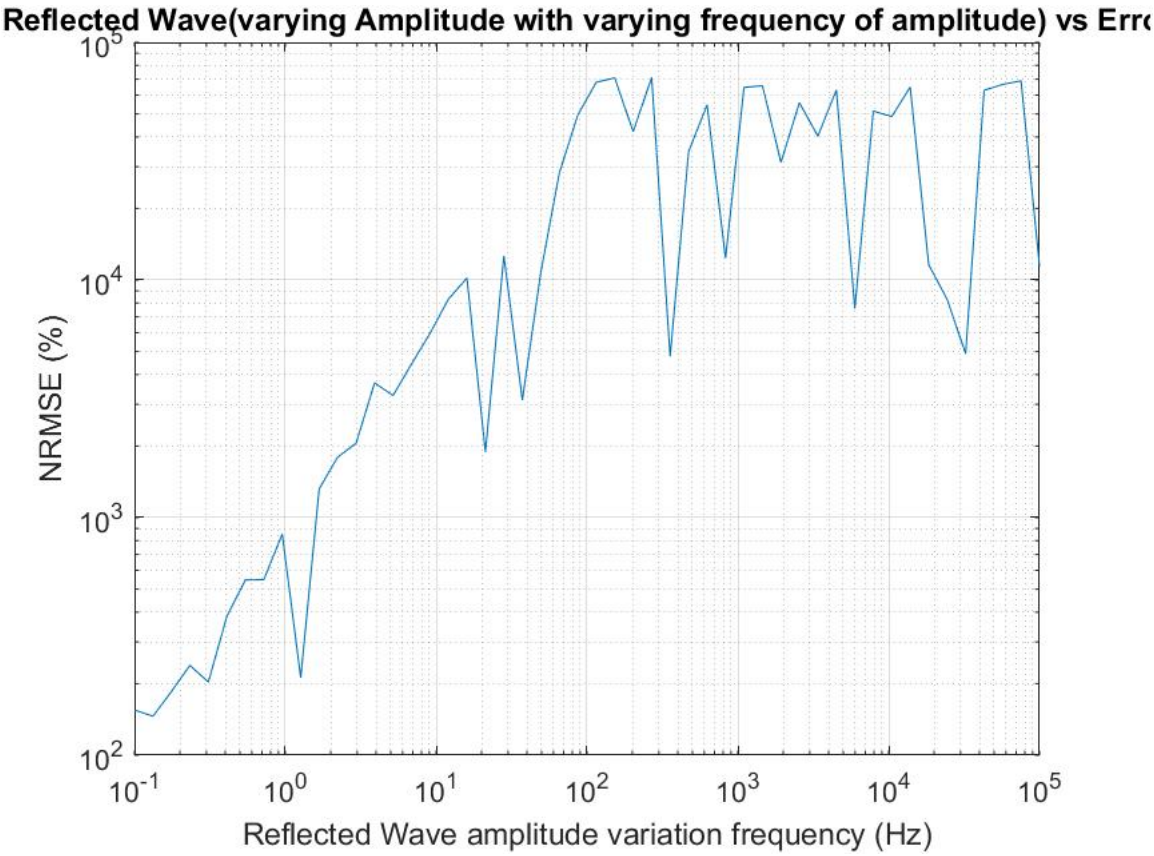

Figure 6.13: EDACM results showing error when the peak amplitude of reflected wave is Time Varying with differing frequencies

Similarily, the EDACM shows increasing susceptibility to rising frequencies of oscillation of the reflected waves peak amplitude.

MDACM Results

The performance of the MDACM algorithm with a time varying frequency of amplitude change differs from the previously recieved results in that it does not experience a zero crossing of the error axis. The results obtained indicated similar performance to the other algorithms, in that the MDACM algorithm is also sensitive to the rate of change of the time varying amplitude.

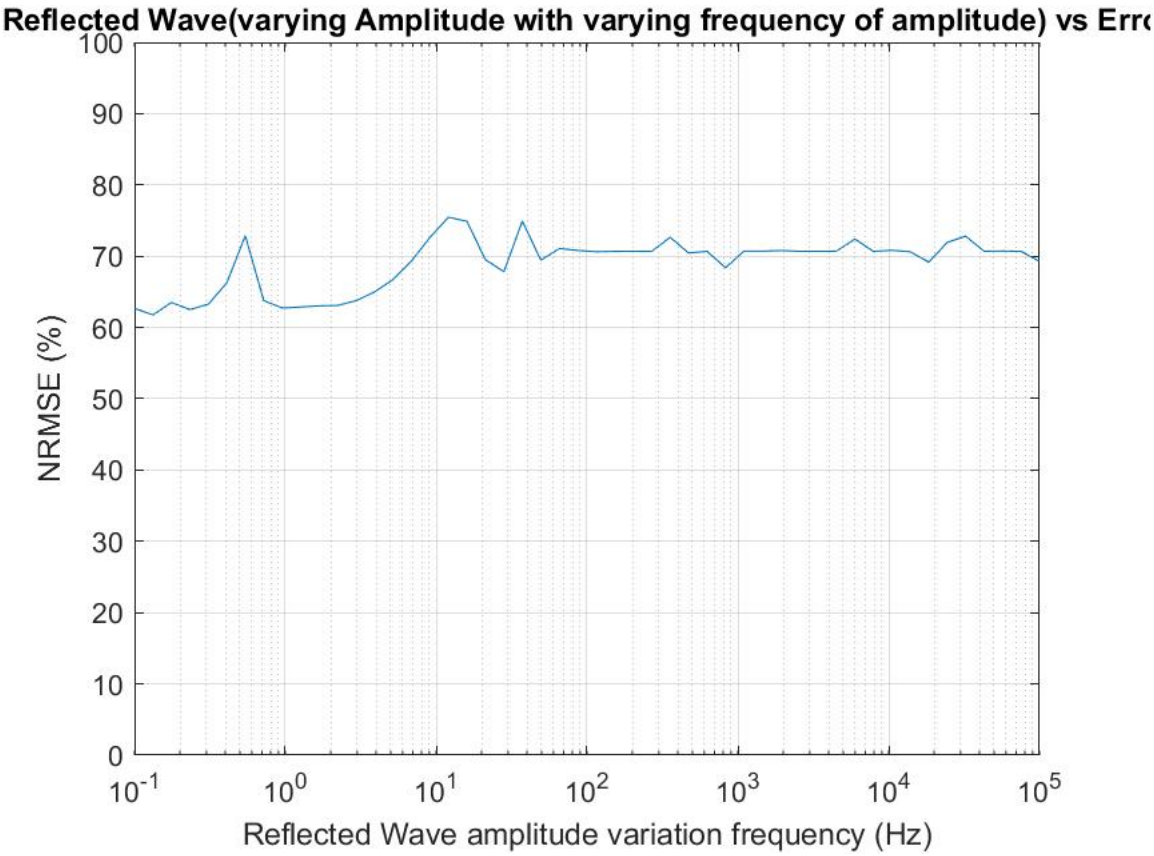

Figure 6.14: MDACM results showing error when the peak amplitude of reflected wave is Time Varying with differing frequencies

6.1.4 Amplitude Testing Summary

The testing completed above highlights each algorithms ability to withstand variations in the reflected waves peak amplitude. The arctan and DACM algorithms showed excellent performance when the reflected waveform exhibited straightforward attenuation or amplification with the accuracy remaining unchanged. The MDACM algorithm that was implemented for this project showed significant suceptibility to amplitude variations.

When the frequency of attenuation or amplification of the reflected waves peak amplitude was varied, both the arctan and EDACM algorithms exhibited suceptability to this situation with the added frequency noise being translated to added phase shift corrupting the reading. Because of EDACM's added mathematical differentiate and cross multiply steps it is particularly affected by this noise, with it translating to a static phase offset in the demodulated output. The MDACM algorithm again indicated an ineffectivness in operation when the amplitude noise is time varying indicating it would be an unsuitable candidate for measuring vibration in environments where electromagnetic noise is prevalent.

Using additional filtering to remove DC offset or the added frequency noise will aid in each algorithms performance when affected by amplitude noise cause by the environment.

6.2 Carrier Frequency Testing

The carrier wave frequency directly relates to the precision of the algorithms. It determines how many times the vibration frequency is sampled and the phase shift detected. The following tests will characterise each algorithms performance with regards to the carrier wave yielding results which will be analysed to identify behaviours.

6.2.1 Test 1 - Varying carrier frequencies measuring a unit vibration frequency

This test captures the relationship between vibration frequency and carrier frequency. This test is conducted on a unit vibration frequency to show the ratio relationship between the two values. Mathematically, the testing being conducted is represented by the w_c

attribute in the carrier wave equation being varied between $0.1...10^6$.

ARCTAN Results

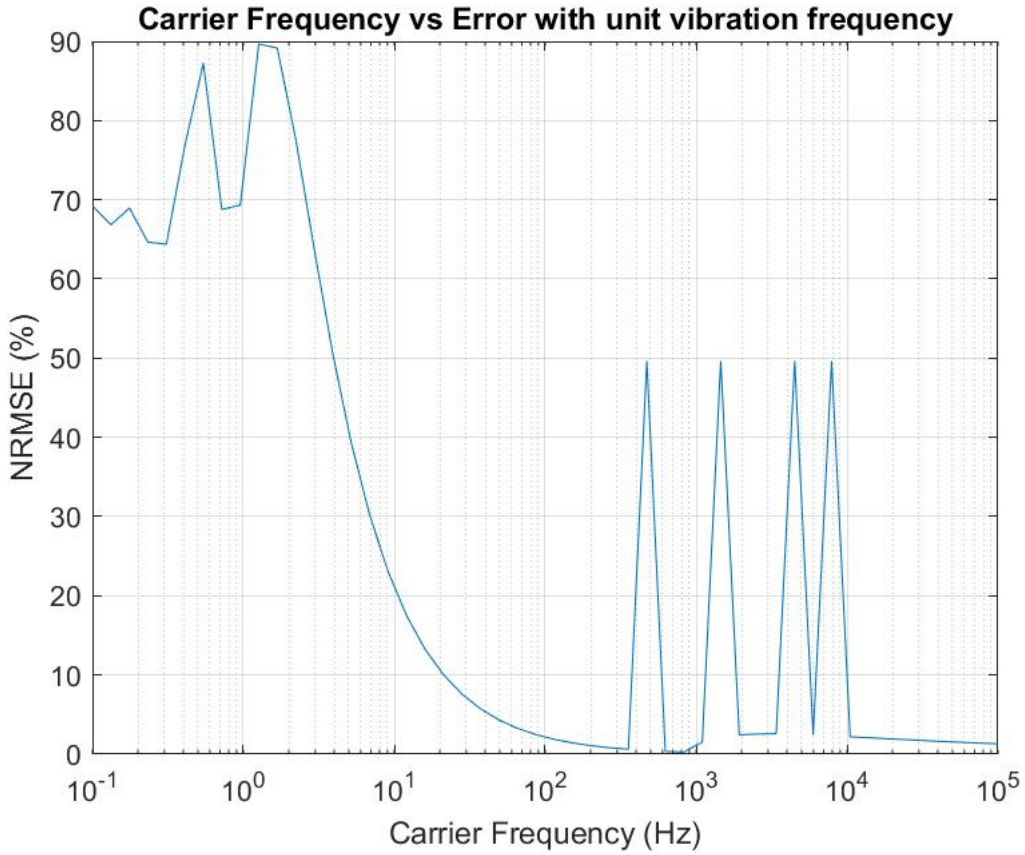

Figure 6.15: Arctan results showing error when the carrier frequency is increased in relation to the vibration frequency.

From the results collected, it is visible that for carrier frequencies less than the vibration frequency, a significant increase in error is present. The optimum relationship between vibration frequency and carrier frequency is visible when the carrier frequency is greater than nineteen times the vibration frequency, with all frequencies beyond this point yielding a less than once percent error. This ratio corresponds with an optimum in error percentage with regards to the data processing power required for higher ratios. The general behaviour can be seen in the figure above that as the carrier frequency increases relative to the vibration frequency so does the accuracy of the measurement.

EDACM Results

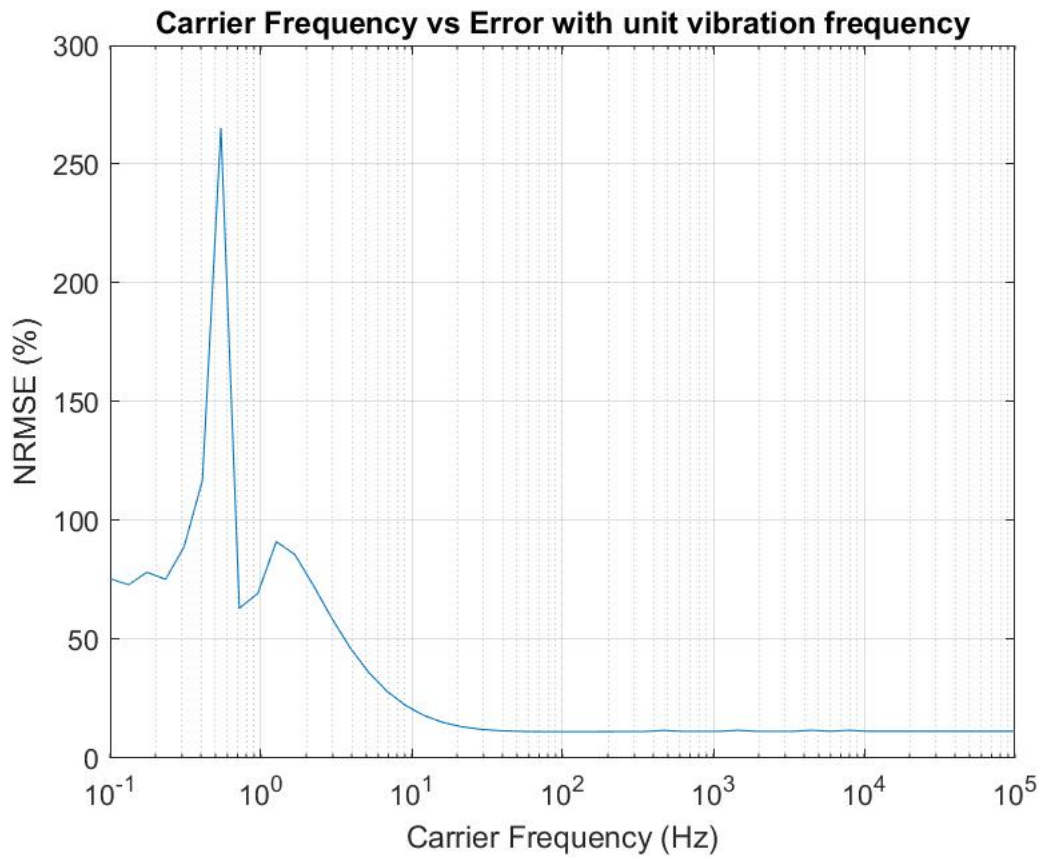

Figure 6.16: Arctan results showing error when the carrier frequency is increased in relation to the vibration frequency.

The EDACM results indicate a similar response to carrier frequency increase, with frequencies below the vibration frequency being measured incountering large errors. The EDACM algorithms optimum point is reached at eighty times the vibration frequency, with frequencies above this yielding an error less than one percent. Again, it is visible that the general impact of carrier frequency variation to the EDACM algorithm is the higher the frequency of the carrier relative to the vibration frequency the higher the accuracy.

MDACM Results

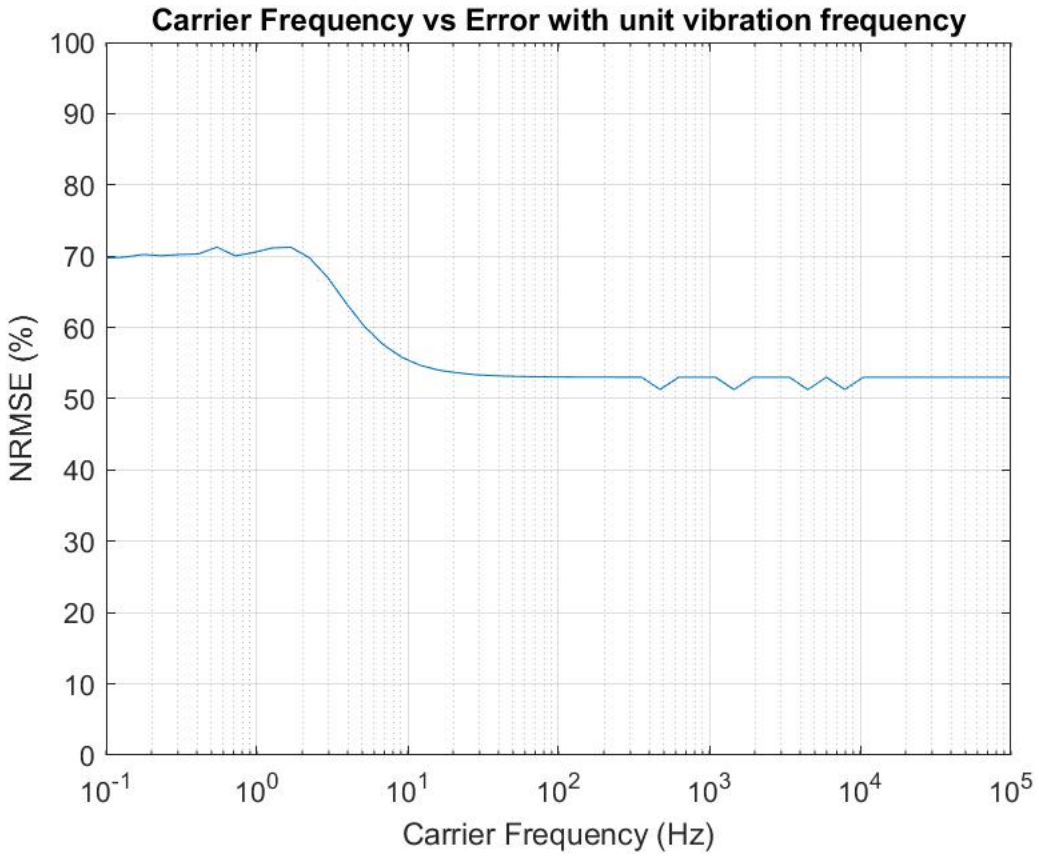

Figure 6.17: MDACM results showing error when the carrier frequency is increased in relation to the vibration frequency.

Similar to the two other alogorithms the MDACM algorithm can be seen to have significant error when the carrier frequency is below the vibration frequency. As the carrier frequency increases the error can be seen to fall to a steady state where no futher error is introduced. The steady state error percentage of $\approx 54\%$ can be seen at 40 times the vibration.

6.2.2 Test 2 - Carrier wave measuring different displacements

This test identifies the relationship between the carrier frequencies wavelength and the displacement of the vibration being measured. To conduct this test the carrier frequency will be a fixed value with the displacement being a fraction of the carriers wavelength represented by $\frac{\lambda}{k}$ where k varies between $0.1...10^6$. Completing this test will identify each algorithms sensitivity to phase shift which relates to the displacement being measured.

ARCTAN Results

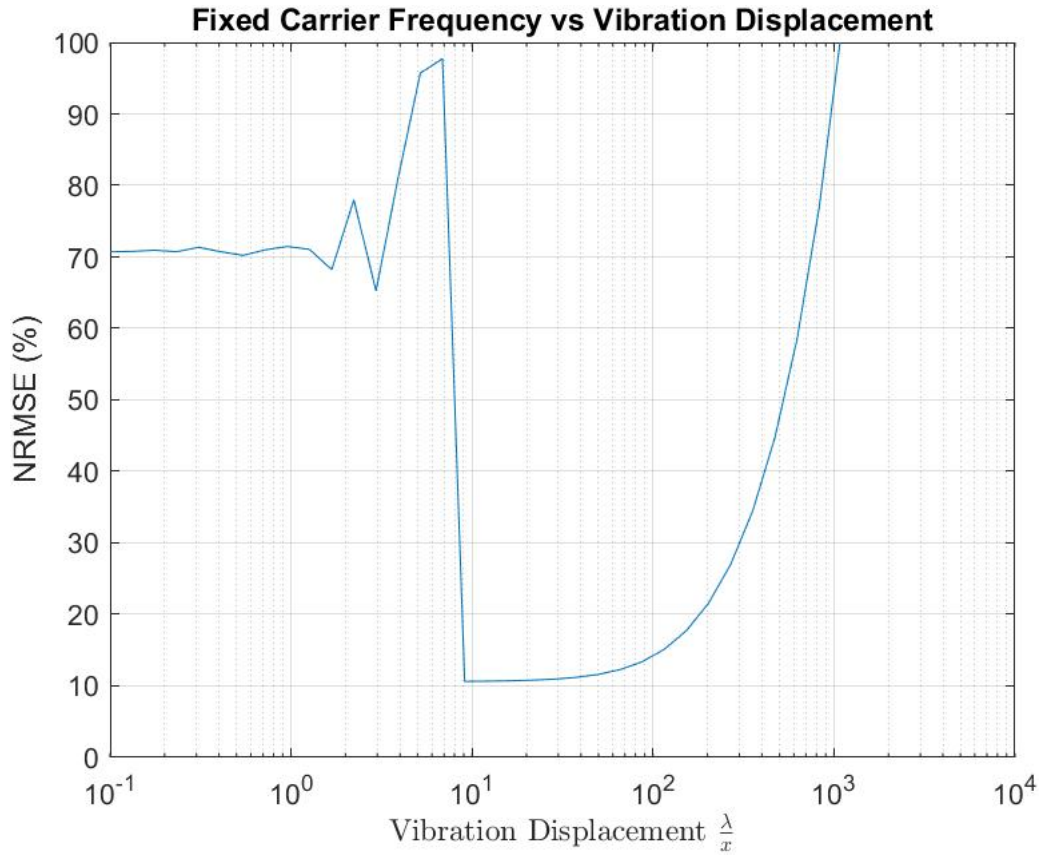

Figure 6.18: Arctan results showing error when the carrier frequency is fixed and different ratios of vibration to wavelength displacement are being measured.

From the collected results it is visible that the arctangent algorithm becomes accurate when the displacement being measured corresponds with $\frac{\lambda}{8}$ when there is no static phase offset present in the demodulated waveform. This is an expected response as the codomain operation of the arctangent function limits the reading of any displacement larger than $\frac{\lambda}{8}$. This limit is represented mathematically by understanding the codomain range of arctangent as being $\frac{\pi}{2}$ to $-\frac{\pi}{2}$ and factoring it into the displacement equation

$$x(t) = \frac{\lambda}{4\pi}\frac{\pi}{2}$$

$$x_{max} = \frac{\lambda}{8}$$

Displacements with in the codomain restiction exhibit a high level of accuracy with the error recorded varying increasingly from 10% to 15% for displacements measuring between $\frac{\lambda}{8}$ down to $\frac{\lambda}{100}$.

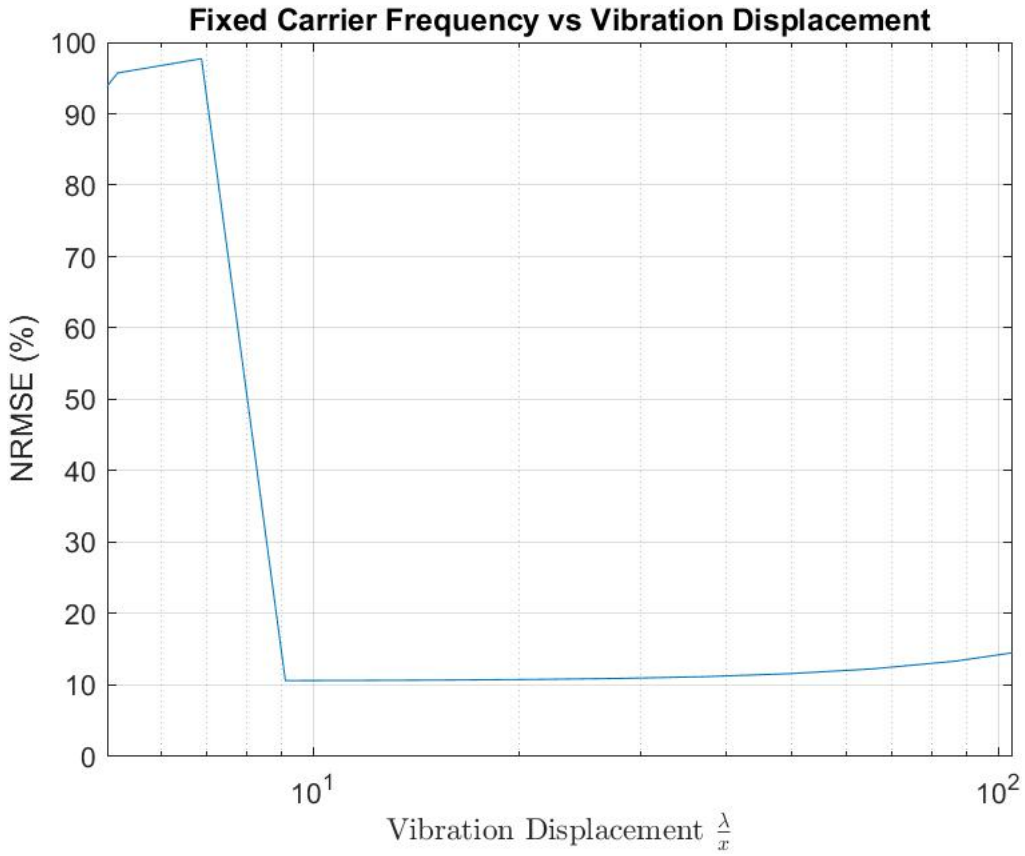

Figure 6.19: Arctan results showing error when the carrier frequency is fixed and different ratios of vibration displacement to wavelength displacement are being measured.

The following graph depicts the waveforms associated with the arctangent measuring a displacement of $\frac{\lambda}{80}$ to showcase the algorithms accuracy.

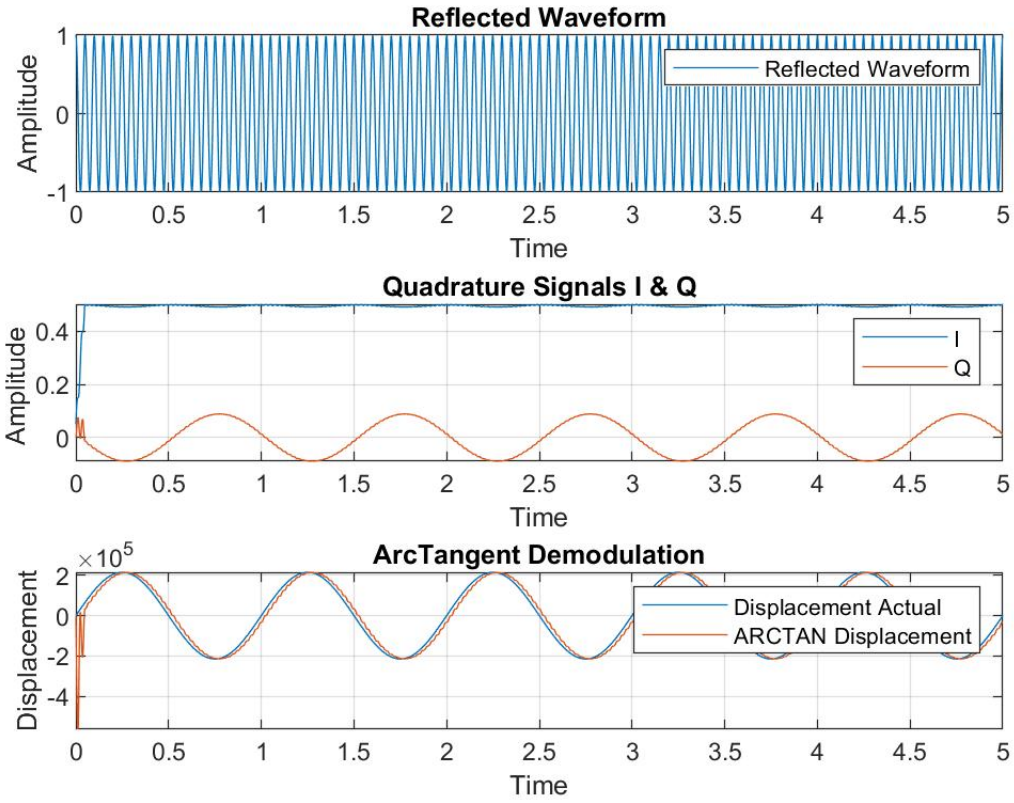

Figure 6.20: Arctan waveforms associated with measuring a displacement of $\frac{\lambda}{80}$.

EDACM Results

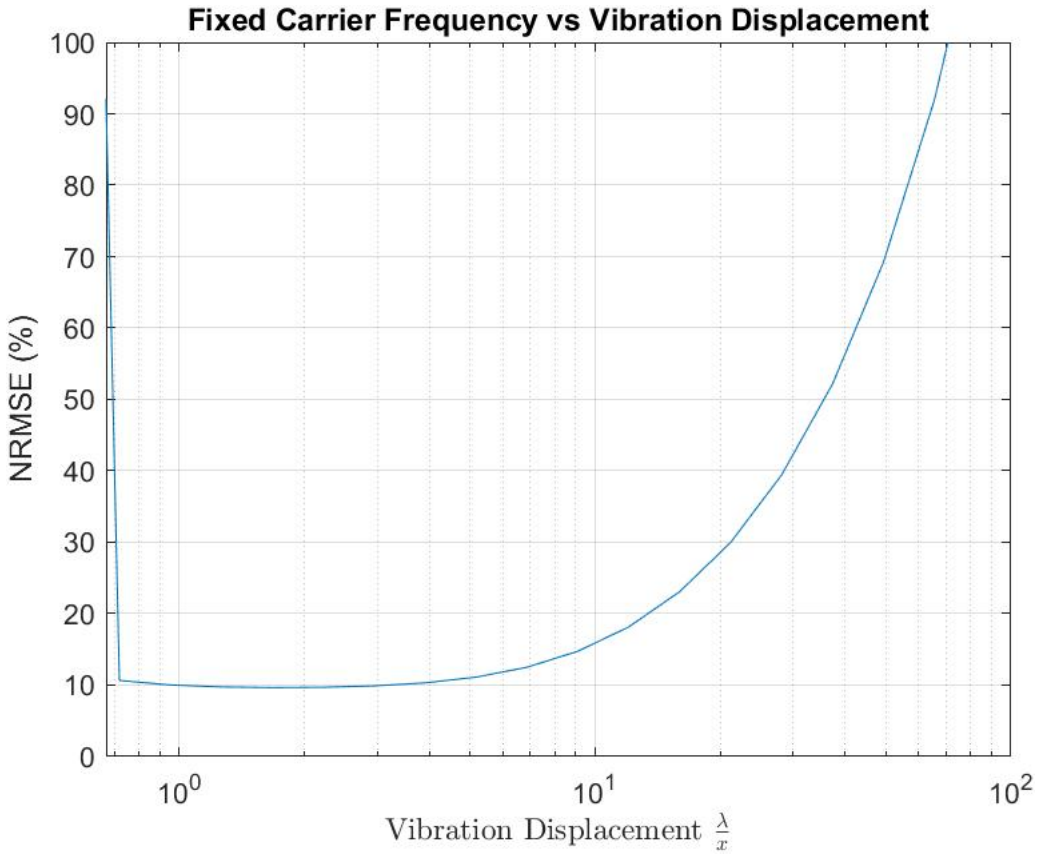

Figure 6.21: EDACM results showing error when the carrier frequency is fixed and different ratios of vibration displacement to wavelength displacement are being measured.

The results of the EDACM algorithm show that this algorithm is capable of measuring outside of the codomain restriction expereienced with the arctangent algorithm. With the error variation from the codomain limit of $\frac{\lambda}{8}$ up to $\frac{\lambda}{0.8}$ equating to approximately one percent or less.

Similar to the arctangent algorithm, the EDACM algorithm reaches a ratio where the error starts to increase. Unlike the artangent however, the EDACM experienced this point after only $\frac{\lambda}{10}$. This indicates that the measurable displacement is more dependent on the carrier wavelength than the arctangent algorithm is.

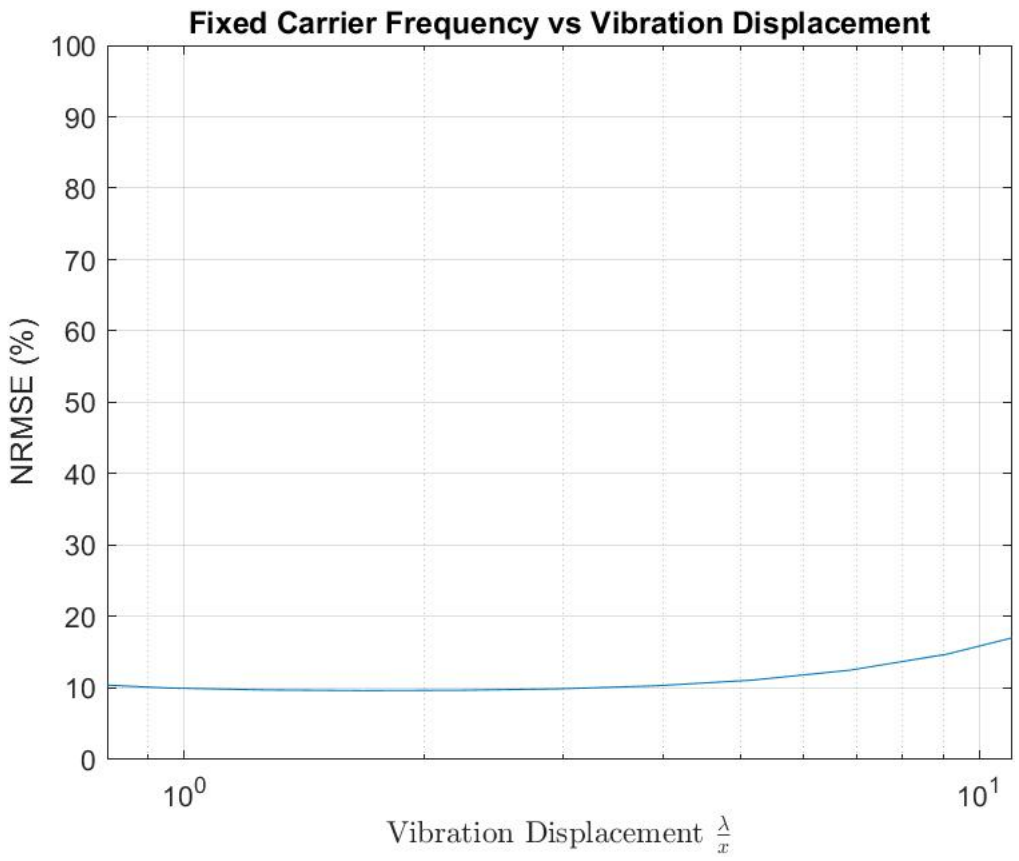

Figure 6.22: EDACM results showing error when the carrier frequency is fixed and different ratios of vibration displacement to wavelength displacement are being measured.

The following waveforms showcase the performance of the EDACM algorithm measuring a displacement larger than $\frac{\lambda}{8}$ which is outside the domain restrictions accompanied with the arctangent algorithm.

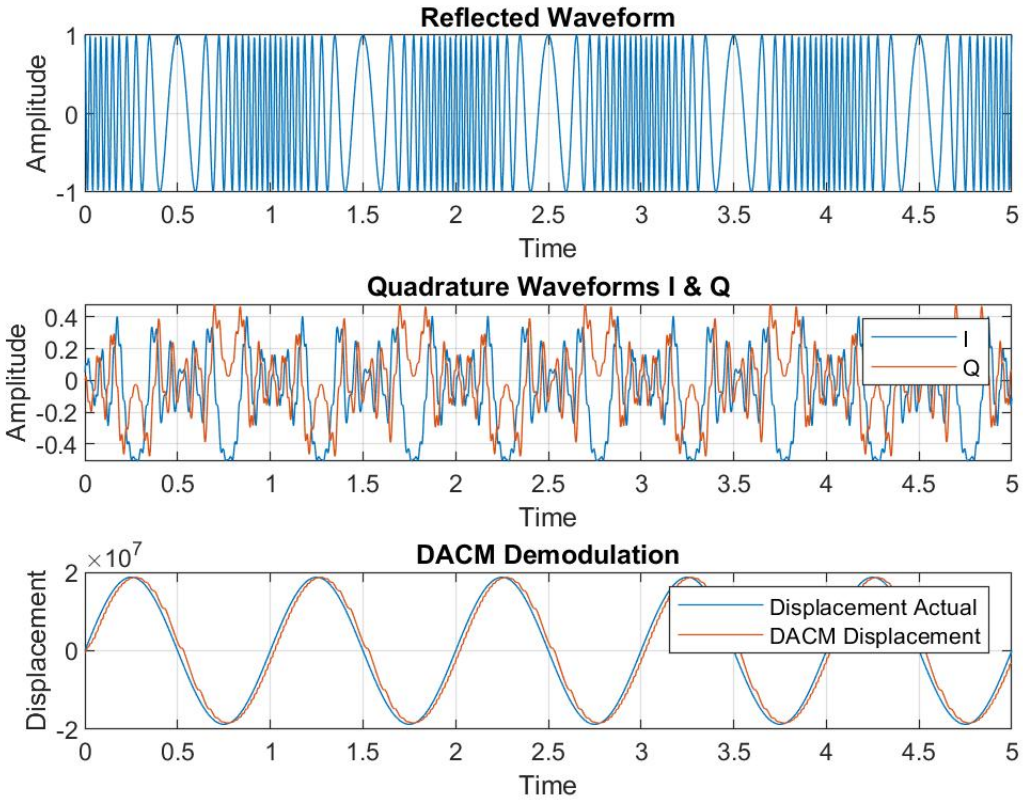

Figure 6.23: EDACM results showing waveforms of measuring a displacement equal to $\frac{\lambda}{0.8}$

MDACM Results

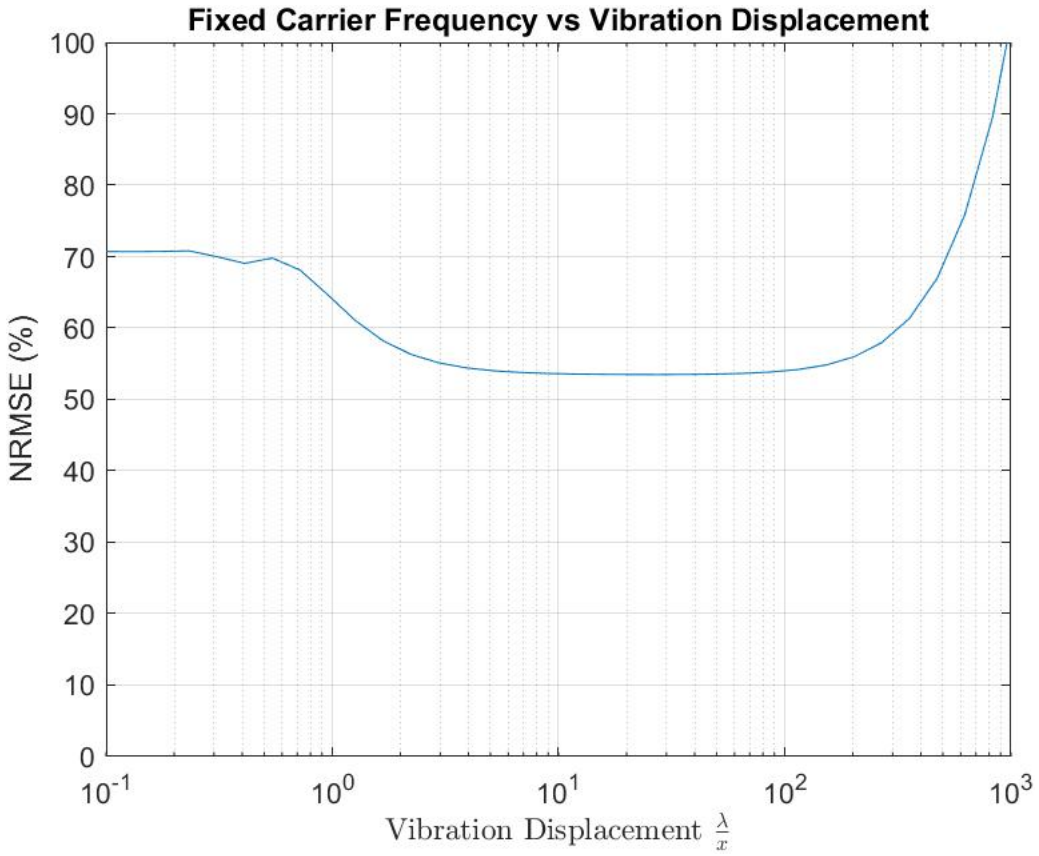

Figure 6.24: MDACM results showing error when the carrier frequency is fixed and different ratios of vibration displacement to wavelength displacement are being measured.

Similar to the performance of the arctangent and DACM algorithms the error present in the MDACM demodulated result increases the smaller the diplacement being measured becomes. The turning point of the curve where the error starts increasing significantly can be seen around the 100 times the vibration frequency mark.

6.2.3 Test 3 - Carrier wave measuring time varying vibration frequency

This test identifies the relationship between error with a fixed carrier frequency and a time varying vibration frequency. .This test aims to replicate the effects of potential noise or time varying vibrations, as is the case found with most machinery. The carrier frequency will be varied between $0.1...10^6$ hertz to showcase the relationship adequately.

ARCTAN Results

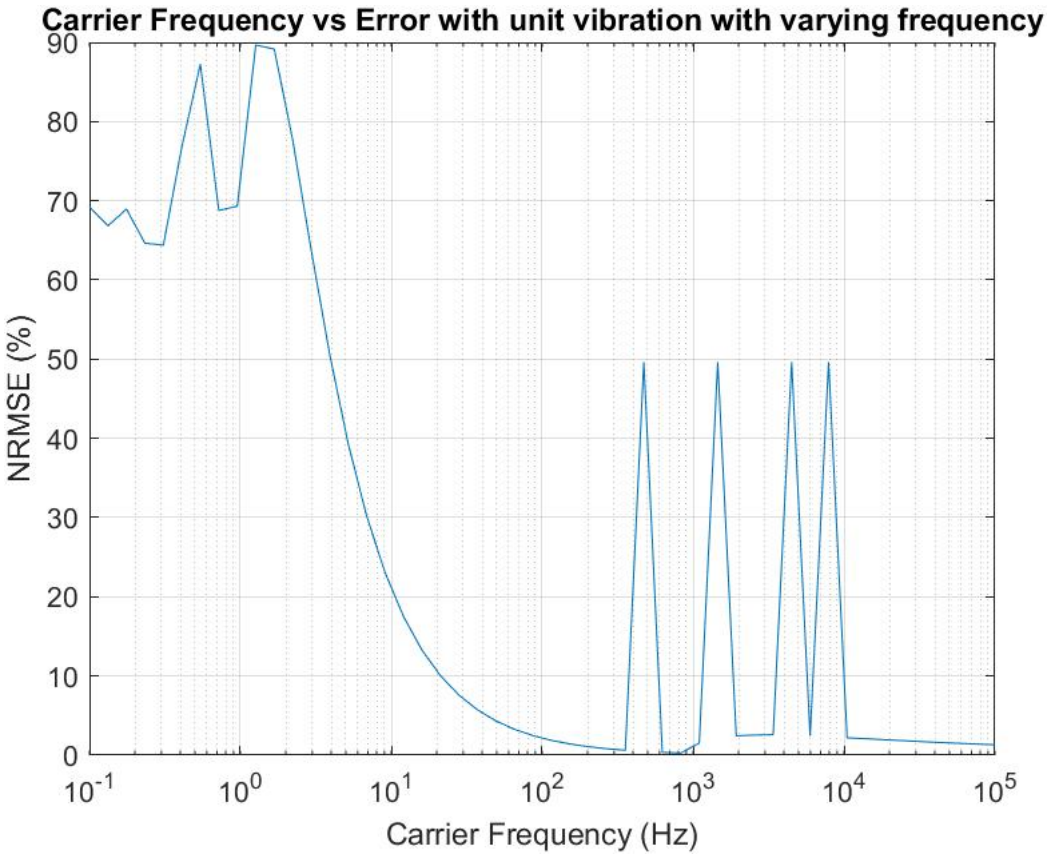

Figure 6.25: Arctan results showing the error present across increasing carrier frequencies with a time varying vibration frequency.

The results of a varying vibration frequency have little to no affect on the error present when the frequency of the carrier is constant. The error starts out rather high when the carrier frequency is less than that of the vibration frequency, but quickly decays as the carrier frequency is increased. Unlike the results captured in test one of the carrier frequency test series, as the carrier frequency is increased above 120 times the vibration frequency the resultant error fluctuates up to 50%. This indicates that the variation in vibration frequency does have an affect on the accuracy of the output.

EDACM Results

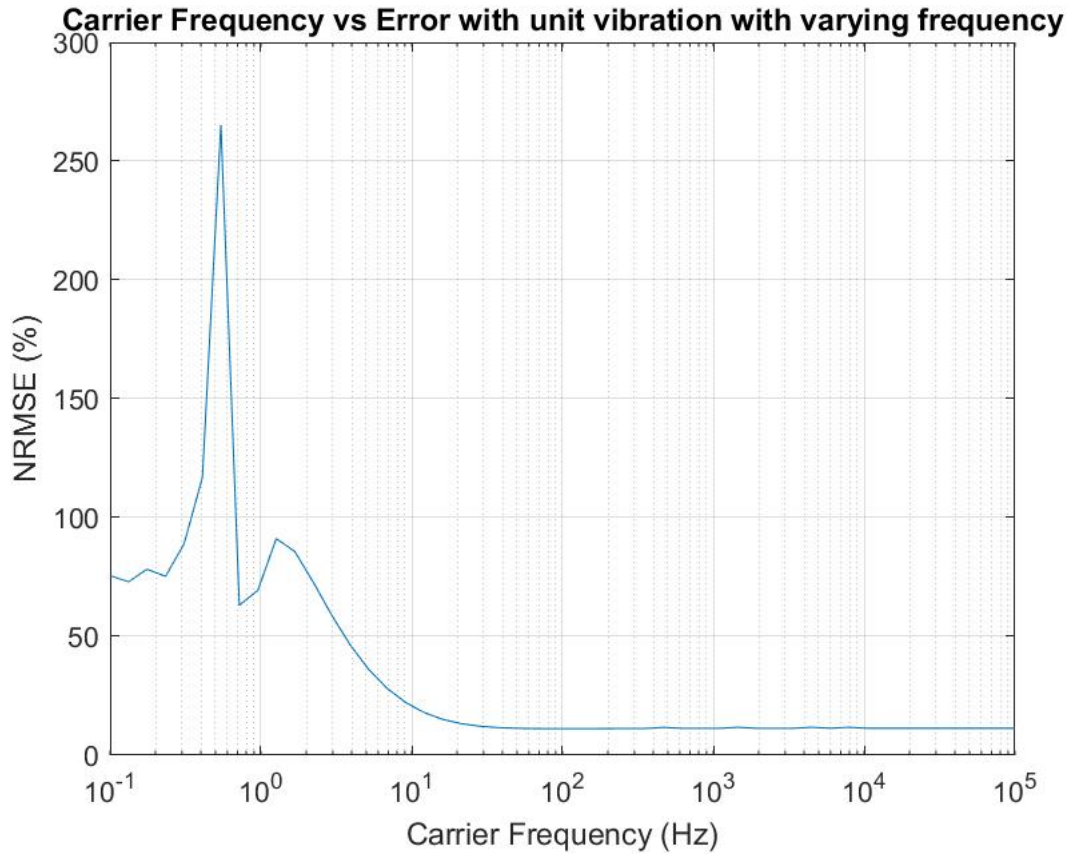

Figure 6.26: EDACM results showing the error present across increasing carrier frequencies with a time varying vibration frequency

As with the arctangent test results for a time varying vibration frequency, the EDACM's performance resembles that of the first test's performance. Unlike the arctangent, there is no fluctuation in the error percentage visible.

MDACM Results

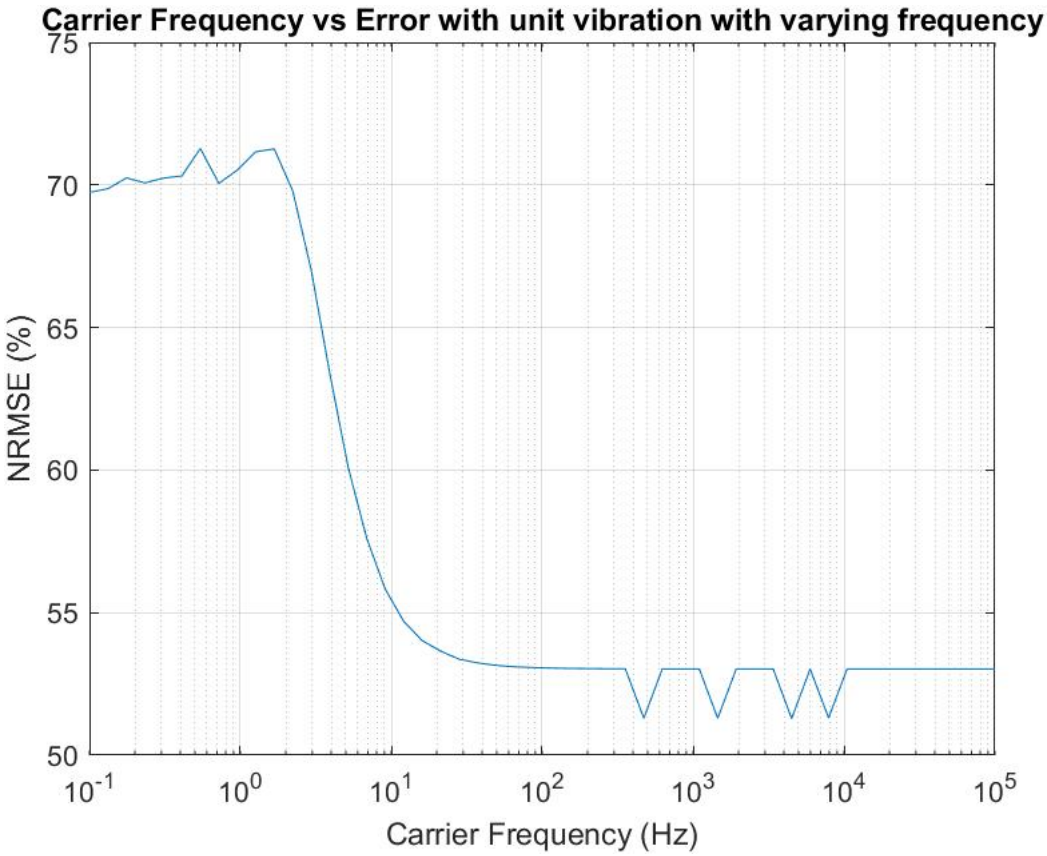

Figure 6.27: MDACM results showing the error present across increasing carrier frequencies with a time varying vibration frequency

Similar to the arctangent and EDACM algorithms performance the introduction of a time varying vibration frequency does not overy affect the error present in the demodulated result. As the carrier frequency is increased a point is reached where the error present is largely steady.

6.2.4 Summary of Carrier Testing

From the testing completed the carrier frequecy error results are similar among the three algorithms. It is apparent that the main concern of the carrier frequency is that it is a large enough multiple of the vibration being measured so that the ratio of carrier to vibration frequency places the error in the steady state region of the graphs.

An important understanding of each algorithm is the limits of displacement that can be

measured. The testing completed varified the codomain restrictions of the arctangent algorithm whilst confiming the EDACM's ability to measure outside of this restriction. A point is visible with each algorithm that dictates where the accuracy of measurement starts to decline. This arises when the displacement being measured is not large enough to be extracted accurately from the reflected waveform.

6.3 Phase Noise Testing

The following results were obtained when testing each algorithms performance with phase manipulation, similar to the other tests completed this use the NRMSE value to convey the error presented.

6.3.1 Test 1 - Static Phase offset

This test highlights the performance of each algorithm with a static wave offset present.

ARCTAN Results

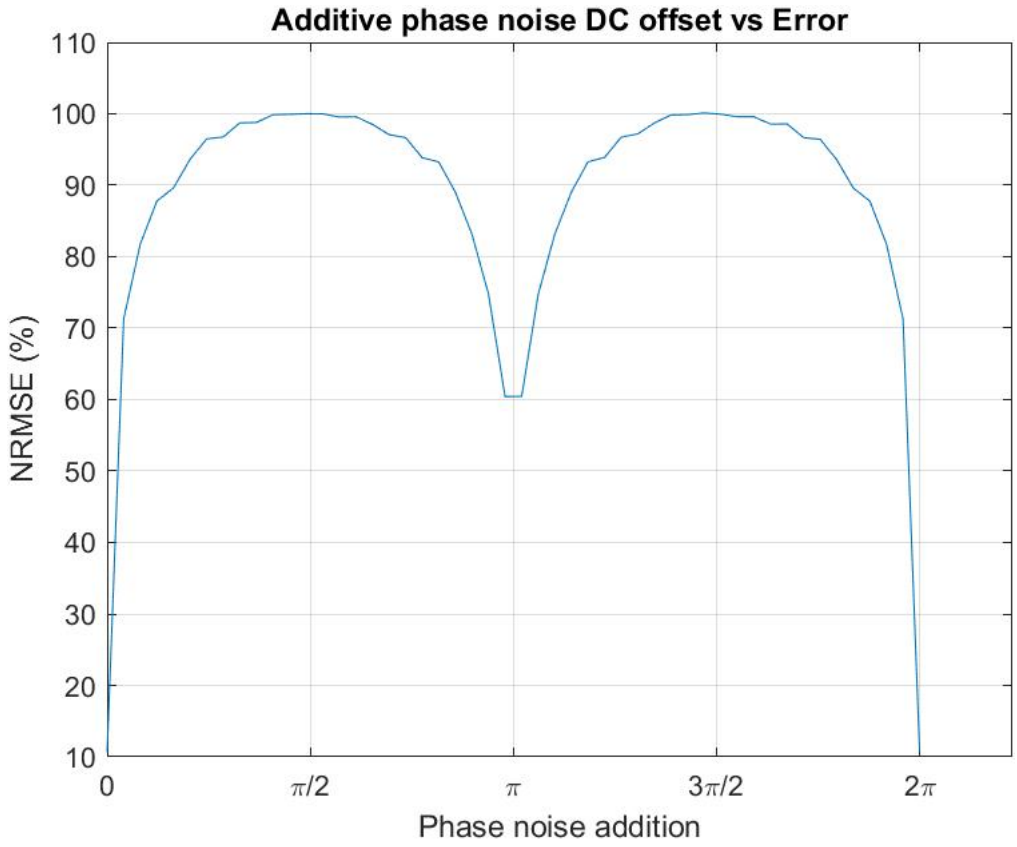

Figure 6.28: Arctan results showing the error introduced with a static phase shift imparted on the reflected waveform

The results obtained from the phase testing indicate that as the phase shift approaches $\pi/2$ the phase demodulation is nearing the limits of the domain restriction of the arctangent operator. The results were captured measuring a displacement of $\lambda/8$ the maximum possible displacement that the arctangent can measure accurately, this was completed to showcase the effects of the domain limits as can be seen below.

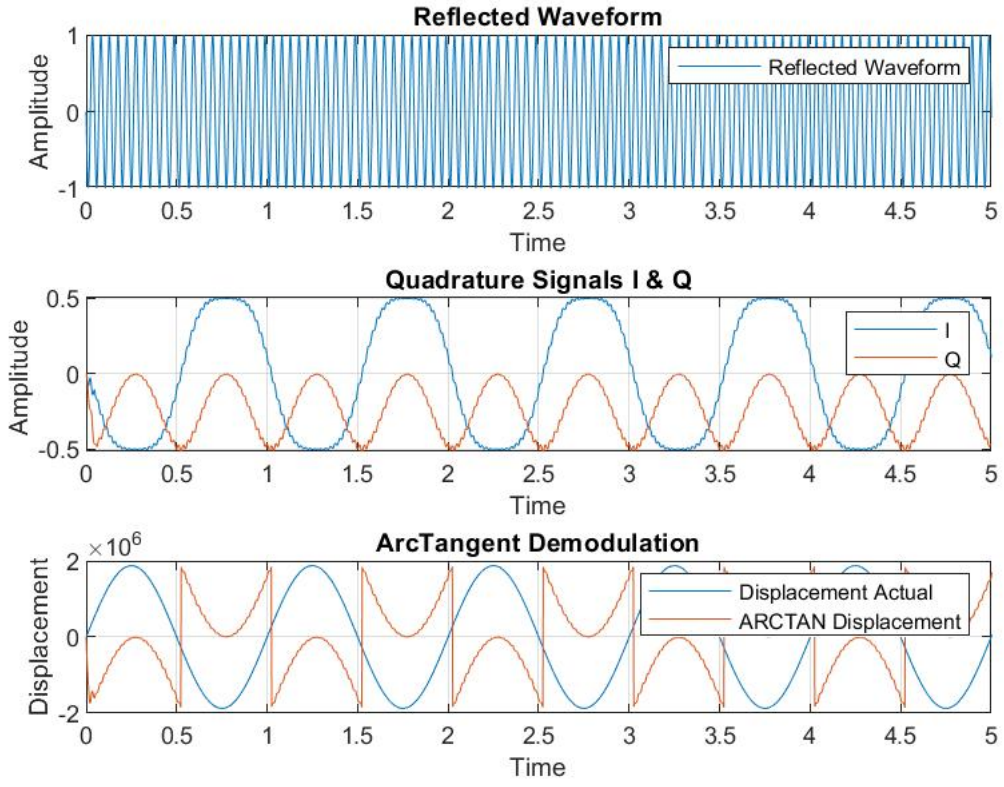

Figure 6.29: Arctan results showing the error introduced with a static phase shift imparted on the reflected waveform at peak error of $\pi/2$

EDACM Results

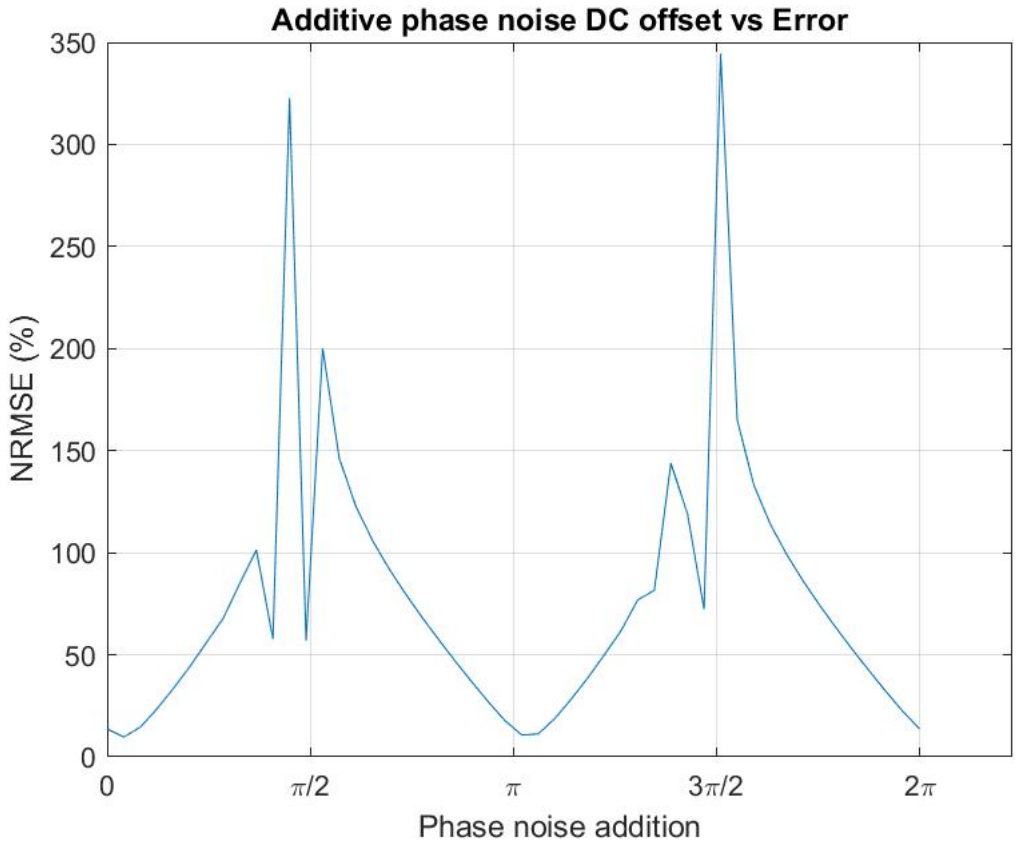

Figure 6.30: EDACM results showing the error introduced with a static phase shift imparted on the reflected waveform

The extended differentiate and cross multiply algorithm shows particular susceptability to static phase shift. The magnitude of error present can be observed to be significantly larger than that present with the arctangent algorithm. Limiting the y axis to display error between 0 and 100% yields the following graph.

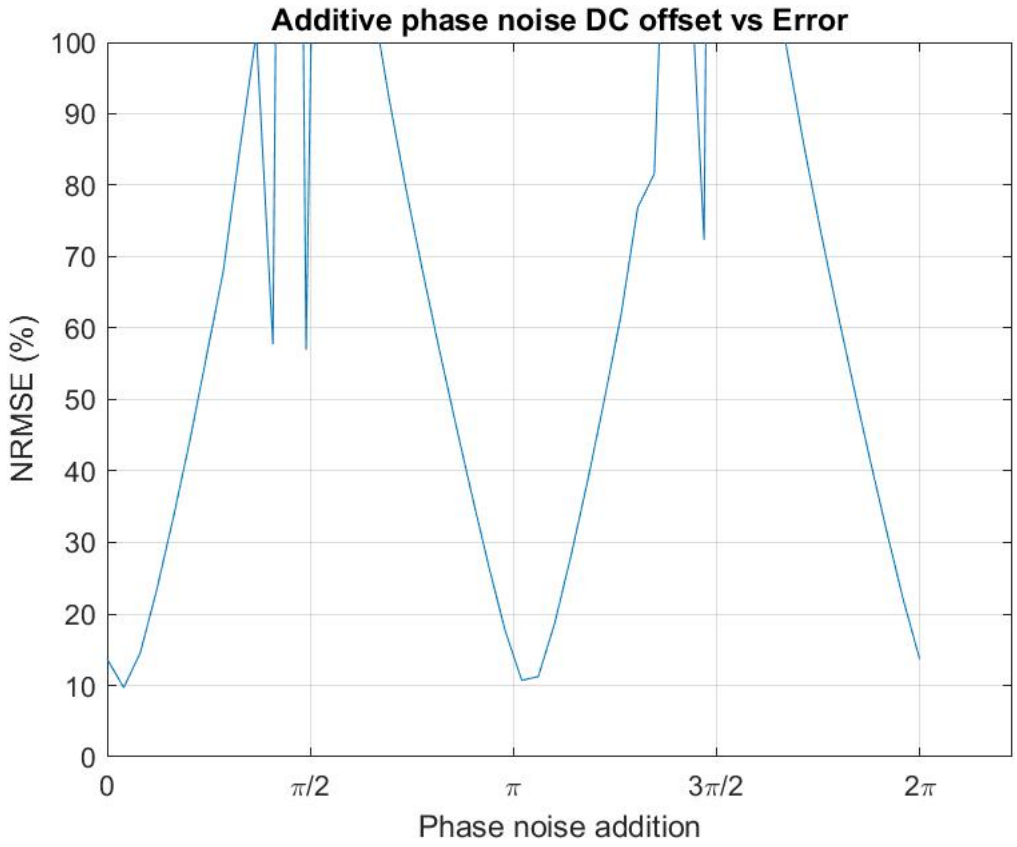

Figure 6.31: EDACM results showing the error introduced with a static phase shift imparted on the reflected waveform

The sensitvity to phase shift observed above is believed to be a biproduct of the differentiate and cross multiply steps of this algorithm. Normally the accumulation process would remove any zero mean noise present in this algorithm however the static offset noise being added to the reflected wave form in this test is not zero mean highlighting a weakness in this algorithms ability to demodulate the vibration accurately.

MDACM Results

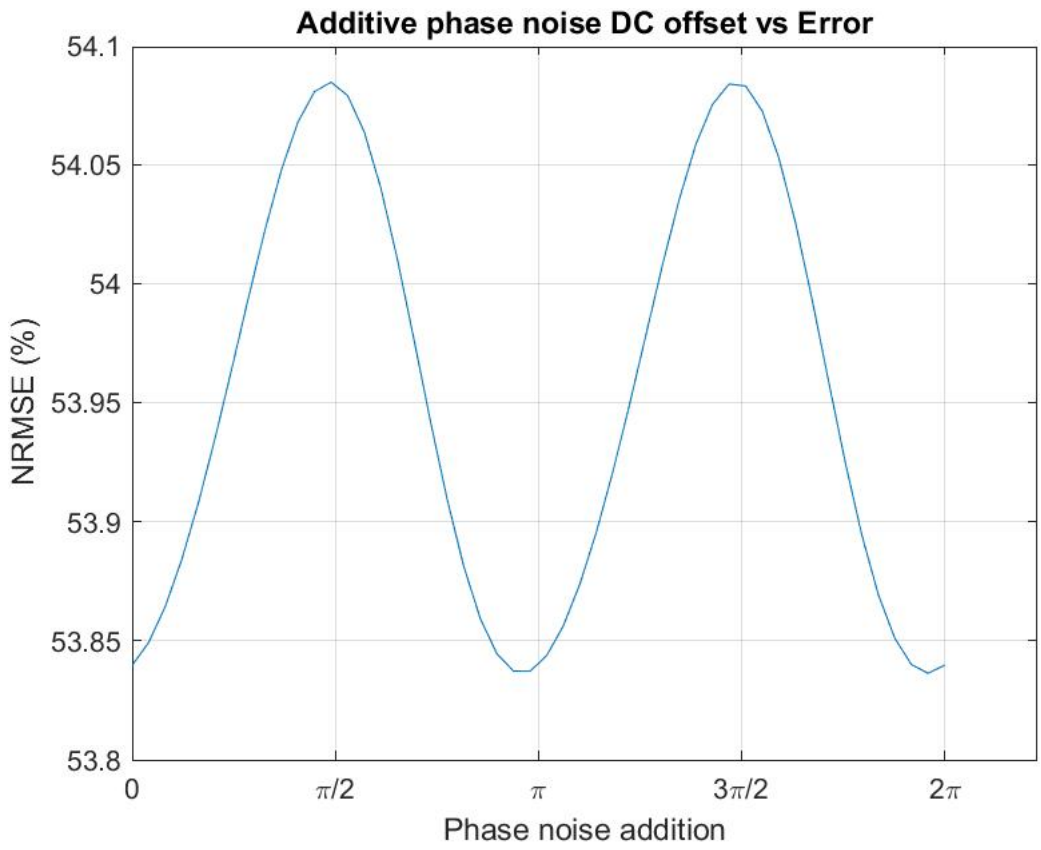

Figure 6.32: MDACM results showing the error introduced with a static phase shift imparted on the reflected waveform

The error present in the modified differentiate and cross multiplies demodulated result mimics the profile of the arctangent algorithm in that the error introduced by phase shift peaks at $\pi/2$. The overall error introduced by the phase shift was considerably less than that of the other algorithms.

6.4 Effects of Sampling

This test identifies the affects of sampling on the accuracy of the demodulation. Completing this testing allows for understanding in the selection of a sampling rate that will allow for consistent accuracy with the algorithms. To complete this testing, the number of samples per cycle will be varied from $10^0...10^4$. A per cycle basis is used to ensure that all frequencies will be sampled at the same rate.

6.4.1 Arctangent Results

The arctangent results can be seen below. As the sampling rate is increased, generally the accuracy of the demodulation also increases. Sampling rates below ten samples per cycle carry significant error in their results, while above twenty samples per cycle signifies the error percentage reaching a steady state value. Above 100 samples per cycle there is very little benifit gained for increases in sampling rates and data processing ability becomes impacted.

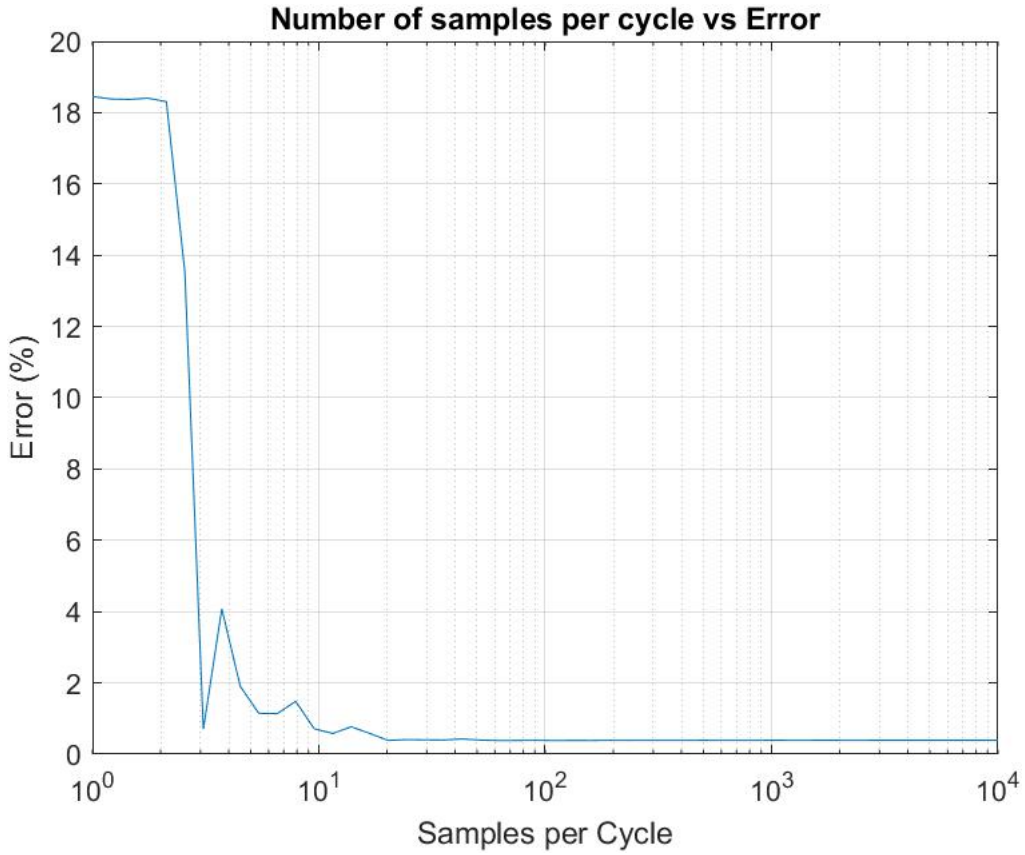

Figure 6.33: Error present in Arctangent demodulation with varied sampling rates.

6.4.2 EDACM Results

The EDACM algorithm, although initially heavily impacted by undersampling of the waveform, recovers quickly with the error percentage being reduced to under one percent when each cycle is sampled four times.

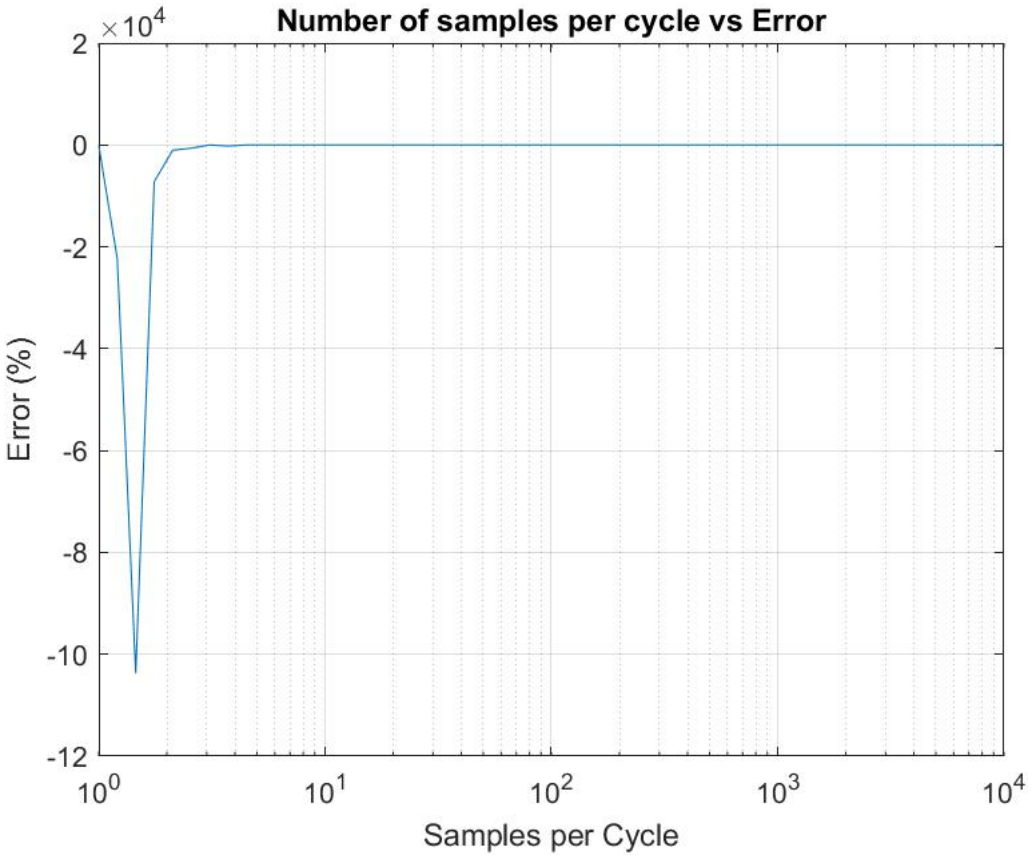

Figure 6.34: Error present in EDACM demodulation with varied sampling rates.

The EDACM algorithm does not reach a steady state error until 10^3 samples per cycle as can be seen below.

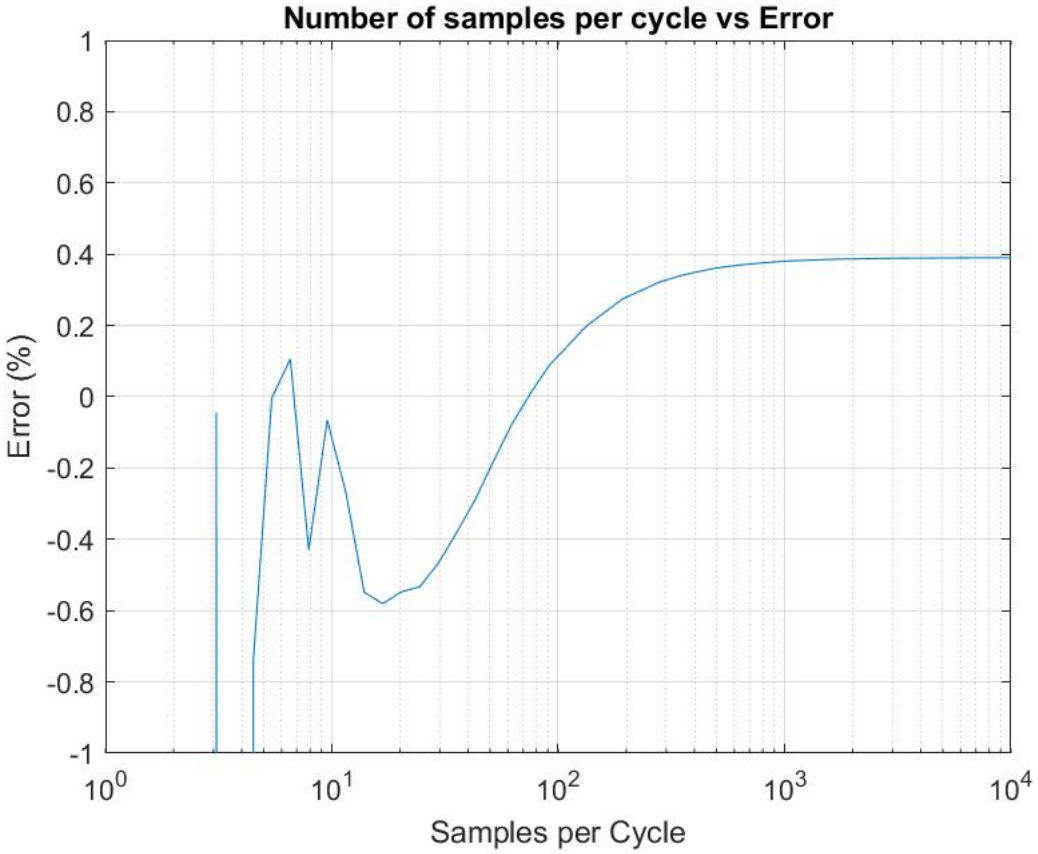

Figure 6.35: Error present in EDACM demodulation with varied sampling rates.

Chapter 7

Statictical Data Analysis - ANOVA

The following section completes the analysis of variance review of the collected data from the theoretical testing completed above. To complete the statistical analysis the built in ANOVA function of excel was utilised.

7.1 Artangent Data

Table 7.1: Arctangent Results summary

Test	Average Error	Std Dev	Variance
Amplitude Test 1	10.6938%	2.63E-15%	6.95E-30%
Amplitude Test 2	87.5472%	6.86E-14%	4.72E-27%
Amplitude Test 3	73.8264%	25.1747%	633.7701%
Carrier Test 1	26.4404%	32.458%	1053.522%
Carrier Test 2	772.4861%	1837.724%	3377230%
Carrier Test 3	27.9219%	31.5196%	993.4887%
Phase Test 1	88.4532%	18.9856%	360.4519%

Completing the ANOVA analysis of the collected data to identify the impact the attributes have on the error present in the demodulated result the Arctangent algorithm had an F-

statistic value of 7.77 whilst the F-critical value was 2.12 coupled with a probability value of 7.48E-18 indicating that the null hypothesis associated with the ANOVA method is void and one or more of the attributes do indeed contribute more to the error than the others.

From the above summary the values indicate that the following attributes have the greatest affect on the error (highest to smallest).

1. Carrier Test 2 - Measures the error when a fixed carrier wave and measures varying vibration displacements
2. Carrier Test 1 - Measures the error present when the carrier frequency is varied against a unit vibration frequency
3. Carrier Test 3 - Measures the error present when a carrier frequency is measuring a time varying vibration frequency
4. Amplitude Test 3 - Measures the error present when the peak amplitude is a time varying value the cycles at varying frequencies
5. Phase Test 1 - This test imparts a phase offset onto the reflect signal.
6. Amplitude Test 2 - Measures the error present when the peak amplitude of the reflected wave is a time varying value in relation to other parameters
7. Amplitude Test 1 - Measures the error present when the peak amplitude of the reflected wave is a static value that is changed in relation to other parameters

7.2 EDACM Data

Table 7.2: EDACM Results summary

Test	Average Error	Std Dev	Variance
Amplitude Test 1	13.7009%	4.6178E-14%	2.1324E-27%
Amplitude Test 2	12861.74%	1.6915E-10%	2.8613E-20%
Amplitude Test 3	24736.08%	713789969.6%	26716.8480%
Carrier Test 1	30.3446%	41.8082%	1747.9234%
Carrier Test 2	11815.63%	28607.3480%	818380357.4%
Carrier Test 3	34.7086%	44.5212%	1982.1397%
Phase Test 1	76.8260%	68.7324%	4724.1486%

Completing the ANOVA analysis of the collected data to identify the impact the attributes have on the error present in the demodulated result the EDACM algorithm had an F-statistic value of 21.5451 whilst the F-critical value was 2.12 coupled with a probability value of 1.746E-21 indicating that the null hypothesis associated with the ANOVA method is void and one of more or the attributes do indeed contribute more to the error than the others.

From the above summary the values indicate that the following attributes have the greatest affect on the error (highest to smallest).

1. Carrier Test 2 - Measures the error when a fixed carrier wave and measures varying vibration displacements
2. Amplitude Test 3 - Measures the error present when the peak amplitude is a time varying value the cycles at varying frequencies
3. Phase Test 1 - This test imparts a phase offset onto the reflect signal.
4. Carrier Test 1 - Measures the error present when the carrier frequency is varied against a unit vibration frequency
5. Carrier Test 3 - Measures the error present when a carrier frequency is measuring a time varying vibration frequency

6. Amplitude Test 2 - Measures the error present when the peak amplitude of the reflected wave is a time varying value in relation to other parameters

7. Amplitude Test 1 - Measures the error present when the peak amplitude of the reflected wave is a static value that is changed in relation to other parameters

7.3 MDACM Data

Table 7.3: MDACM Results summary

MDACM Summary			
Test	Average Error	Std Dev	Variance
Amplitude Test 1	7.998E+09%	2.883E+10%	8.3119E+20%
Amplitude Test 2	5.06E+08%	1.824E+09%	3.3260E+18%
Amplitude Test 3	68.9788%	3.7177%	13.8212%
Carrier Test 1	58.1191%	7.6178%	58.0308%
Carrier Test 2	752.4002%	1760.6719%	3099965.407%
Carrier Test 3	57.9124%	7.5892%	57.5958%
Phase Test 1	53.9529%	0.0891%	0.0079%

Completing the ANOVA analysis of the collected data to identify the impact the attributes have on the error present in the demodulated result the MDACM algorithm had an F-statistic value of 3.766 whilst the F-critical value was 2.12 coupled with a probability value of 0.0012 indicating that the null hypothesis associated with the ANOVA method is void and one or more of the attributes do indeed contribute more to the error than the others.

From the above summary the values indicate that the following attributes have the greatest affect on the error (highest to smallest).

1. Amplitude Test 1 - Measures the error present when the peak amplitude of the reflected wave is a static value that is changed in relation to other parameters

2. Amplitude Test 2 - Measures the error present when the peak amplitude of the reflected wave is a time varying value in relation to other parameters

3. Carrier Test 2 - Measures the error when a fixed carrier wave and measures varying vibration displacements

4. Carrier Test 1 - Measures the error present when the carrier frequency is varied against a unit vibration frequency

5. Carrier Test 3 - Measures the error present when a carrier frequency is measuring a time varying vibration frequency

6. Amplitude Test 3 - Measures the error present when the peak amplitude is a time varying value the cycles at varying frequencies

7. Phase Test 1 - This test imparts a phase offset onto the reflect signal.

7.4 Discussion

From the results collected and analysed, all three of the algorithms under investigation confirmed that the null hypothesis is indeed invalid. This indicates that for each of the algorithms the attributes under test had varying impacts on the demodulated signals error. The testing completed highlighted that one of the most important factors of non contact distance and vibration measurement is the selection of carrier frequency versus the vibration displacement being investigated with this relationship introducing significant error if not adequately selected.

The environmental impacts on the electromagentic wave were summarised into attenuation or amplification and phase manipulation of the reflected waveform. The arctangent algorithm results show that the phase noise added to the reflected waveform introduced an average error of 88.4521% and had a variance of 360.4519% and the varying frequency of amplitude noise inducing an average error of 73.8264% and a variance of 633.7701%. These results show that the arctangent algorithms inherent ability to handle phase noise is better than its ability to handle amplitude frequency noise.

The EDACM algorithms performance resembles that of the artangents in that the algorithms ability to handle amplitude frequency is worse than that of the phase noise with averages of 24736.08% and 76.8260% and variances of 26716.8480% and 4724.1486% respectively.

The MDACM algorithm's results showed that the noise introduced by varying frequency of amplitude was significantly less than that of the artangent or EDACMs algorithm with the MDACM showing considerable suceptibility to static variations in the amplitude of the refelected waveform. The MDACM algorithm results showed the algorithm to be considerably unaffected by phase noise with an average error of 53.9529% and a variance of 0.0079%.

Chapter 8

Empirical Test Rig creation

This section of the report details the design and creation of the emperical test rig.

8.1 Housing & Speaker

Creation of the Chladni plate will involve a horizontally placed speaker that will have it's cone attached to a thin metallic plate. When the speaker is supplied with a signal, the cone will vibrate and the metallic plate will vibrate in time with the speaker's cone. The speaker being used to construct this device is a 50 Watt five inch speaker (Res 2023).

To facilitate the horizontal mounting, the speaker has been fixed to some plyboard via M4 threaded rod and the base of the speaker has been fixed to another piece of plywood with ninety degree brackets. The CAD below and the image showcases how the speaker is fixed.

8.2 Speaker design

In order to ensure the speaker had enough power to vibrate the metallic plate via movement of its cone, a 50W 5 inch speaker (Res 2023) was chosen. The selection of this speaker allowed for the power source to be facilitated via benchtop sources simplifying the design of the vibration source considerably.

In order to control the frequency the speaker cone will vibrate at, a circuit has been designed and built that facilitates full control of the audio signal being transmitted to the speaker. This circuit was designed around the XR-2206 monolithic function generator chip. This integrated circuit is well known in the electrical engineering space as a reliable function generator and suitable for use. Control of the signal amplitude and frequency is facilitated through two potentiometers (EXA July 1997). This translates to being able to directly control the displacement of the cone as well as the frequency of that displacement.

The below circuit shows the XR-2206 IC design (EXA July 1997) that was constructed:

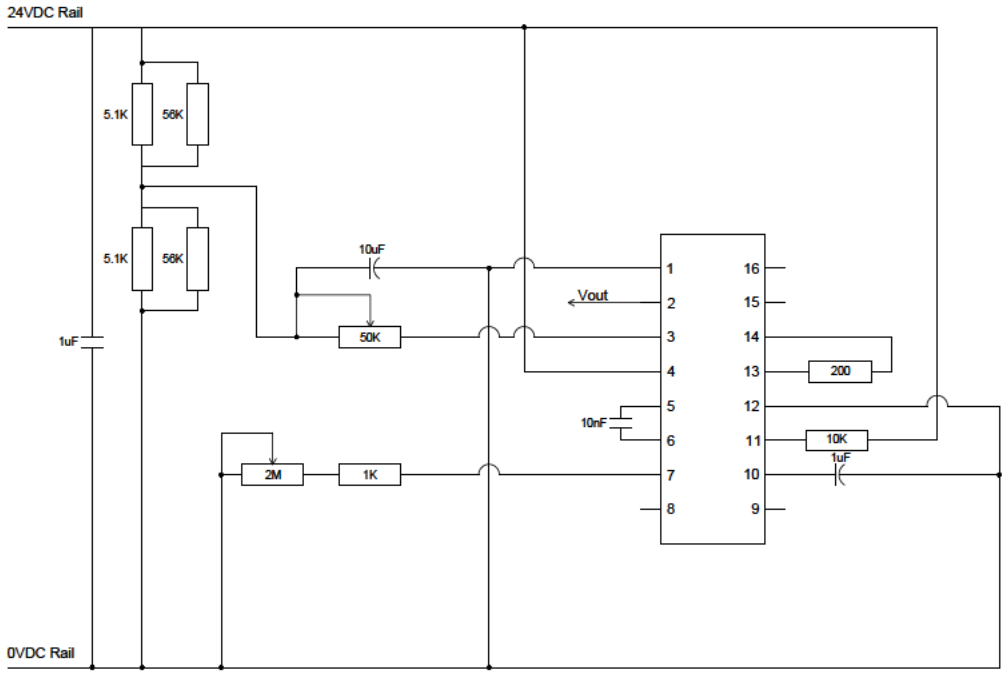

Figure 8.1: XR2206 Function Generator Circuit

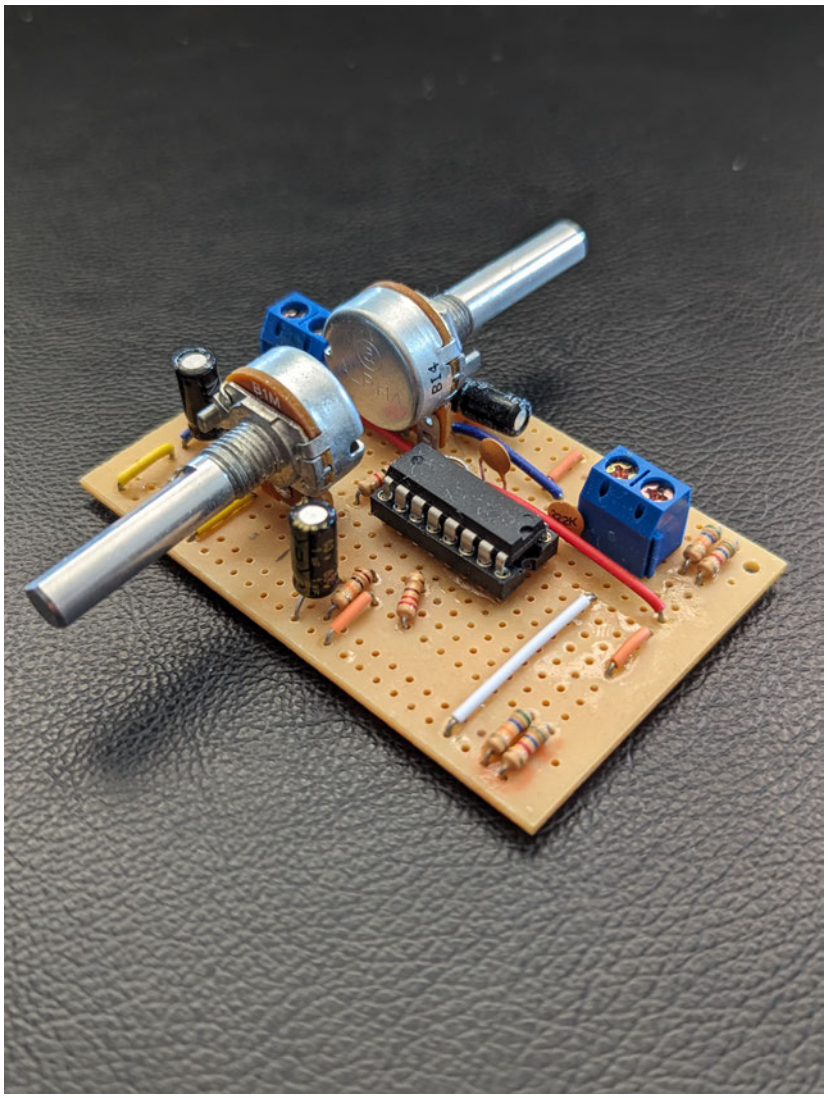

Figure 8.2: Image of the contructed function generator circuit

Amplification of the signal produced by the XR-2206 chip is required so as to adequetly power the 50W speaker. To achieve this a 2N3055 transistor has been used to create a transistor amplifier circuit with the rails being supplied by a Meanwell PSC-160B-C 100W dual rail 24V power supply (MEA 2021).

To measure the vibration being induced in the plate by the speaker an Arduino acelerometer has been used in conjunction with an arduino UNO to measure the acceleration and combined with the time to determine displacement.

8.3 Ultrasonic Sensors

The transmitter and recievers used for the emperical testing are the CUSA-AT75-18-2400-TH and the CUSA-R75-18-2400-TH these sensors were chosen through review of the datasheet determining suitability for application and bench test results showcasing the capability of the units (CUI 2020*a*, CUI 2020*b*). The units will be supplied with a frequency of approx 40kHz (determined by potentiometer accuracy) by a second XR-2206 chip, and will be sampled by a Pico2204 benchtop oscilloscope. The bench top oscilloscope is capable of sampling the sensors at speeds up to 100MHz allowing it to be significantly over specified for the frequency trying to be measured (Pic 2022).

Chapter 9

Conclusions and Further Work

9.1 Conclusions

In conclusion, the results obtained in this research project show that the arctangent and EDACM algorithms are effective at extracting the vibration displacement measurement through the imparted phase shift on a reflected wave when conditions are perfect. This project found that the MDACM algorithm was able to extract the vibration wave profile from the reflected wave, with the resultant demodulation being heavily attenuated when being used to measure vibration displacement under ideal conditions.

The results obtained showed that both the arctangent and EDACM algorithms were able to accurately measure the demodulation with static amplitude noise applied, however when the amplification/attenuation noise applied to the amplitude was time varying both algorithms showed increased error in the result, the EDACM algorithm more so than the Arctangent algorithm due to its arithmetic.

The carrier wave testing highlighted the importance of the correct selection of carrier wave versus the displacement attempting to be measured. The main learning being that the arctangent and EDACM algorithm both showed increases in error when smaller displacements relative to a fixed carrier wavelength were being measured this indicates a limit to the effectiveness of one carrier frequency.

The phase noise testing showed that the arctangent and EDACM algorithms were susceptible to additional phase noise on the reflected signal with all algorithms being adversly

affected by the addition of the noise, with the error introduced by the noise rendering the result unaffective. The MDACM algorithm showed robustness to the addition of phase noise on the signal, with its error varying less than 0.5% through the full 2π range of added noise.

The results of the sampling tests indicated that the more samples per cycle of a waveform the more accurate the demodulated result is. There is a point reached where further computational stress yields negligable error improvement, this was identified as being twenty samples per cycle.

The statistical analysis proved that the algorithms are more susceptible to different sources of noise, and that the different algorithms did handle these noise sources differently. All theoretical results taken, do determine that noise present with any algorithm does yield an unusable result, with each algorithm exceeding acceptable measurement limits at the onset of noise.

Its therefore the conclusion of this project that while the algorithms show large potential and accuracy for measurement in ideal conditions, when introduced to the affects of the elements the usability of this technology and algorithms in there current form drops off. Further investigation into the filtering of noise and additional work to develop the algorithms may yield in a more usable result.

9.2 Project Objectives

9.3 Statement of objectives

Starting this research project objectives were identified that would signify a successful conclusion to this research project The objectives are detailed below with the summary of how each has been achieved.

1. ***Conduct research on algorithms used in the continuous Doppler wave phase demodulation space.*** Research into algorithms avilable for noncontact distance and vibration measurement using the Doppler wave phase demodulation methodology were identified by an extensive literature review in which three algo-

rithms were identified as being suitable for investigation.

2. ***Conduct investigation into adverse environmental impacts on radio/acoustic waves.*** Through literature review the impacts of environmental effects were identified to be attenuation of the reflected signal and an imparted phase shift.

3. ***Investigate appropriate testing configurations and Doppler radio system designs.*** Multiple testing arrangements were investigated in completing this project, the settled upon design for the testing was to be an ultrasonic transmitter/reciever emitting a carrier wave at a thin sheet of aluminium. The induced phase shift on the reflected wave was then recieved by the reciever. Both carrier and reflected wave were measured using a picoscope capturing the waveform data that could then be processed by the algorithms.

4. ***Determine the properties that the algorithms are to be assessed on related to the accuracy of measurement and consistency of performance.*** To determine each algorithms performance through out the testing the root mean square error between the demodulated vibration signal and the known vibration signal was taken. This provided a metric to then assess the impacts each test was having on the results.

5. ***Conceptualize and design test arrangements for both synthetic and real data signals.*** Through the literature review the factors describing the reflected waveform of concern relating to this project, were identified as the amplitude and the phase constant. By varying these values and replicating the behaviour that the environment would have on these parameters the impacts of the environment has been simulated. In addition the carrier frequency attribute, although not directly affected by environmental factors was also included in the investigation as it contributes significantly to the error present in the output. As mentioned above the real data set was to be collected using a chladni setup, and processed using the algorithms.

6. ***Select hardware and a suitable software development environment.*** Hardware selection for the real world data collection rig was selected and details provided. In addition to this the designed circuits have been included with schematics. The testing environment chosen was MATLAB as it has the data processing capability required for this project and was familiar.

7. ***Develop the software algorithms and the synthetic data signals that are to be tested.*** The three algorithms under review were developed in MATLAB and were tested against a known source to confirm accuracy and operation. The synthetic data signal creation resulted in being the manipulation of the reflected waveforms attributes and this was completed with the use of the additive noise model.

8. ***Test demodulation algorithms theoretically in the software environment with synthetic signals to prove understanding and operation of algorithms.*** The testing completed identified the limits of operation of each algorithm, detailing where error is introduced. This provides an understanding of the limitations of operation of each as well showcasing a foundational understanding of how each algorithm operates.

9.4 Further Work

The field of noncontact distance and vibration measurement is a vast field and contains many avenues of research that could be taken to build upon the work completed in this research project. The identified work that could be completed further to this project are as follows:

- Completion of practical testing element associated with this project
- Investigation into filtering tecniques to improve the demodulated result

Bibliography

Abuhdima, E. M. & Saleh, I. M. (2010), Effect of sand and dust storms on microwave propagation signals in southern libya, *in* 'Melecon 2010 - 2010 15th IEEE Mediterranean Electrotechnical Conference', pp. 695–698.
URL: *https://doi.org/10.1109/MELCON.2010.5475995*

Australia, E. (2022), 'Code of Ethics and Guidelines on Proffessional Conduct', PDF on website. [Online; accessed May-01-2023].
URL: *https://www.engineersaustralia.org.au/publications/code-ethics*

CAS & DataLoggers (2016), 'Basic Techniques of Vibration Measurement and Diagnosis', Https://dataloggerinc.com/. [Online; accessed October-02-2022].
URL: *https://dataloggerinc.com/resource-article/basic-techniques-of-vibration-measurement-and-diagnosis/*

Chandrakantha, L. (2014), Learning anova concepts using simulation, *in* 'Proceedings of the 2014 Zone 1 Conference of the American Society for Engineering Education', pp. 1–5.
URL: *https://doi.org/10.1109/ASEEZone1.2014.6820644*

CUI (2020*a*), *ULTRASONIC SENSOR*. Rev. 1.
URL: *https://au.mouser.com/datasheet/2/670/cusa_r75_18_2400_th-2306667.pdf*

CUI (2020*b*), *ULTRASONIC SENSOR*. Rev. 1.
URL: *https://au.mouser.com/datasheet/2/670/cusa_t75_18_2400_th-2306801.pdf*

EXA (July 1997), *Monolithic Function Generator*. Rev. 1.3.
URL: *https://www.sparkfun.com/datasheets/Kits/XR2206_104_020808.pdf*

Fares, M., Fares, S. & Ventrice, C. (1997), Attenuation and phase shift of the electromagnetic waves due to moist snow, *in* 'Proceedings IEEE SOUTHEASTCON '97.

'Engineering the New Century", pp. 109–112. [Online; accessed May-01-2023].
URL: *https://doi.org/10.1109/SECON.1997.598621*

Fluke (2022), 'Most Common Causes of Machine Vibration', Fluke Resource Center. [Online; accessed September-19-2022].
URL: *https://www.fluke.com/en-au/learn/blog/vibration/most-common-causes-of-machine-vibration#: :text=Vibration can accelerate machine wear,issues and diminished working conditions.*

Hanly, S. (2021), '3 Types of Non-Contact Vibration Sensors', Endaq Blog. [Online; accessed September-21-2022].
URL: *https://blog.endaq.com/types-of-non-contact-vibration-sensors*

Hepburn, B. & Andersen, H. (2021), Scientific Method, *in* E. N. Zalta, ed., 'The Stanford Encyclopedia of Philosophy', Summer 2021 edn, Metaphysics Research Lab, Stanford University.
URL: *https://plato.stanford.edu/archives/sum2021/entries/scientific-method/*

Kia, S. H., Henao, H. & Capolino, G.-A. (2009), 'Torsional vibration effects on induction machine current and torque signatures in gearbox-based electromechanical system', *IEEE Transactions on Industrial Electronics* **56**(11), 4689–4699. [Online; accessed September-19-2022].
URL: *https://doi.org/10.1109/TIE.2009.2026772*

Leis, J. W. (2011), *Digital signal processing using MATLAB for students and researchers*, 1st ed. edn, Wiley, Hoboken.
URL: *https://doi.org/10.1002/9781118033623*

Leis, J. W. (2018), *Communication Systems Principles Using MATLAB*, 1 edn, Wiley, Newark.

Li, S., Xiong, Y., Ren, Z., Gu, C. & Peng, Z. (2020), Ultra-micro vibration measurement method using cw doppler radar, *in* '2020 International Conference on Sensing, Measurement & Data Analytics in the era of Artificial Intelligence (ICSMD)', pp. 235–237. [Online; accessed September-15-2022].
URL: *https://doi.org/10.1109/ICSMD50554.2020.9261640*

MEA (2021), *160W Single Output with Battery Charger(UPS Function)*. Rev. 1.
URL: *https://www.meanwell.com/productPdf.aspx?i=506*

Pic (2022), *PicoScope® 2000 Series Like a benchtop oscilloscope, only smaller and better.* Rev. 1.

URL: *https://www.picotech.com/oscilloscope/2000/picoscope-2000-specifications*

Rakshit, R., Roy, D. & Chakravarty, T. (2018), On characterization of vibration measurement using microwave doppler radar, *in* '2018 IEEE SENSORS', pp. 1–4. [Online; accessed October-11-2022].

URL: *https://doi.org/10.1109/ICSENS.2018.8589725*

Res (2023), *Woofer/Midrange Speaker Driver - 5 Inch.* Rev. 1.

URL: *https://www.jaycar.com.au/medias/sys_master/images/images/9959297581086/CW2192-dataSheetMain.pdf*

Sadiku, M. N. O. (2018), *Elements of electromagnetics*, The Oxford series in electrical and computer engineering, seventh edition. edn, Oxford University Press, New York. [Textbook; accessed May-07-2023].

Sauro, J. (2015), '5 Advanced Stats Techniques & When to Use Them'.

URL: *https://https://measuringu.com/advanced-stats/*

Sen, A., Majumder, M. C., Mukhopadhyay, S. & Biswas, R. K. (2017), 'Condition Monitoring of Rotating Equipment Considering the Cause and effects of Vibration: A Brief Review'. [Online; accessed September-18-2022].

URL: *https://d1wqtxts1xzle7.cloudfront.net/53754001/F7113649-with-cover-page-v2.pdf?Expires=1663495882&Signature=gPNNlr33DhZvBqlTznJEheOnEPQT0G1yOTmVutVRQrxwb*
pqr6TG592iQVIgEJ0PCL5eROcckKReazAcAyTkFXXUfpnCAHLjdDQtZ3hvZXf7hbaujY5pfQGIB0Agu
Pair-Id=APKAJLOHF5GGSLRBV4ZA

Singh, H., Bonev, B., Petkov, P. & Kumar, R. (2018), A novel approach for predicting attenuation of radio waves caused by rain, *in* '2018 2nd IEEE International Conference on Power Electronics, Intelligent Control and Energy Systems (ICPEICES)', pp. 1193–1198.

URL: *https://doi.org/10.1109/ICPEICES.2018.8897481*

Union, I. T. (n.d.), Propagation data and prediction methods required for the design of earth-space telecommunication systems, Technical report.

Wang, J., Wang, X., Chen, L., Huangfu, J., Li, C. & Ran, L. (2014), 'Noncontact distance and amplitude-independent vibration measurement based on an extended dacm algorithm', *IEEE Transactions on Instrumentation and Measurement* **63**(1), 145–153.

[Online; accessed September-15-2022].

URL: *https://doi.org/10.1109/TIM.2013.2277530*

Wright, J. (2010), 'What Causes Machinery Vibration?', Machinery Lubrication. [Online; accessed September-21-2022].

URL: *https://www.machinerylubrication.com/Read/25974/signs-tips-machinery-vibration#: :text=Unchecked machine vibration can accelerate,and may damage product quality.*

Xiong, Y., Chen, S., Dong, X., Peng, Z. & Zhang, W. (2017), 'Accurate measurement in doppler radar vital sign detection based on parameterized demodulation', *IEEE Transactions on Microwave Theory and Techniques* **65**(11), 4483–4492. [Online; accessed October-09-2022].

URL: *https://doi.org/10.1109/TMTT.2017.2684138*

Xu, W., Gu, C. & Mao, J.-F. (2020), Noncontact high-linear motion sensing based on a modified differentiate and cross-multiply algorithm, *in* '2020 IEEE/MTT-S International Microwave Symposium (IMS)', pp. 619–622. [Online; accessed October-9-2022].

URL: *https://doi.org/10.1109/IMS30576.2020.9223896*

Zhang, L., Fu, C.-H., Zhuang, Z., Yang, X., Ding, G., Hong, H. & Zhu, X. (2022), 'Kalman filter and cross-multiply algorithm with adaptive dc offset removal', *IEEE Transactions on Instrumentation and Measurement* **71**, 1–10.

URL: *https://doi.org/10.1109/TIM.2022.3147317*

Chapter 10

Appendices

10.1 Appendix A - Project Specification

ENG 4111/2 Research Project

Project Specification

For:	**Matthew Boden**
Title:	Non-Contact Distance and Vibration Measurement
Major:	Electrical and Electronic Engineering
Supervisors:	John Leis
Enrolment:	ENG4111 - EXT S1, 2023 ENG4111 - EXT S2, 2023
Project Aim:	The aim of this project is to investigate the different algorithms related to the demodulation of phase encoded distance and vibration data and to then test the performance of the algorithms in adverse conditions. These conditions include high heat environments, atmospheres that are contaminated with dust particles, atmospheres subject to multiple sources of interference. To accomplish this the project will have two main points of focus, the first being the Implementation and testing of the algorithms using synthetic data and the second will be the use of the created algorithms on real data.

Programme: Version 1.0, 12^{th} **March 2023**

1. Conduct background research on algorithms used in the continuous Doppler wave phase demodulation space.
2. Conduct investigation into adverse environmental impacts on radio/acoustic waves.
3. Investigate appropriate testing configurations, and Doppler radio system designs.
4. Determine the properties that the algorithms are to be assessed on related to the accuracy of measurement and consistency of performance.
5. Conceptualize and design test arrangements for both synthetic and real data signals.
6. Select hardware and a suitable software development environment.
7. Develop the software algorithms and the synthetic data signals that are to be tested.
8. Test demodulation algorithms theoretically in software environment with synthetic signals to prove understanding and operation of algorithms.

As time and resources permit:

1. Complete testing of algorithms using real world data in place of synthetic data.
2. Process and evaluate data from tests and recommend methods of improving algorithm performance.

10.2 Appendix B

UniSC

Risk Assessment [Ref Number: 2691] - Live

Date Printed: Thursday, 6 July 2023

Name	Boden_Matthew_DissertationRA	Current Rating	Residual Rating
		Low	Low
Location	Off Campus: Toowoomba, Private Residence		

Business Unit	Last Review Date	Risk Owner
School of Engineering	3/07/2023	Matt Boden

Risk Assessment Team	Risk Approver
John Leis	John Leis

Additional Notes

Describe task / use

Beng dissertation project, relating to the testing and data collection of phase demodulation algorithms used to interpret vibration data from a continuous Doppler wave form.

ENG4111 and ENG4112 are the courses this relates to.

Risk Factors

Risk Factor	Electrical

Description

Access to power to facilitate use of equipment, Battery usage for electronics.

Environmental tests provide access to usage of electronics in a wet environment.

Voltages that will present through out the experimentation include the following: 240Vac outlets, 5-24VDC control circuitry and microcontroller.

- Does the work involve:
- Low Voltage Electricity -- Yes
- Static Electricity -- Yes
- Stored Electricity e.g. batteries -- Yes
- Could hazards be caused by:
- Exposed electrical parts? -- Yes
- Faulty equipment or appliances? -- Yes
- Incorrect installation? -- Yes
- Overloaded circuits? -- Yes
- Will the work be affected by the loss of power? -- No
- Will electricity be used in wet or potentially wet conditions? -- Yes

Low	Very Low		
Existing Controls	**Proposed Controls**		
• 4 - Engineering: Low voltage equipment designed and constructed to AS3000, preventing general access to exposed live parts	Description	Responsibility	Target Date
	Where possible low voltage equipment use will be minimised.		31/10/2023
	Where needed access/work to low voltage equipment will be limited to licensed electricians.		31/10/2023
	IP68 rated equipment will be used to mitigate the risk introduced by a wet environment. RCD protected circuits will be used to supply power to all equipment.		31/10/2023

Risk Factor	Mechanical and Fixed Plant

Description

The experiment rig being created will utilise fans and pumps to create the atmospheric requirements for testing.

- Is there the potential for:
- Crushing and pinch points? -- Yes
- Moving and rotating equipment? -- Yes
- Stored Energy? -- Yes
- Wearing / Scraping? -- Yes
- Could hazards be caused by equipment or structural failure? -- No

Low	Very Low		
Existing Controls	**Proposed Controls**		
• 4 - Engineering: Fans and motors being used are generally covered by a shield to prevent access.	Description	Responsibility	Target Date
	Use of rotating equipment will be restricted to installation behind a barrier that will protect user from any objects.		31/10/2023
	Pinch points will be clearly marked with appropriate warning labels to prevent access.		31/10/2023
	An exclusion zone will be established around test site to prevent unintended entry.		31/10/2023
	Appropriate PPE will be used to protect the user. - Face Shield - Gloves		31/10/2023

Risk Factor	Lighting

Description

The test rig will use a perspex material to create an enclosed environment. This has the potential to reflect the light in the test space. The test space lighting needs to be adequate enough to allow for proper utilisation of the equipment.

- Is there the potential for:
- Glare? -- Yes
- Low level lighting? -- Yes

Low	Low		
Existing Controls	**Proposed Controls**		
• No existing controls required: No existing controls	Description	Responsibility	Target Date
	Correct wattage bulbs will be used to ensure a 160lux environment as specified in the "Managing the work environment and facilities code of practice 2021".		31/10/2023
	Use of tinted safety glasses will minimize the effects of glare to acceptable levels.		31/10/2023

Risk Factor	Thermal, Fire and Explosion

Description

In creating the environment for the testing, there is a need to create and environment with an elevated temperature

- Is there the potential for:
- Contact with hot or cold object, surface, liquid or gas -- Yes
- Extremes of heat or cold including personal exposure -- Yes
- Fire – Equipment, vehicle or building -- Yes
- Radiant Heat -- Yes
- Will hot works be performed? e.g. welding and grinding -- No

Low	Very Low		
Existing Controls	**Proposed Controls**		
• 4 - Engineering: Heaters and thermal elements are enclosed behind frames that prevent direct contact.	Description	Responsibility	Target Date
	Use of heating equipment will be restricted to installation behind a barrier that will protect user.		31/10/2023
	An exclusion zone will be established around test site to prevent unintended entry.		31/10/2023
	Appropriate PPE will be used to protect the user. - Long sleeve shirts - Gloves		31/10/2023

Risk Factor	Other

Description

Equipment Failure - Electronics being used are susceptible to damage from voltage spikes and over current that may be present when incorrect connection or short circuit occurs.

- -- --

10.3 Appendix C

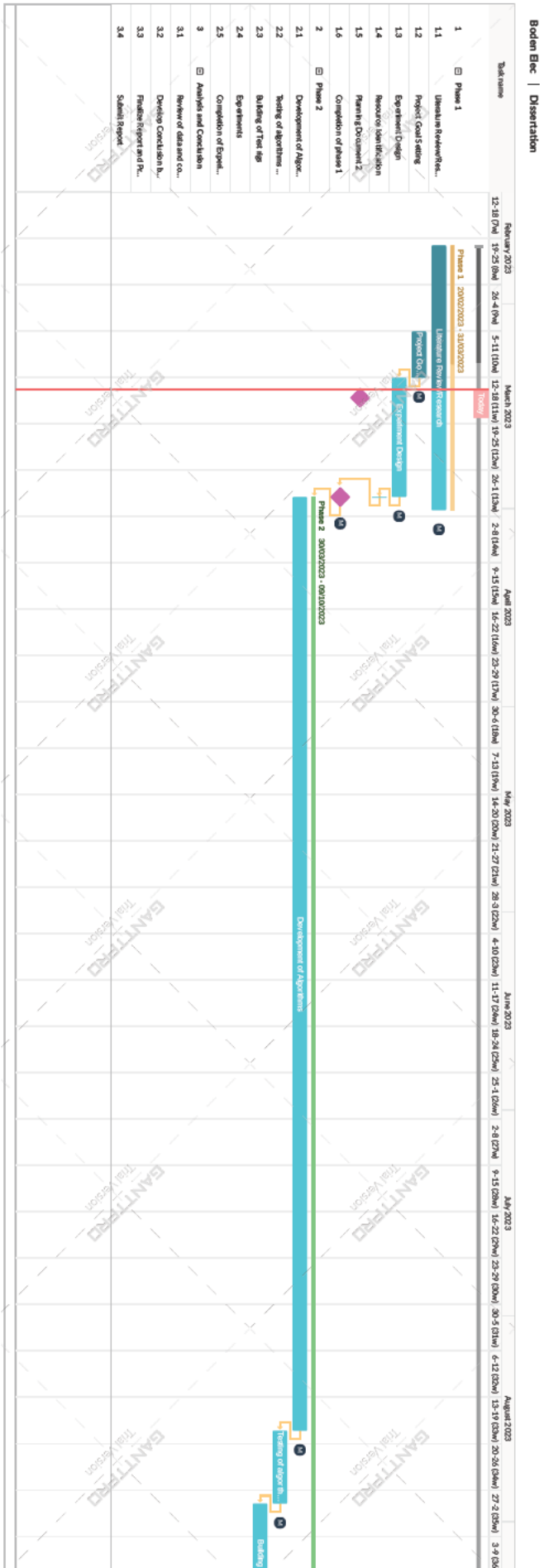

10.4 Appendix D - Arctangent Algorithm Code

```
function error = ATAN(N,Tmax,fc,fm,k,A,t,Theta)

    %Author:Matthew Boden
    %Date: 17/08/2023
    %Project: Noncontact and distance vibration measurement
    %Description: This script creates the Arctangent

    %Reference:
    %J.Leis, "Communication Systems Principles Using Matlab", 2018, Page 22
    %% Initialisation
    %% Variable
    v = 2.998*10^8;

    %%
    %carrier signal creation
    wc = 2*pi*fc;               %omega of carrier
    xc = cos(wc*t);             %creation of carrier signal
    lambda = (v/fc);          %calcualting the wavelength of the carrier

    %%
    %PM modulation
    wm = 2*pi*fm;            %omega of vibration
    Am = 1;                  %amplitude of vibration signal
    xm = Am*sin(wm*t);       %creation of vibration signal

    %%
    %modulation parameteres
    %displacement
    k = lambda/k;
    alpha = (4*pi*k)/lambda;

    %%
    %Noise
    Noise = Theta;

    %%
    %phase modulation equation
    xpm = A.*cos(wc*t + (alpha*xm) + Noise);

    %%
    %displacement actual calculation
    dispact = (lambda/(4*pi))*(alpha.*xm);
    dispmax = (lambda/(4*pi))*alpha;

    %% Setting Filter parameters
    window = floor((1/(fc))/((Tmax)/(N)));
    b = (1/window)*ones(1,window);
    a = 1;
    %%
    %PM Demodulation
    I = cos(wc*t).*xpm;        %Creation of in phase Quadrature Signal
    I = filter(b,a,I);
    Q = sin(wc*t).*xpm;        %Creation of phase shifted Quadrature Signal
    Q = filter(b,a,Q);

    %multiply by -1 to phase shift 180 to be in phase with source
    d = -1*atan(Q./I);
    %Converting the phaseshift waveform extracted by Arctan into displacement
```

```
    % in meters
    dmeas = ((lambda/(4*pi))*d);

    %determining maximum value of calculated displacement waveform
    Dispmeas = sqrt((2/length(d))*sum(dmeas.^2));

    %% Error Calcualtion
    %error = ((dispmax-Dispmeas)/dispmax)*100;

    %NRMSE
    error = ((sqrt((sum((dispact-dmeas).^2))/(length(dispact))))/dispmax)*100;

end
```

10.5 Appendix E - EDACM Algorithm Code

```
function error = DACM(N,Tmax,fc,fm,k,A,t,Theta)
    %Author:Matthew Boden
    %Date: 20/05/2023
    %Project: Noncontact and distance vibration measurement
    %Description: This script creates the vibration signal with noise
    %parameters applied - DACM

    %Reference:
    %J.Leis, "Communication Systems Principles Using Matlab", 2018, Page 22

    %Change Log:
    %% Initialisation
    %% Variable definition
    v = 2.998*10^8;

    %% Carrier signal creation
    wc = 2*pi*fc;             %omega of carrier
    xc = cos(wc*t);           %creation of carrier signal
    lambda = (v/fc);          %calculating the wavelength of the carrier

    %% Waveform creation for vibration
    %
    wm = 2*pi*fm;             %omega of vibration
    Am = 1;                   %amplitude of vibration signal
    xm = Am*sin(wm*t);        %creation of vibration signal

    %Displacement
    k = lambda/k;

    %% Modulation parameteres
    %
    alpha = (4*pi*k)/lambda;            %Displacement set to an eight of a ↙
wavelength
    %% Noise Models
    %
    Noise = Theta;               %Offset due to hardware or noise

    %% Phase Modulation Equation (reflected waveform)
    %
    xpm = A.*cos(wc*t + (alpha*xm) + Noise);   %currently set to a fixed displacement

    %% Actual Displacement Value
    %
    dispact = (lambda/(4*pi))*(alpha.*xm);   %division by 1000 to change to km
    dispmax = (lambda/(4*pi))*alpha;         %Peak displacement shown by xm sin wave

    %% Filter Parameters
    window = floor((1/(fc))/((Tmax)/(N)));
    b = (1/window)*ones(1,window);
    a = 1;
    %% Creation and Calibration of IQ signals
    I = cos(wc*t).*xpm;                      %Creation of in phase Quadrature Signal
    I = filter(b,a,I);

    Q = sin(wc*t).*xpm;                      %Creation of phase shifted Quadrature ↙
Signal
    Q = filter(b,a,Q);
```

```
    %% Matrix manipulation for Vectorisation
    Ifd = [I(1,2:end) 0];
    Qfd = [Q(1,2:end) 0];
    %% Phase Demodulation Algorithm - EDACM
    %
    %EDACM
    %Calculation of differentiation
    w = ((Ifd.*(Qfd-Q))-(Qfd.*(Ifd-I)))./((I.^2)+(Q.^2)); %
    %Accumulation of differentiation
    O = cumsum(w);
    %displacement waveform
    x = -1*((lambda*O)/(4*pi));  %mulitply by -1 to add 180degree phase shift

    %determining maximum value of calculated displacement waveform
    Dispmeas = sqrt((2/length(x))*sum(x.^2));

    %% Error Calculation
    %error = ((dispmax-Dispmeas)/dispmax)*100;
    %NRMSE
    error = ((sqrt((sum((dispact-x).^2))/(length(dispact))))/dispmax)*100;
end
```

10.6 Appendix F - MDACM Algorithm Code

```
function error = MDACM(N,Tmax,fc,fm,k,A,t,Theta)
    %Author:Matthew Boden
    %Date: 20/05/2023
    %Project: Noncontact and distance vibration measurement
    %Reference:
    %J.Leis, "Communication Systems Principles Using Matlab", 2018, Page 22

    %Change Log:
    %% Initialisation
    %% Variable
    v = 2.998*10^8;

    %% carrier signal creation
    wc = 2*pi*fc;           %omega of carrier
    xc = cos(wc*t);         %creation of carrier signal
    lambda = (v/fc);         %calculating the wavelength of the carrier

    %% PM modulation
    wm = 2*pi*fm;           %omega of vibration
    Am = 1;                 %amplitude of vibration signal
    xm = Am*sin(wm*t);      %creation of vibration signal

    %% Noise Models
    Noise = Theta;                  %Offset due to hardware or noise

    %% Modulation parameteres
    %
    %Displacement
    k = lambda/k;
    alpha = (4*pi*k)/lambda;
    %% phase modulation equation (reflected waveform)
    xpm = A.*cos(wc*t + (alpha*xm) + Noise);

    %% Actual Displacement Value
    dispact = (lambda/(4*pi))*(alpha.*xm);   %division by 1000 to change to km
    dispmax = (lambda/(4*pi))*alpha;         %Peak displacement shown by xm sin wave

    %% Filter Parameters
    window = floor((1/(fc))/((Tmax)/(N)));
    b = (1/window)*ones(1,window);
    a = 1;

    %% Creation and Calibration of IQ signals
    I = cos(wc*t).*xpm;                     %Creation of in phase Quadrature Signal
    I = filter(b,a,I);
    Q = sin(wc*t).*xpm;                     %Creation of phase shifted Quadrature ↙
Signal
    Q = filter(b,a,Q);

    %% Phase Demodulation
    %MDACM
    for K = 2:length(I)
        w(K) = (I(K-1)*Q(K))-(Q(K-1)*I(K));
    end
    %w = filter(b,a,w);
    w = w - mean(w);
    %Accumulation of w
    O = cumsum(w);
```

```
    %Displacement
    x = -1*((O.*lambda)/(4*pi));

    %determining maximum value of calculated displacement waveform
    Dispmeas = sqrt((2/length(x))*sum(x.^2));

    %% Error Calculation
    %error = ((dispmax-Dispmeas)/dispmax)*100;
    %NRMSE
    error = ((sqrt((sum((dispact-x).^2))/(length(dispact))))/dispmax)*100;

end
```

10.7 Appendix H - Carrier Frequency Test Sequence - Code

Carrier Test sequence

Setting test parameters to run through.

```
%% Test Script to run tests on Atan Function
clc
clear all
close all

%% Parameter Definition
Testrange = logspace(-1,5);
%Setting amplitude of reflected wave default
A = 1;
%Setting Carrier Frequency default
fc = 20;
%Setting Modulation frequency default
fm = 1;
%setting displacement of frequency default  (lambda/k)
k = 8;
%Setting run time of simulation and setting parameters so that each cycle
%of carrier frequency is created with a set number of points.
Tmax = 20;

%%Setting phase noise.
Theta = 0;

%filepath 'F:\My Drive\Thesis\ENG4111 - Research Project Semester 1\Progress Report\Progress Re
```

Test 1

Analysis of error present when carrier frequency is varied against a unit vibration frequency.

$x_c(t) = A_c * \sin(w_c t)$

where

A_c is the amplitude peak value

w_c is the angular velocity equal to $2\pi f_c$

t is the time sequence

```
%% test 1
for C = 1:length(Testrange)
    Nfreq = Tmax/(1/Testrange(C));
    N = Nfreq*20;
    dt = Tmax/(N-1);
    t = 0:dt:Tmax;
    ATTest1Er(C) = ATAN(N,Tmax,Testrange(C),fm,k,A,t,Theta);
    DACMTest1Er(C) = DACM(N,Tmax,Testrange(C),fm,k,A,t,Theta);
    MDACMTest1Er(C) = MDACM(N,Tmax,Testrange(C),fm,k,A,t,Theta);
end
```

Plotting:

```
%Plot of Test1
txt = "ArcTan_Carrier_Testing_Test1";
EDtxt = "DACM_Carrier_Testing_Test1";
MDtxt = "MDACM_Carrier_Testing_Test1";

% Error Plotting
    figure
    semilogx(Testrange,ATTest1Er);
    grid on
    title("Carrier Frequency vs Error with unit vibration frequency");
    xlabel("Carrier Frequency (Hz)");
    ylabel("NRMSE (%)");
    ax = gca;
    exportgraphics(ax,'F:\My Drive\Thesis\ENG4111 - Research Project Semester 1\Progress Report
```

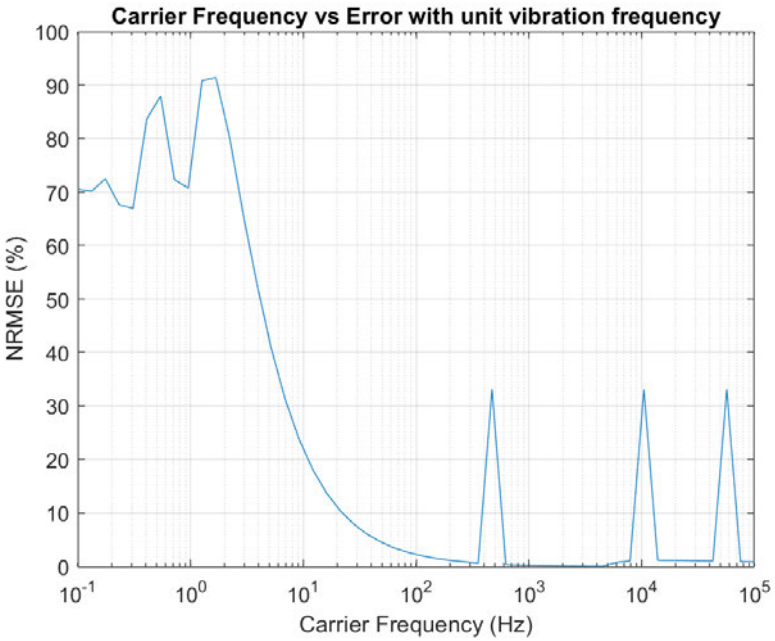


```
    writematrix(ATTest1Er','ArcTan_Results\' + txt + '.xlsx');

 % Error Plotting
    figure
    semilogx(Testrange,DACMTest1Er);
    grid on
    title("Carrier Frequency vs Error with unit vibration frequency");
    xlabel("Carrier Frequency (Hz)");
    ylabel("NRMSE (%)");
    ax = gca;
```

```
exportgraphics(ax,'F:\My Drive\Thesis\ENG4111 - Research Project Semester 1\Progress Report
```

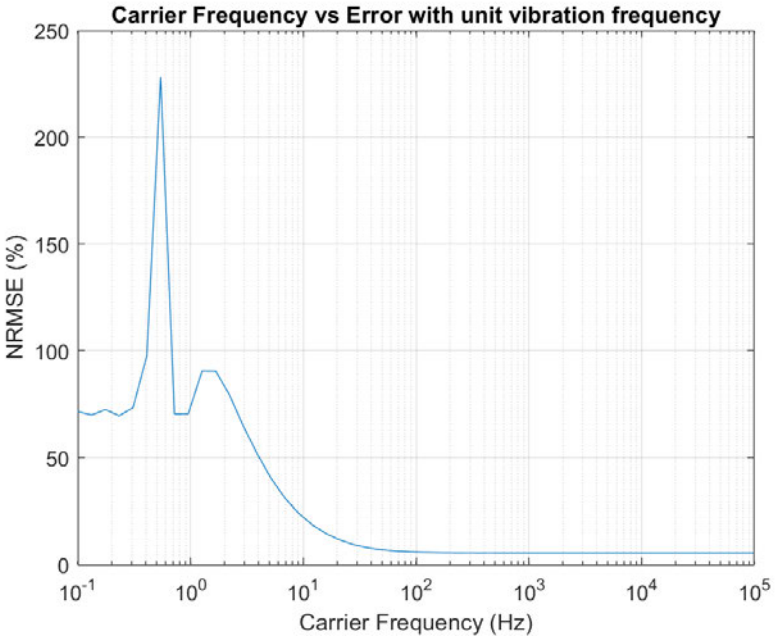


```
writematrix(DACMTest1Er','DACM_Results\' + EDtxt + '.xlsx');

 % Error Plotting
figure
semilogx(Testrange,MDACMTest1Er);
grid on
title("Carrier Frequency vs Error with unit vibration frequency");
xlabel("Carrier Frequency (Hz)");
ylabel("NRMSE (%)");
ylim([0 100]);
ax = gca;
exportgraphics(ax,'F:\My Drive\Thesis\ENG4111 - Research Project Semester 1\Progress Report
```

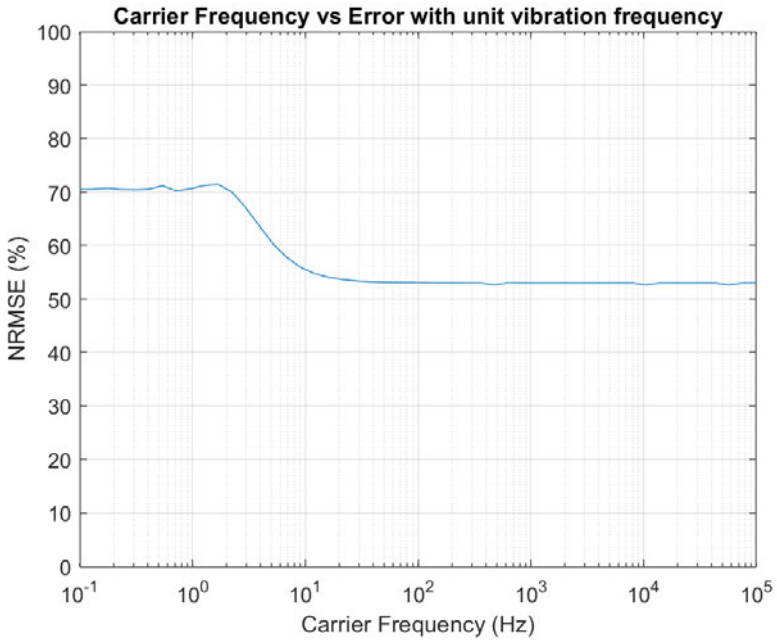


```
    writematrix(MDACMTest1Er','MDACM_Results\' + MDtxt + '.xlsx');
```

Test 2

This test identifies the relationship between the carrier frequencies wavelength and the displacement of the vibration being measured. The carrier frequency will be a fixed value with the displacement being a fraction of the carriers wavelength represented by $\frac{\lambda}{k}$ where k varies between $0.1...10^6$. Completing this test will identify each algorithms sensitivity to phase shift which relates to the displacement being measured.

```
%% test 2
Nfreq = Tmax/(1/fc);
N = Nfreq*20;
dt = Tmax/(N-1);
t = 0:dt:Tmax;

for C = 1:length(Testrange)
    ATTest2Er(C) = ATAN(N,Tmax,fc,fm,Testrange(C),A,t,Theta);
    DACMTest2Er(C) = DACM(N,Tmax,fc,fm,Testrange(C),A,t,Theta);
    MDACMTest2Er(C) = MDACM(N,Tmax,fc,fm,Testrange(C),A,t,Theta);
end
```

Plotting:

```
%Plot of Test1
txt = "ArcTan_Carrier_Testing_Test2";
```

```
EDtxt = "DACM_Carrier_Testing_Test2";
MDtxt = "MDACM_Carrier_Testing_Test2";

% Error Plotting
    figure
    semilogx(Testrange,ATTest2Er);
    grid on
    title("Fixed Carrier Frequency vs Vibration Displacement");
    xlabel("Vibration Displacement $\frac{\lambda}{x}$","Interpreter","latex");
    ylabel("NRMSE (%)");
    ylim([0 100]);
    ax = gca;
    exportgraphics(ax,'F:\My Drive\Thesis\ENG4111 - Research Project Semester 1\Progress Report
```

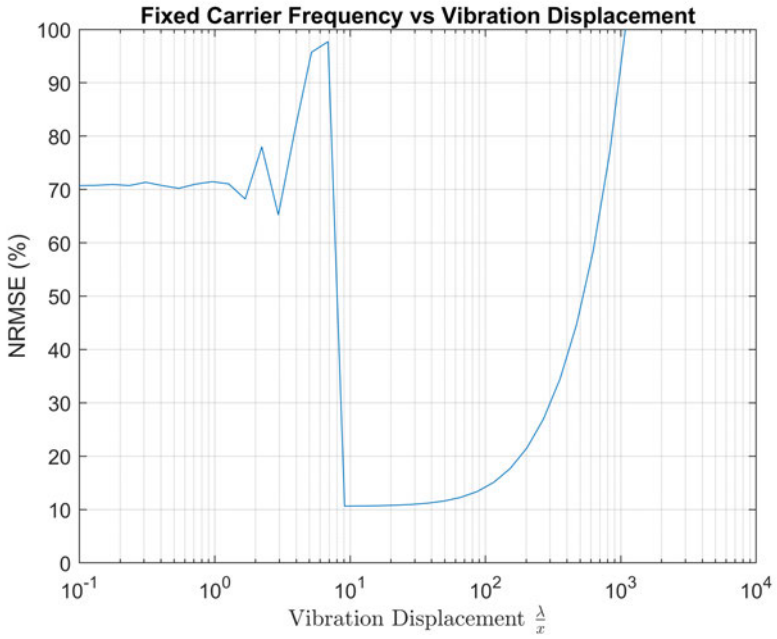


```
    writematrix(ATTest2Er','ArcTan_Results\' + txt + '.xlsx');

    figure
    semilogx(Testrange,ATTest2Er);
    grid on
    title("Fixed Carrier Frequency vs Vibration Displacement");
    xlabel("Vibration Displacement $\frac{\lambda}{x}$","Interpreter","latex");
    ylabel("NRMSE (%)");
    ylim([0 100]);
    ax = gca;
    exportgraphics(ax,'F:\My Drive\Thesis\ENG4111 - Research Project Semester 1\Progress Report
```

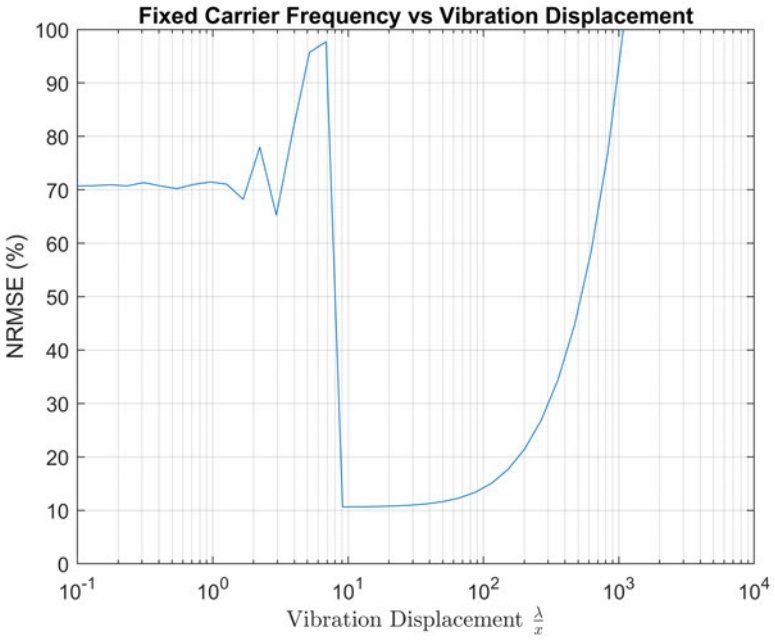


```
figure
semilogx(Testrange,ATTest2Er);
grid on
title("Fixed Carrier Frequency vs Vibration Displacement");
xlabel("Vibration Displacement $\frac{\lambda}{x}$","Interpreter","latex");
ylabel("NRMSE (%)");
ylim([0 100]);
ax = gca;
exportgraphics(ax,'F:\My Drive\Thesis\ENG4111 - Research Project Semester 1\Progress Report
```

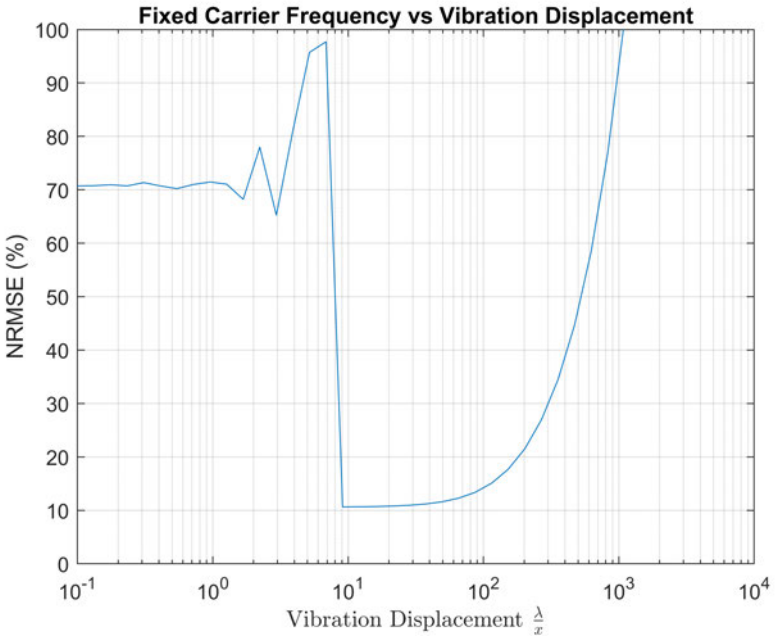


```
% Error Plotting
    figure
    semilogx(Testrange,DACMTest2Er);
    grid on
    title("Fixed Carrier Frequency vs Vibration Displacement");
    xlabel("Vibration Displacement $\frac{\lambda}{x}$","Interpreter","latex");
    ylabel("NRMSE (%)");
    ylim([0 100]);
    ax = gca;
    exportgraphics(ax,'F:\My Drive\Thesis\ENG4111 - Research Project Semester 1\Progress Report
```

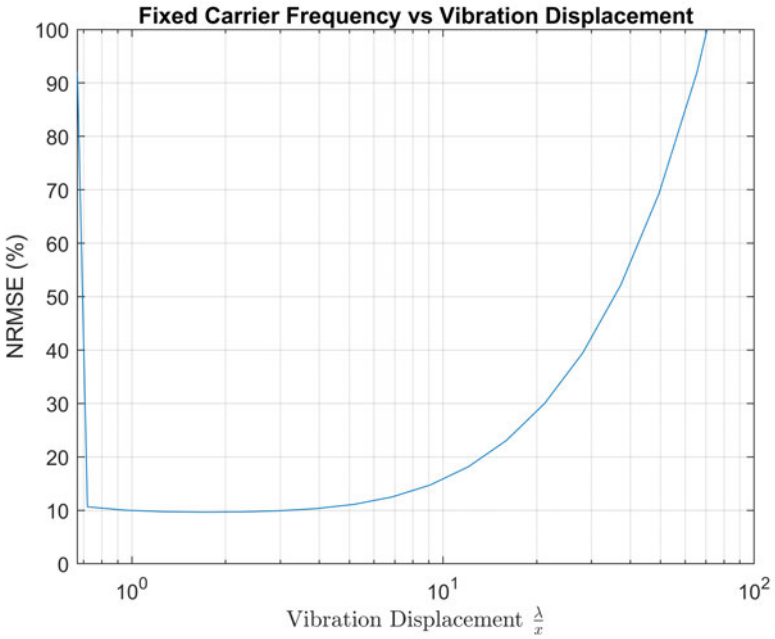


```
writematrix(DACMTest2Er','DACM_Results\' + EDtxt + '.xlsx');

 % Error Plotting
figure
semilogx(Testrange,DACMTest2Er);
grid on
title("Fixed Carrier Frequency vs Vibration Displacement");
xlabel("Vibration Displacement $\frac{\lambda}{x}$","Interpreter","latex");
ylabel("NRMSE (%)");
ylim([0 100]);
ax = gca;
exportgraphics(ax,'F:\My Drive\Thesis\ENG4111 - Research Project Semester 1\Progress Report
```

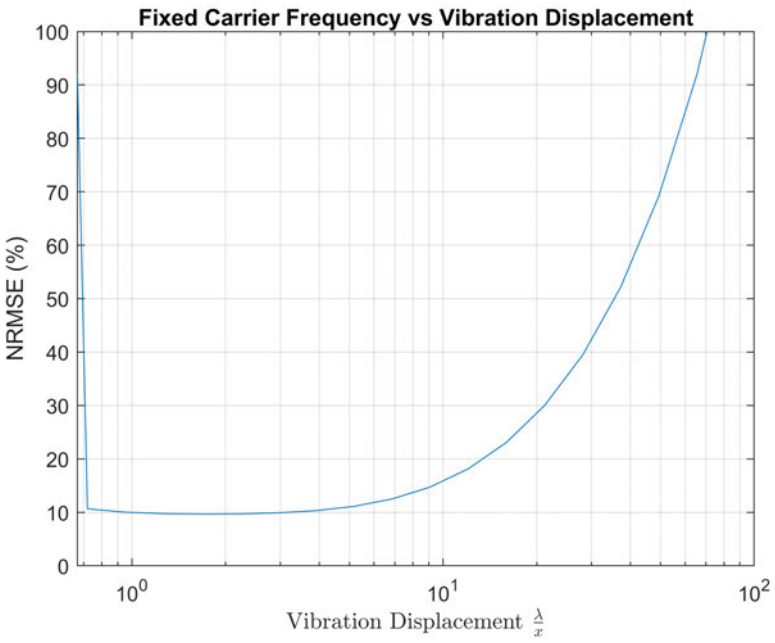


```
 % Error Plotting
figure
semilogx(Testrange,DACMTest2Er);
grid on
title("Fixed Carrier Frequency vs Vibration Displacement");
xlabel("Vibration Displacement $\frac{\lambda}{x}$","Interpreter","latex");
ylabel("NRMSE (%)");
ylim([0 100]);
ax = gca;
exportgraphics(ax,'F:\My Drive\Thesis\ENG4111 - Research Project Semester 1\Progress Report
```

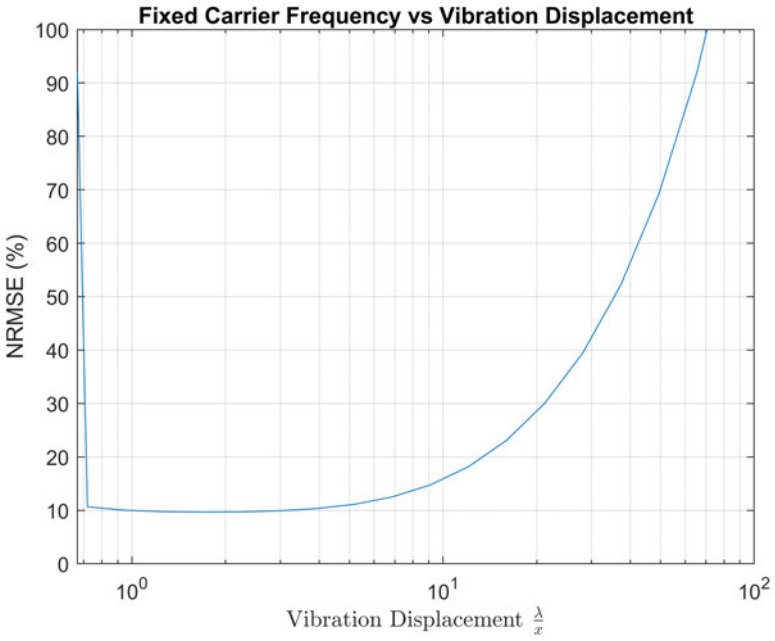


```
% Error Plotting
figure
semilogx(Testrange,MDACMTest2Er);
grid on
title("Fixed Carrier Frequency vs Vibration Displacement");
xlabel("Vibration Displacement $\frac{\lambda}{x}$","Interpreter","latex");
ylabel("NRMSE (%)");
ylim([0 100]);
ax = gca;
exportgraphics(ax,'F:\My Drive\Thesis\ENG4111 - Research Project Semester 1\Progress Report
```

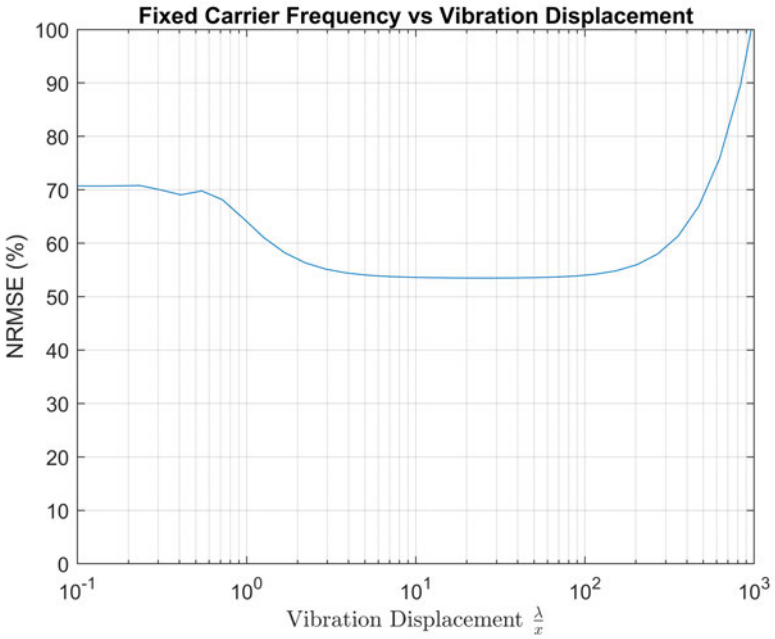


```
writematrix(MDACMTest2Er','MDACM_Results\' + MDtxt + '.xlsx');

    % Error Plotting
figure
semilogx(Testrange,MDACMTest2Er);
grid on
title("Fixed Carrier Frequency vs Vibration Displacement");
xlabel("Vibration Displacement $\frac{\lambda}{x}$","Interpreter","latex");
ylabel("NRMSE (%)");
ylim([0 100]);
ax = gca;
exportgraphics(ax,'F:\My Drive\Thesis\ENG4111 - Research Project Semester 1\Progress Report
```

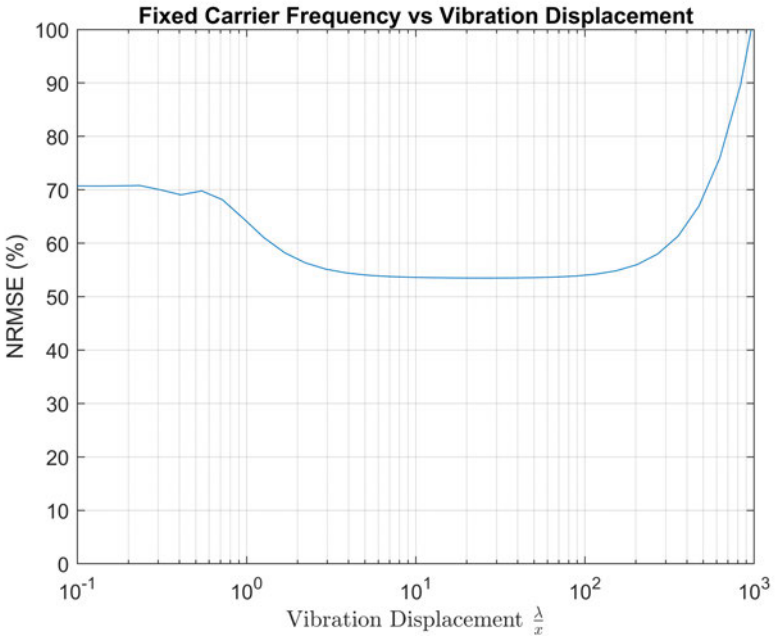

Test 3

This test identifies the relationship between error carrier frequency and a time varying vibration frequency .This test aims to replicate the effects of potential noise or time varying vibrations as is the case found with most machinery. The carrier frequency will be varied between $0.1...10^6$ hertz to showcase the relationship adequately.

```
%Creation of time ranges for waveform creation, A second range is required
%for the creation of the vibration signal as it is operating at differnet
%frequencies compared to the carrier wave form.


for C = 1:length(Testrange)
    Nfreq = Tmax/(1/Testrange(C));
    N = Nfreq*20;
    dt = Tmax/(N-1);
    t = 0:dt:Tmax;
    fm = 1*cos(2*pi*fc);
    ATTest3Er(C) = ATAN(N,Tmax,Testrange(C),fm,k,A,t,Theta);
    DACMTest3Er(C) = DACM(N,Tmax,Testrange(C),fm,k,A,t,Theta);
    MDACMTest3Er(C) = MDACM(N,Tmax,Testrange(C),fm,k,A,t,Theta);
end
```

Plotting:

```
%Plot of Test1
txt = "ArcTan_Carrier_Testing_Test3";
EDtxt = "DACM_Carrier_Testing_Test3";
MDtxt = "MDACM_Carrier_Testing_Test3";

% Error Plotting
    figure
    semilogx(Testrange,ATTest3Er);
    grid on
    title("Carrier Frequency vs Error with unit vibration with varying frequency");
    xlabel("Carrier Frequency (Hz)");
    ylabel("NRMSE (%)");
    ax = gca;
    exportgraphics(ax,'F:\My Drive\Thesis\ENG4111 - Research Project Semester 1\Progress Report
```

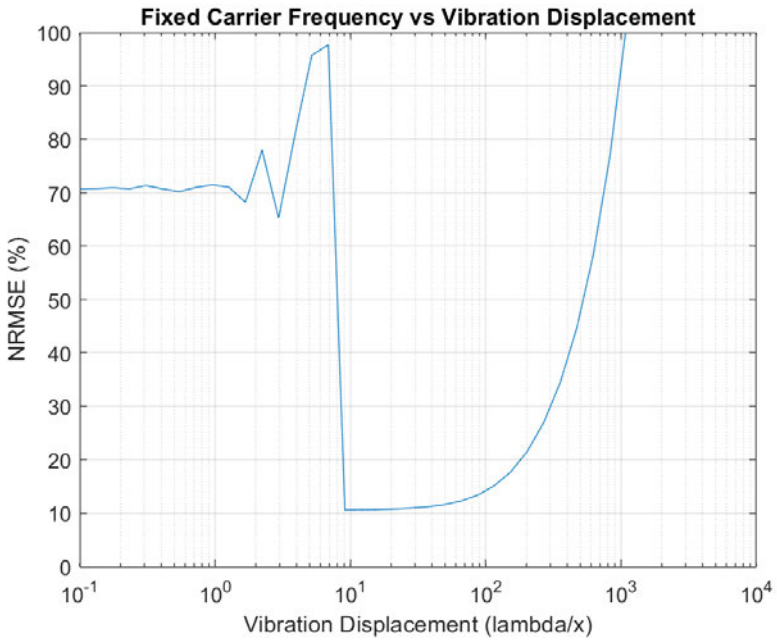

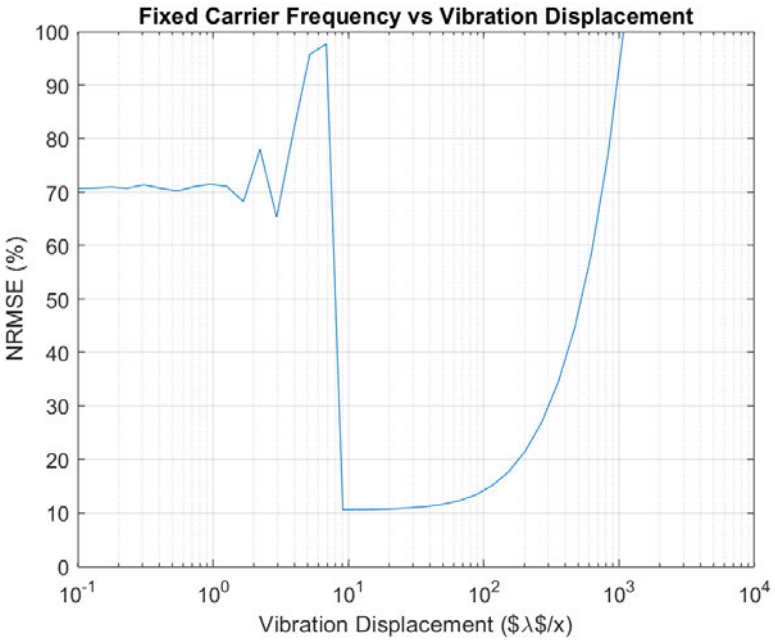
Fixed Carrier Frequency vs Vibration Displacement
NRMSE (%)
Vibration Displacement ($λ$/x)

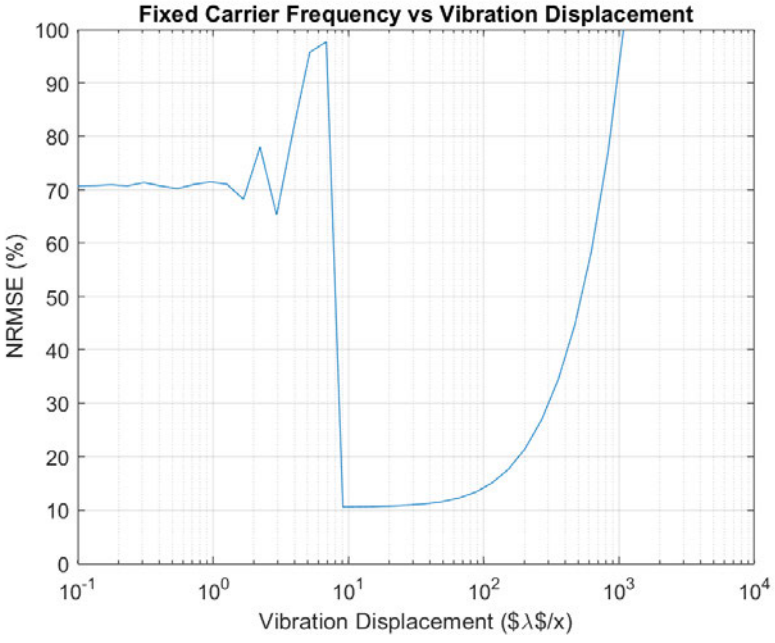
Fixed Carrier Frequency vs Vibration Displacement
NRMSE (%)
Vibration Displacement ($λ$/x)

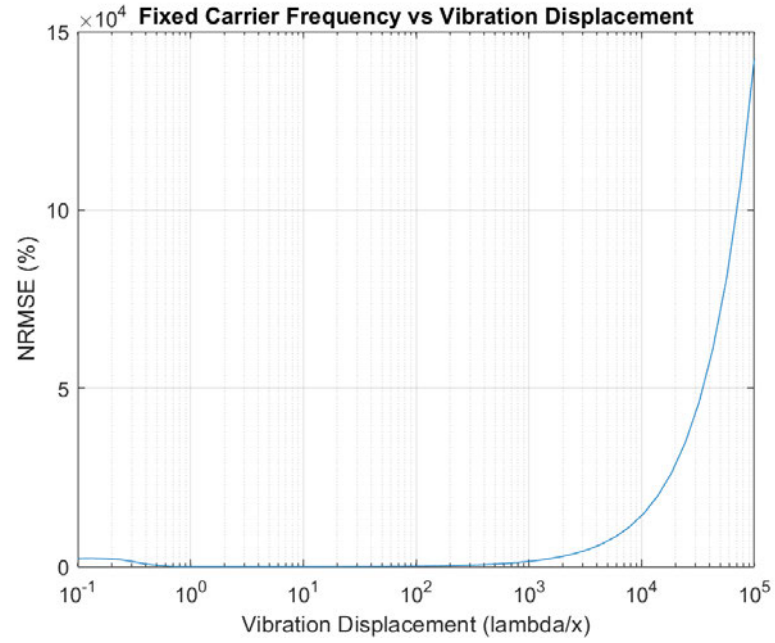
×10^4
Fixed Carrier Frequency vs Vibration Displacement
15
10
5
0
NRMSE (%)
10^-1
10^0
10^1
10^2
10^3
10^4
10^5
Vibration Displacement (lambda/x)

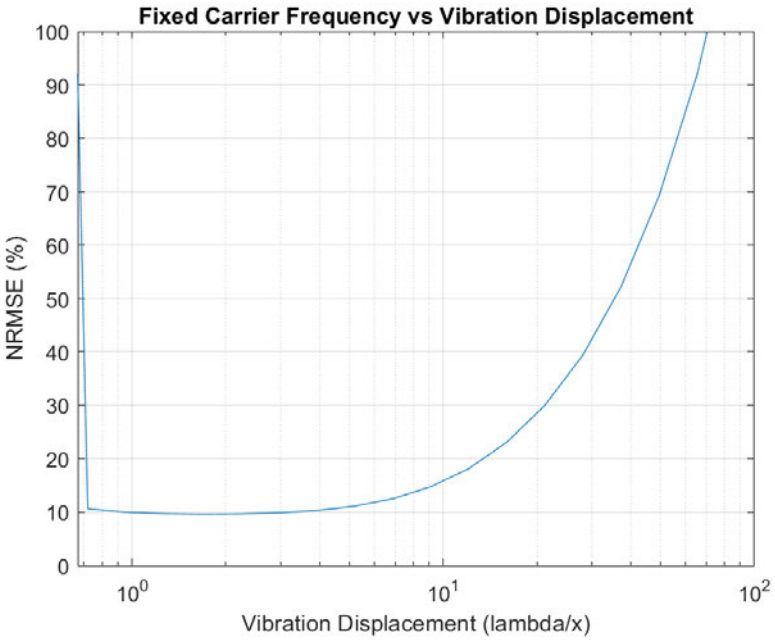
Fixed Carrier Frequency vs Vibration Displacement
100
90
80
70
60
50
40
30
20
10
0
NRMSE (%)
10^0
10^1
10^2
Vibration Displacement (lambda/x)

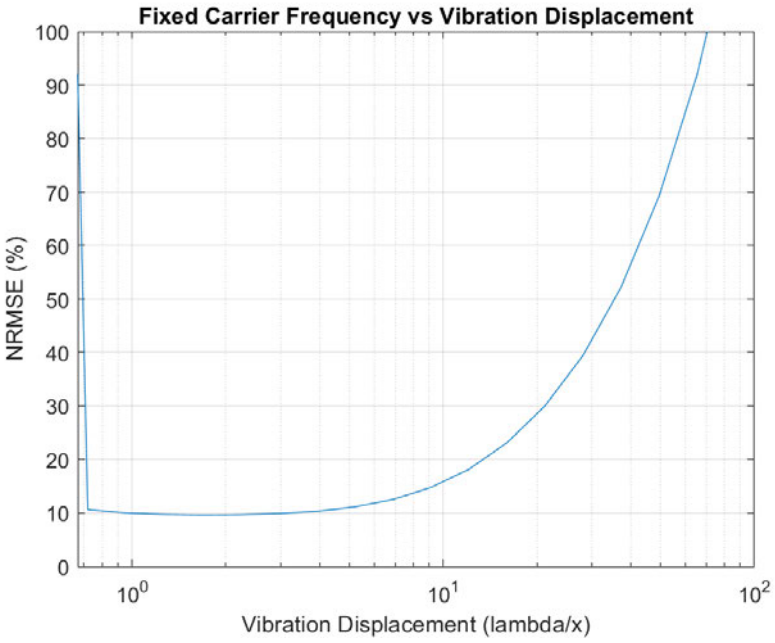
Fixed Carrier Frequency vs Vibration Displacement
NRMSE (%)
Vibration Displacement (lambda/x)

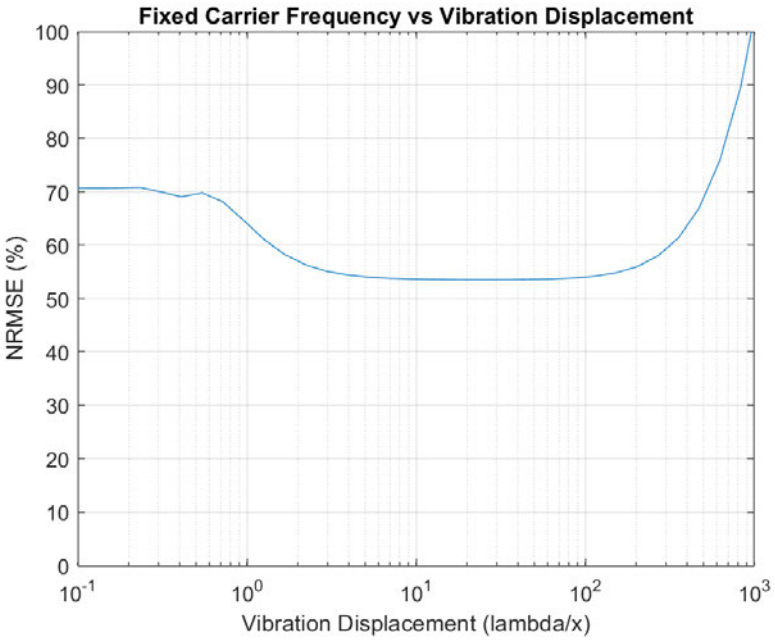
Fixed Carrier Frequency vs Vibration Displacement
NRMSE (%)
Vibration Displacement (lambda/x)

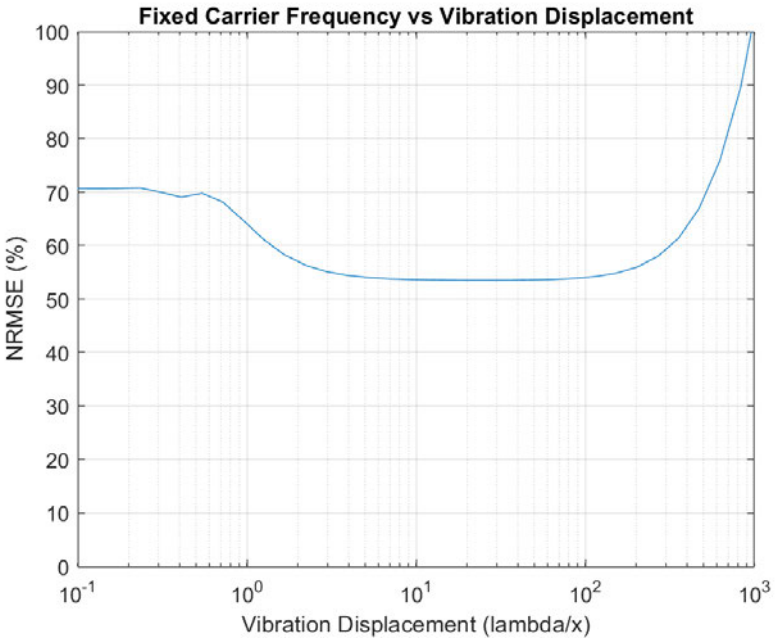

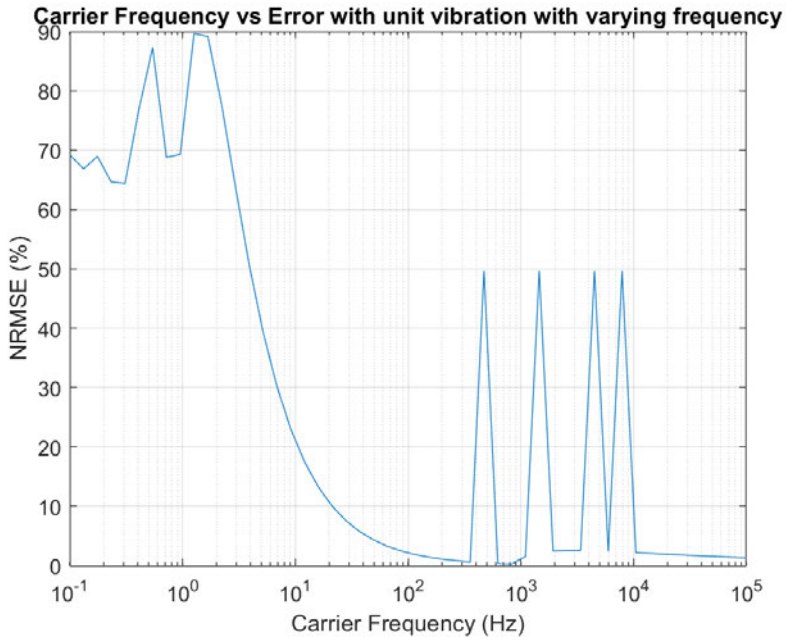


```
    writematrix(ATTest3Er','ArcTan_Results\' + txt + '.xlsx');
% Error Plotting
    figure
```

```
    semilogx(Testrange,ATTest3Er);
    grid on
    title("Carrier Frequency vs Error with unit vibration with varying frequency");
    xlabel("Carrier Frequency (Hz)");
    ylabel("NRMSE (%)");
    ylim([0 10])
    ax = gca;
    exportgraphics(ax,'F:\My Drive\Thesis\ENG4111 - Research Project Semester 1\Progress Report
```

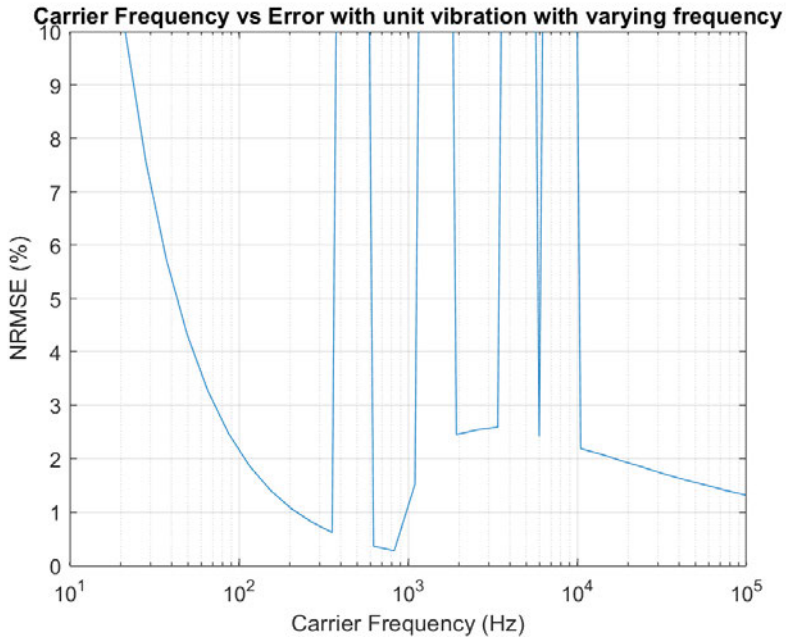


```
% Error Plotting
    figure
    semilogx(Testrange,DACMTest3Er);
    grid on
    title("Carrier Frequency vs Error with unit vibration with varying frequency");
    xlabel("Carrier Frequency (Hz)");
    ylabel("NRMSE (%)");
    ax = gca;
    exportgraphics(ax,'F:\My Drive\Thesis\ENG4111 - Research Project Semester 1\Progress Report
```

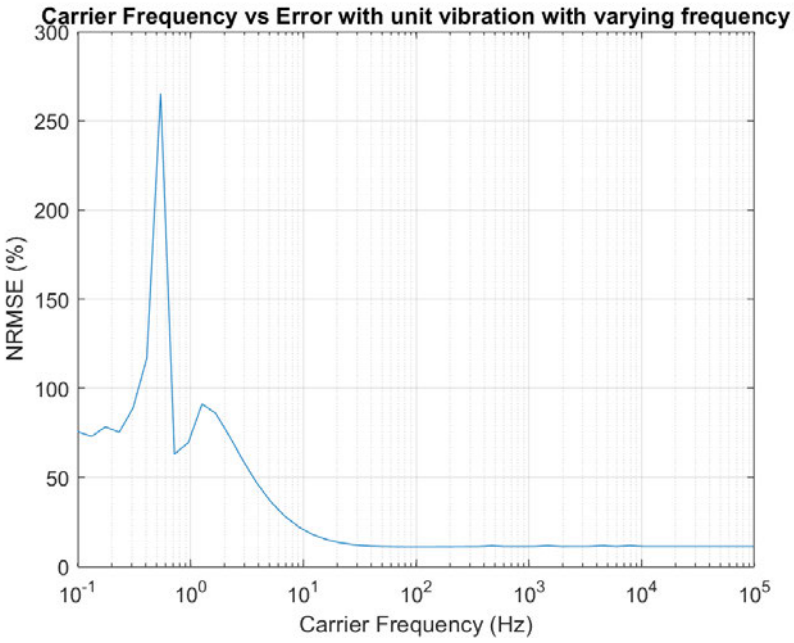


```
writematrix(DACMTest3Er','DACM_Results\' + EDtxt + '.xlsx');

 % Error Plotting
figure
semilogx(Testrange,MDACMTest3Er);
grid on
title("Carrier Frequency vs Error with unit vibration with varying frequency");
xlabel("Carrier Frequency (Hz)");
ylabel("NRMSE (%)");
ax = gca;
exportgraphics(ax,'F:\My Drive\Thesis\ENG4111 - Research Project Semester 1\Progress Report
```

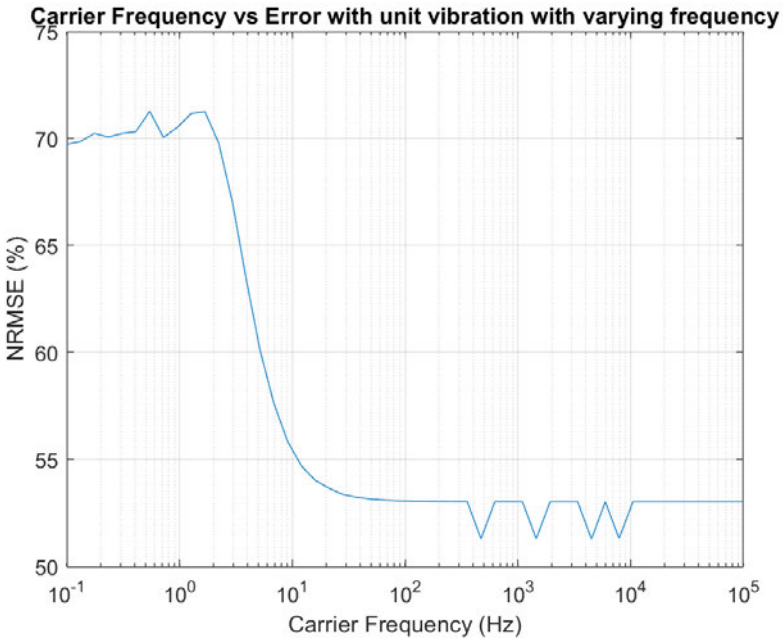


```
writematrix(MDACMTest3Er','MDACM_Results\' + MDtxt + '.xlsx');
```

10.8 Appendix I - Phase Noise Test Sequence - Code

Random Phase noise Test

Setting test parameters to run through.

```
%% Test Script to run tests on Atan Function
clc
clear all
close all

%Setting amplitude of reflected wave default
A = 1;
%Setting Carrier Frequency default
fc = 20;
%Setting Modulation frequency default
fm = 1;
%setting displacement of frequency default  (lambda/k)
k = 8;
%Setting run time of simulation and setting parameters so that each cycle
%of carrier frequency is created with a set number of points.
Tmax = 5;
Nfreq = Tmax/(1/fc);
N = Nfreq*20;
dt = Tmax/(N-1);
t = 0:dt:Tmax;

%Setting TestRange
Testrange = linspace(0, 2*pi,50);

%%Setting phase noise.
Theta = 0;
```

Test 1

This test introduces a standard DC offset to the phase on the reflected signal.

```
%% test 1
for C = 1:length(Testrange)
    ATPHTest1Er(C) = ATAN(N,Tmax,fc,fm,k,A,t,Testrange(C));
    DACMPHTest1Er(C) = DACM(N,Tmax,fc,fm,k,A,t,Testrange(C));
    MDACMPHTest1Er(C) = MDACM(N,Tmax,fc,fm,k,A,t,Testrange(C));
end
```

Plotting

```
txt = "ArcTan_Phase_Testing_Test1";
EDtxt = "DACM_Phase_Testing_Test1";
MDtxt = "MDACM_Phase_Testing_Test1";

%% Arctan Plotting
    figure
    plot(Testrange,ATPHTest1Er);
    grid on
```

```
title("Additive phase noise DC offset vs Error");
xlabel("Phase noise addition");
ylabel("NRMSE (%)");
xticks([0 pi/2 pi 3*pi/2 2*pi]);
xticklabels({'0','\pi/2','\pi','3\pi/2','2\pi'});
ax = gca;
exportgraphics(ax,'F:\My Drive\Thesis\ENG4111 - Research Project Semester 1\Progress Report
```

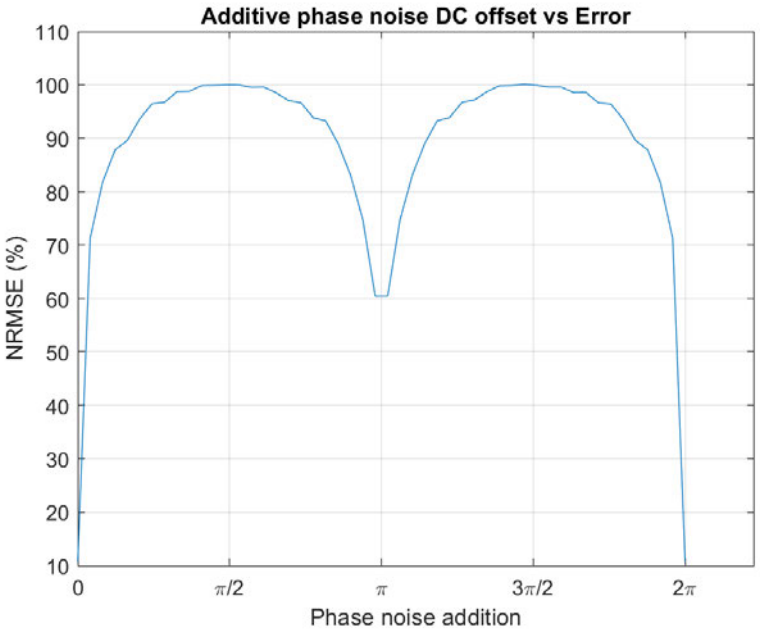


```
writematrix(ATPHTest1Er','ArcTan_Results\' + txt + '.xlsx');

%% EDACM Plotting
figure
plot(Testrange,DACMPHTest1Er);
grid on
title("Additive phase noise DC offset vs Error");
xlabel("Phase noise addition");
ylabel("NRMSE (%)");
xticks([0 pi/2 pi 3*pi/2 2*pi]);
xticklabels({'0','\pi/2','\pi','3\pi/2','2\pi'});
ax = gca;
exportgraphics(ax,'F:\My Drive\Thesis\ENG4111 - Research Project Semester 1\Progress Report
```

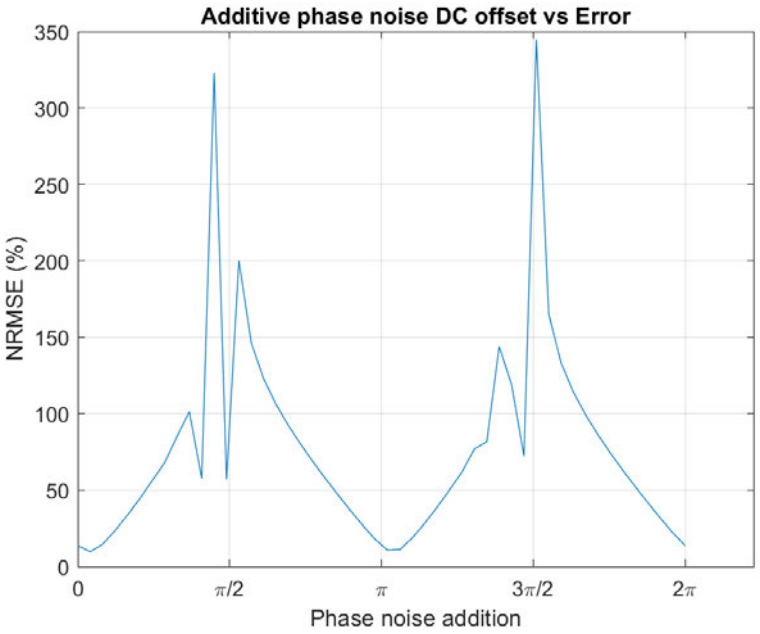


```
writematrix(DACMPHTest1Er','DACM_Results\' + EDtxt + '.xlsx');

%% EDACM Plotting
figure
plot(Testrange,DACMPHTest1Er);
grid on
title("Additive phase noise DC offset vs Error");
xlabel("Phase noise addition");
ylabel("NRMSE (%)");
xticks([0 pi/2 pi 3*pi/2 2*pi]);
xticklabels({'0','\pi/2','\pi','3\pi/2','2\pi'});
ylim([0 100]);
ax = gca;
exportgraphics(ax,'F:\My Drive\Thesis\ENG4111 - Research Project Semester 1\Progress Report
```

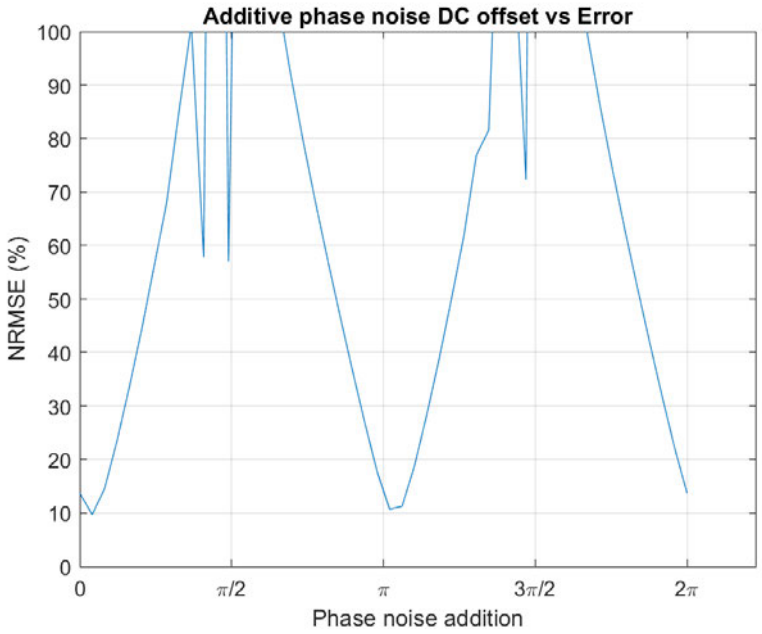


```
%% MDACM Plotting
figure
plot(Testrange,MDACMPHTest1Er);
grid on
title("Additive phase noise DC offset vs Error");
xlabel("Phase noise addition");
ylabel("NRMSE (%)");
xticks([0 pi/2 pi 3*pi/2 2*pi]);
xticklabels({'0','\pi/2','\pi','3\pi/2','2\pi'});
ax = gca;
exportgraphics(ax,'F:\My Drive\Thesis\ENG4111 - Research Project Semester 1\Progress Report
```

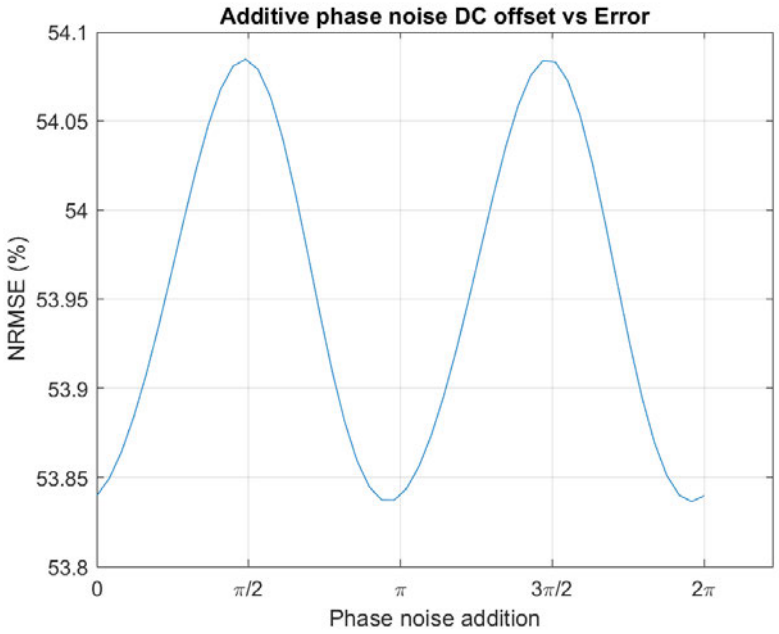


```
writematrix(MDACMPHTest1Er','MDACM_Results\' + MDtxt + '.xlsx');
```

10.9 Appendix J - Sampling Test Sequence - Code

Sampling Test Sequence

Setting test parameters to run through.

```
%% Test Script to run tests on Atan Function
clc
clear all
close all

%% Parameter Definition
Testrange = logspace(0,4);
%Setting amplitude of reflected wave default
A = 1;
%Setting Carrier Frequency default
fc = 20;
%Setting Modulation frequency default
fm = 1;
%setting displacement of frequency default  (lambda/k)
k = 8;
%Setting run time of simulation and setting parameters so that each cycle
%of carrier frequency is created with a set number of points.
Tmax = 20;
Nfreq = Tmax/(1/fc);

%%Setting phase noise.
Theta = 0;
```

Test 1

Analysis of error present when carrier frequency is varied against a unit vibration frequency.

$x_c(t) = A_c * \sin(w_c t)$

where

A_c is the amplitude peak value

w_c is the angular velocity equal to $2\pi f_c$

t is the time sequence

```
%% test 1
for C = 1:length(Testrange)
    N = Nfreq*Testrange(C);
    dt = Tmax/(N-1);
    t = 0:dt:Tmax;
    ATTest1Er(C) = ATAN(N,Tmax,fc,fm,k,A,t,Theta);
    DACMTest1Er(C) = DACM(N,Tmax,fc,fm,k,A,t,Theta);
    MDACMTest1Er(C) = MDACM(N,Tmax,fc,fm,k,A,t,Theta);
end
```

Plotting:

```
%Plot of Test1
txt = "ArcTan_Sample_Testing_Test1";
EDtxt = "DACM_Sample_Testing_Test1";
MDtxt = "MDACM_Sample_Testing_Test1";

% % Error Plotting
%     figure
%     semilogx(Testrange,ATTest1Er);
%     grid on
%     title("Number of samples per cycle vs Error");
%     xlabel("Samples per Cycle");
%     ylabel("Error (%)");
%     ax = gca;
%     exportgraphics(ax,'ArcTan_Results\'+txt+'.jpg');
%     writematrix(ATTest1Er','ArcTan_Results\' + txt + '.xlsx');
%
%  % Error Plotting
%     figure
%     semilogx(Testrange,DACMTest1Er);
%     grid on
%     title("Number of samples per cycle vs Error");
%     xlabel("Samples per Cycle");
%     ylabel("Error (%)");
%     ax = gca;
%     exportgraphics(ax,'DACM_Results\'+EDtxt+'.jpg');
%     writematrix(DACMTest1Er','DACM_Results\' + EDtxt + '.xlsx');

 % Error Plotting
    figure
    semilogx(Testrange,MDACMTest1Er);
    grid on
    title("Number of samples per cycle vs Error");
    xlabel("Samples per Cycle");
    ylabel("Error (%)");
    ax = gca;
    exportgraphics(ax,'MDACM_Results\'+MDtxt+'.jpg');
```

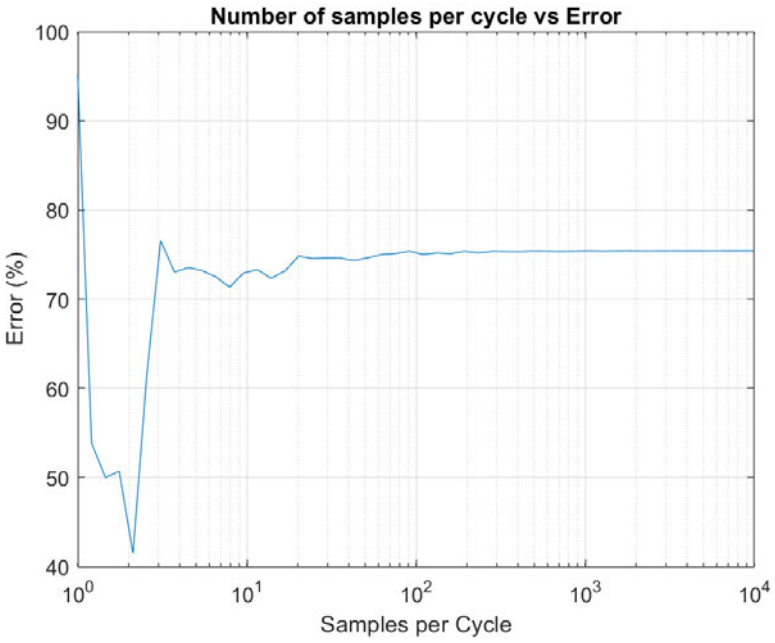


```
writematrix(MDACMTest1Er','MDACM_Results\' + MDtxt + '.xlsx');
```